Germ Cells and the Origins of Mammalian Pluripotent Cells

Ewart W. Kuijk

ISBN: 978-90-393-4992-2

Printed in the Netherlands by F&N Boekservice, Eigen Beheer, Amsterdam
Printing of this thesis was financially supported by the Jurriaanse Stichting

Cover design and layout by Marije Brouwer, Bureau Multimedia, Faculty of Veterinary Medicine
Cover illustration: hatching bovine blastocyst stage embryo

The research described in this thesis was performed at the Department of Farm Animal Health, Faculty of Veterinary Medicine, Utrecht University, the Netherlands

Germ Cells and the Origins of Mammalian Pluripotent Cells

Kiemcellen en de oorsprong van
pluripotente cellen bij zoogdieren

(met een samenvatting in het Nederlands)

Proefschrift
ter verkrijging van de graad van doctor aan de Universiteit Utrecht op gezag van de rector magnificus, prof.dr. J.C. Stoof, ingevolge het besluit van het college voor promoties in het openbaar te verdedigen op dinsdag 17 februari 2009 des middags te 12.45 uur

door

Ewart Willem Kuijk
geboren op 12 januari 1975, te Eindhoven

Promotoren:	Prof.dr. B. Colenbrander Prof.dr. H.P. Haagsman Prof.dr. J. Rothuizen
Co-promotor:	Dr. B.A.J. Roelen

Voor mijn ouders,
Voor Karin, Veerle & Morris

TABLE OF CONTENTS

Chapter I

Introduction: On the origins of pluripotent cells

On the origins of pluripotent cells

Background

Mammalian embryonic stem (ES) cells are derived from preimplantation embryos and can be propagated indefinitely without loss of pluripotency; i.e. the potential to develop into any embryonic cell type [1]. For several reasons, ES cells are powerful research tools in the field of developmental biology. They offer the opportunity to study mammalian differentiation processes in a culture dish. Furthermore, ES cells can be transplanted into host embryos and participate in their development. Labeling of the cells before transplantation can give insight in cell contribution to specific organs and tissues. Another major advantage of ES cells is the opportunity they provide for targeting genes and the creation of knock-out and knock-in animals (Fig. 1)[2].

Moreover, ES cells hold great potential in future regenerative medicine, especially since the derivation of ES cell lines from human embryos [1]. The capacity of ES cells of infinite self-renewal combined with the potency to develop into any cell type evokes that ES cells can regenerate damaged organs and cure a variety of diseases that are caused by malfunction of certain cell types. Candidate diseases for ES based cell therapy are muscular dystrophies, ischaemic heart disease, juvenile-onset diabetes mellitus, and neuro-degenerative diseases such as Parkinson's, and Alzheimer's [1, 3]. Various hurdles need to be overcome before ES-based therapy can be practiced. A major safety concern is the potential risk of not fully differentiated cells that cause tumor formation after transplantation [4]. Another barrier is the risk of immunerejection after allogeneic transplantation. This can be circumvented by the generation of patient specific pluripotent cells through therapeutic cloning; i.e. the derivation of patient specific ES cells from embryos that were obtained upon somatic cell nuclear transfer. However, there are obvious ethical issues to cloning humans [5]. Moreover, this technique requires the use of donor oocytes, availability of which is limited [6].

Because of obvious ethical reasons, research with human ES cell lines has its limitations, when compared to their murine counterparts. The potential risks and long-term capacity of human ES cells to regenerate damaged tissues should be investigated before ES-based therapies can be applied in human medicine. ES-based regeneration should first be examined in a proper model organism. Since the mouse falls short as a good model for humans in terms of life span and organ sizes, the pig has been proposed as a candidate model organism for ES cell-based therapy [4, 7-9]. Furthermore, pig ES cell lines, but also bovine ES cell lines, could allow genetic engineering of these livestock species to enhance production efficiencies or to promote disease resistance [10]. For these reasons, multiple groups have tried to generate porcine and bovine ES cell lines, but so far no cell lines have been described that can be cultured for a long period without loss of pluripotency [7, 9].

Another source of pluripotent cells are mouse and human primordial germ cells from which pluripotent embryonic germ (EG) cell lines can be derived. Recently, ES-like pluripotent cell lines have also been described that originate from murine neonatal and adult male germ cells. Pluripotent cells that originate from mouse testis are called multipotent germ stem (mGS) cells. EG and mGS cell lines are in many respects similar to ES cell lines and therefore share the advantages of ES cells. Primordial germ cells and male germline stem cells are in-

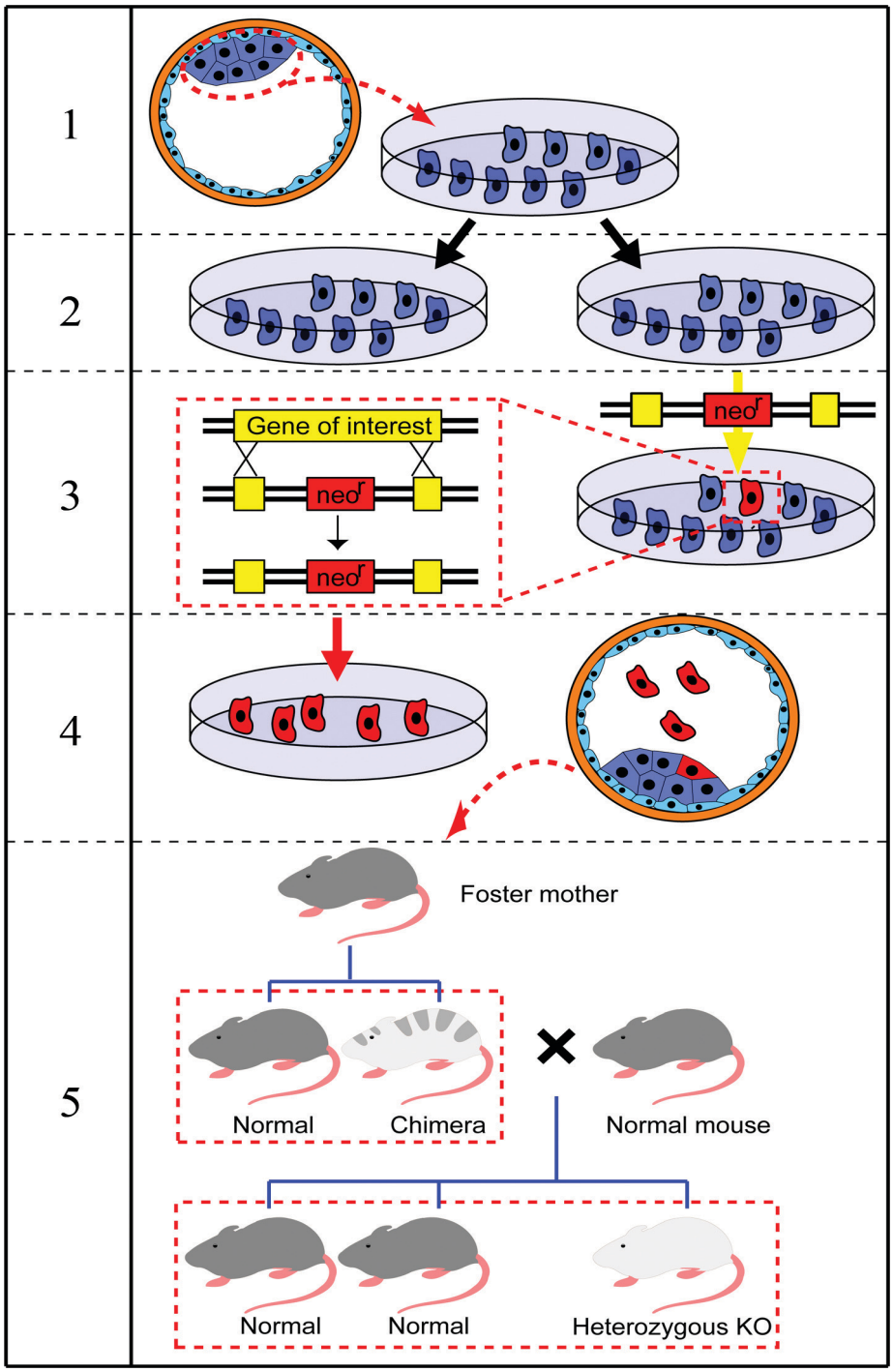
1
2
3
4
5
Gene of interest
neo^r
neo^r
neo^r
Foster mother
Normal
Chimera
Normal mouse
Normal
Normal
Heterozygous KO

teresting alternative sources of pluripotent cell lines from animals other than mouse and man that have scarcely been explored. Here, we will briefly discuss the origin of various pluripotent cell types and the molecular mechanisms that are involved in the development or maintenance of these cell types.

The first segregation: the formation of trophectoderm and inner cell mass

The developmental potential of mammalian cell types is reflected by the morphology of the chromatin. Loosely packed chromatin is called euchromatin and a more condense appearance is called heterochromatin. In general, cells with high plasticity have more euchromatin, which permits active transcription, and cells with limited developmental potential have more heterochromatin, which constrains transcription. Numerous covalent modifications of histone tails have been described that influence the density of chromatin, for instance methylation, acetylation, phosphorylation, sumoylation, and ubiquitination. These and other heritable non-genetic alterations that affect cellular phenotypes are called epigenetics [11]. Through epigenetic programming of cells a fertilized oocyte can give rise to all different cell types of an adult organism even though these cells share the same genome.

The first phases in mammalian development are similar between species. Fusion of a haploid sperm cell with a haploid oocyte results in the formation of a diploid zygote. After fertilization, zygotes first go through several successive cleavage divisions. Zygotes and individual cells of the first cleavage stages are totipotent, which means they can form all extraembryonic and embryonic cell types including new germ cells. In later stages of mammalian development, cells become more specialized and differentiation plasticity is reduced.

From around the 16-cell stage, embryos are mulberry-shaped and therefore called morulae (Latin: morus = mulberry). At subsequent stages, it is more difficult to recognize individual cells due to a process known as compaction. The transition of the compacted morula stage to the blastocyst stage is marked by the formation of a cavity named blastocoel. By cavitation, two morphologically distinct cell populations are segregated. The first population is called

Figure 1: Schematic representation for the derivation of an embryonic stem cell line and production of a knockout mouse

(1) The inner cell mass of a blastocyst stage embryo is isolated and put into culture conditions that favour self renewal; (2) under favourable culture conditions, cells will proliferate and cell numbers will expand; (3) through electroporation, cell membranes are temporarily permeabilized, which allows gene constructs (in this case a neomycin resistance gene cassette which is depicted in red), to enter the cells. The yellow boxes of the gene construct represent regions that are homologous to the gene of interest. In a number of cells (in the cartoon the single red cell in the dish), this homology will allow genetic recombination to occur and the gene of interest will be substituted by the gene construct (depicted in the box with the dashed line). Subsequent culture of the cells in presence of neomycin will positively select for those cells in which recombination has occurred (petri dish will only red cells). Next, gene targeted ES cells can be introduced in preimplantation embryos, which are allowed to develop in a foster mother (5). Since ES cells are pluripotent, they will contribute to all embryonic tissues, including the germ cells. The foster mother will give rise to chimaeric animals. Breeding of a germline chimaera with a normal mouse will result in normal offspring and in offspring heterozygous for the gene target. Further crossing of animals heterozygous for the targeted gene will result in animals homozygous for the knock out. This figure was adapted from a freely useable scalable vector graphics file.

the trophectoderm and consists of the outer epithelial cells that surround the blastocoel. The second group of cells is called the inner cell mass (ICM), which is composed of a cluster of pluripotent cells that sit on the inside of the trophectoderm layer.

Specification of cell lineages in early mouse development depends largely on transcription factors that influence gene expression patterns and, as a result, cell character (Fig. 2). A key player in specification of the ICM is transcription factor OCT4 that has a bipartite DNA binding domain referred to as the POU domain. OCT4 expression is restricted to the ICM of early blastocysts and the epiblast of later blastocyst stages [12]. Although the trophectoderm of *Oct4* null embryos is functional and embryos implant at the blastocyst stage, *Oct4* null embryos fail to develop an ICM or any of its derivatives; resulting in embryos that are entirely composed of trophectoderm cells instead. As a consequence, *Oct4* null embryos are embryonic lethal and die shortly after implantation [13]. The key role of *Oct4* in lineage specification is reinforced by studies in which conditional repression of *Oct4* in mouse ES cells resulted in formation of trophectoderm-like cells [14].

A key transciption factor involved in specification of the trophectoderm lineage is caudal-related homeodomain protein CDX2. Expression of CDX2 in mouse blastocysts is the inverse of OCT4 expression and is restricted to the trophectoderm [15]. Embryos deficit of *Cdx2* cannot maintain the trophectoderm lineage after its initial formation and as a result, *Cdx2* null embryos fail to implant [16, 17]. Early blastocysts of *Cdx2*$^{-/-}$ embryos have trophectoderm cells with an ICM character, as demonstrated by ectopic expression of OCT4 in the outer cells [18]. From the trophectoderm lineage, trophectoderm stem (TS) cell lines can be isolated. When cultured under the appropriate conditions, the individual cells can self-renew without losing the capacity to differentiate within the trophectoderm lineage [19]. However, TS cells cannot be established from *Cdx2* mutant embryos. The key role of CDX2 in trophectoderm specification is also emphasized by the conversion of ES cells to TS cells after forced expression of *Cdx2* [20].

OCT4 and CDX2 are mutually expressed in all cells of 8-cell stage embryos. Remarkably, these transcription factors repress the expression of each other [20] and it has been hypothesized that mutual repression in early morulae results in segregation of CDX2 expressing- and OCT4 expressing- cells and specification of the inner cell mass and trophectoderm lineages as a consequence (Fig. 2)[17, 20, 21].

The second segregation: the formation of primitive endoderm and pluripotent epiblast

At embryonic day 3.5 (E3.5), ICM cells of mouse blastocysts are largely restricted in their fate and can develop into primitive endoderm or into epiblast, which is the second lineage segregation event in mouse development [18]. This heterogeneity is reflected by a complementary mottled expression of GATA6 and NANOG (Fig. 2). GATA6 contributes to specification of primitive endoderm, since imposed expression of *Gata6* in mouse ES cells is sufficient to direct these cells to a primitive endoderm fate [22]. However, *Gata6* is not essential as demonstrated by primitive endoderm formation in *Gata6* null embryos [23]. The primitive endoderm can give rise to extraembryonic endoderm (XEN) stem cell lines [24]. Comparable to ES and

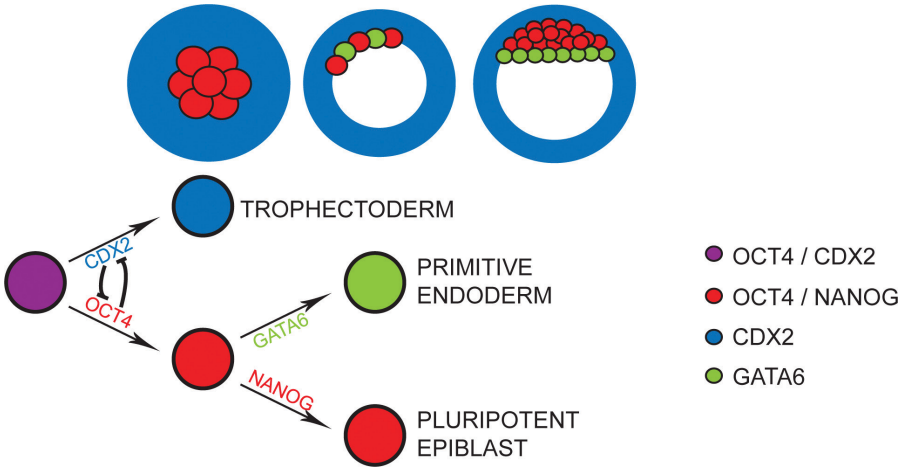

Figure 2: Two successive differentiation events in early mouse embryonic development result in the segregation of three committed lineages that together form the blastocyst.
The first segregation occurs at the compacted morula stage. In this model, mutual repression of OCT4 and CDX2 in early morulae results in CDX2- expressing and OCT4-expressing cells, with loss of CDX2 expression in the ICM as a primary event, and with consequent segregation of the inner cell mass and trophectoderm lineages. The second segregation of lineages divides the inner cell mass into the primitive ectoderm and the primitive endoderm (PE). Before the PE is formed, its precursors can already be detected by expression of Nanog and Gata6, which show a so-called "pepper-and-salt" distribution. NANOG-positive cells become epiblast cells and GATA6-positive cells become PE. This model was adapted from a review by A. Ralston [21].

TS cell lines, the cells from XEN cell lines have the capacity of self-renewal and the differentiation potential of their *in vivo* counterparts.

Specification of the pluripotent epiblast in mouse embryos requires *Nanog*, which is a homeobox transcription factor named after a mythical Celtic land of the forever young. Expression of NANOG in peri-implantation embryos is restricted to the pluripotent epiblast and its precursors [25-27]. *Nanog* $^{-/-}$ embryos lack pluripotent epiblast cells and ICM cells of E3.5 *Nanog* mutants differentiate into parietal endoderm-like cells when cultured *in vitro* [26]. ES cells also express *Nanog* and loss or inhibition of *Nanog* expression increases the propensity of ES cells to differentiate [25, 26, 28]. Moreover, forced expression of *Nanog* reduces responsiveness of ES cells to differentiation signals [25].

Embryos in which the gene that encodes signal adapter protein GRB2 has been disrupted fail to develop a primitive endoderm and lack GATA6 expression, but have a homogeneous ICM that consists of cells equally expressing NANOG [18, 29, 30]. The *Grb2*$^{-/-}$ phenotype mimics that of embryos in which the genes *Fgf4* and *Fgfr2* have been disrupted [31-33]. FGF4, FGFR2, and GRB2 are components of the receptor tyrosine kinase-Ras-MAP kinase (MAPK)-signaling pathway. Therefore, a model has been proposed in which FGF4 binding to FGFR2 activates the GRB2-MAPK pathway, which then initiates GATA6 expression [30]. The onset of GATA6 expression serves as a switch that puts an end to NANOG dominance. Activation of GATA6 target genes further specifies primitive endoderm formation. The shift in transcription factor dominance from NANOG to GATA6 also affects genes involved in cell adhesion, which physically allows the newly formed primitive endoderm cells to segregate

from the epiblast [30].

The differentiation potential of embryo-derived stem cells is most clearly demonstrated by experiments with chimaeras (from Greek: χίμαιρα = monster). Chimaeric embryos can be made by transplantation of cultured stem cells into host blastocyst stage embryos. The developmental contribution of transplanted cells can be easily examined if the cells have been marked with a label beforehand. Such experiments in combination with classical lineage tracing experiments have established the paradigm that the three cell types present in late mouse blastocysts are three committed lineages with separate fates [18]. Trophectoderm cells form the major embryonic contribution to the placenta and donor TS cells exclusively contribute to the fetal portion of the placenta [19]. Primitive endoderm cells give rise to the yolk sac and donor XEN cells solely participate in extra-embryonic endoderm development in chimeras [24]. The extra-embryonic tissues derived from trophectoderm and primitive endoderm support the growth and development of the fetus that originates from the epiblast. Donor ES cells, similar to epiblast cells, contribute to all fetal tissues and the extra-embryonic mesoderm, but colonize trophectoderm and primitive endoderm at low frequency [34].

The pluripotent epiblast of mouse embryos is defined by two segregation events that principally depend on the transcription factors OCT4, CDX2¸GATA6 and NANOG. The lack of success in generating porcine and bovine ES cell lines has been attributed to differences in early embryonic development [7, 9]. Morphologically, there are no major differences between mammals in the development from fertilized oocyte to blastocyst, but from the blastocyst stage onwards, there is more variation between species. Implantation of mouse and human embryos occurs at the blastocyst stage and results in a haemochorial placenta [35]. Conversely, porcine and bovine blastocysts implant at later stages in development. In these species, the trophectoderm first elongates to a long, thin filament before the embryos implant, giving rise to a loose diffuse non-invasive epitheliochorial placenta [36].

At the molecular level, bovine and porcine blastocysts differ from their murine counterparts in OCT4 expression, which is not restricted to the ICM [37, 38]. This indicates that pigs and cows do not share the interplay between OCT4 and CDX2 that is supposed to cause the first lineage segregation in mouse embryos. However, little is known about the other molecular mechanisms that define the pluripotent cell population in bovine and porcine embryos and if *NANOG*, *CDX2*, or *GATA6* are involved in this process. An increase of our understanding on the mechanisms that define the pluripotent cell populations in cows and pigs could facilitate the derivation of pluripotent cells from these species. A first step would be to study the differences and similarities between different species in the expression patterns of the key transcription factors. In comparison with a model organism as the mouse, porcine and bovine genome sequence information is more fragmented and availability of species-specific antibodies, valuable tools in studies on protein expression, is limited. Therefore, development of the appropriate molecular biological tools is a challenging aspect of studies on the factors that determine porcine and bovine pluripotency.

Primordial germ cells

From mouse embryos, pluripotent cell lines can also be established from primordial germ cells. In a diversity of animals, such as sea urchins [39, 40], ascidians [41], flies [42, 43], and nematodes [42], developmental fate of germ cells in embryonic development is regulated by maternal components that are inherited differentially. Mammalian development seems more regulative, with germ cell fate established dynamically through cell interactions. In mouse embryos, PGCs are specified in the proximal pluripotent epiblast between E6.25 and E7.25. In a classic transplantation experiment, embryonic tissue from the distal epiblast that would otherwise have a somatic fate, contributed to the germ cell population after transplantation to the proximal epiblast [44]. This clearly demonstrates that in the mouse, the formation of PGCs is not the result of inherited maternal determinants but by local interactive signals instead.

Instructive bone morphogenetic protein - (BMP) signalling from the extraembryonic ectoderm [45] and visceral endoderm [46] triggers the expression of *fragilis*/*Ifitm3* in adjacent proximal epiblast cells at E5.5/E6, which thereby acquire primordial germ cell competence. At E6.25, approximately six *fragilis*/*Ifitm3*-positive cells become also positive for B-lymphocyte maturation-induced protein 1 (*Blimp1*), which are the first PGC ancestors [47]. In the following period, more *Blimp1*-expressing cells are recruited that eventually become the PGC founder population of approximately 40 PGCs that express *Stella* and are positive for alkaline phosphatase. *Blimp1*-positive cells initially have a mesodermal character as demonstrated by the expression of mesodermal genes *Hoxb1*, *T brachyury*, *Fgf8*, and *Snail* [48]. Upon *Blimp1* expression, PGC precursors escape the somatic fate of the surrounding cells that do not express *Blimp1*. As a consequence, the preliminary mesodermal character becomes repressed and is gradually replaced by an expression pattern that, through the expression of pluripotency-associated genes *Nanog* [25, 27], *Oct4*, and *Sox2*, is reminiscent of ES cells and the pluripotent epiblast. Transciptional similarities between PGCs and ES cells are maintained between E8.5 and E11.5. In this developmental period, when PGCs migrate through the hindgut towards the developing gonads, embryos are permissive for the derivation of pluripotent cell lines from primordial germ cells [49, 50].

In porcine embryonic development, presumptive PGCs have been detected as a small population of OCT4 expressing cells in the endoderm of the primitive streak stage at 13 days post-insemination (d.p.i.) [51]. Alleged PGCs have also been observed in the allantoic endoderm and mesoderm of 14-15 d.p.i. somite stage embryos [51], in the dorsal mesentery of the hindgut of day 18 and 20 embryos, and in the primordium of the gonad at day 23 [52]. In the bovine embryo, PGCs primordial germ cells can be detected in the caudal wall of the proximal yolk sac of day 18 embryos. As in pigs, bovine PGCs also migrate through the hindgut and arrive at the mesonephros before the gonadal ridges start to develop [53]. Thus, porcine and bovine trajectories of PGCs seem to correspond largely to that of migratory PGCs in mouse development. Remarkably, porcine PGCs show little alkaline phosphatase activity before reaching the gonads, but murine and bovine migrating PGCs have high alkaline phosphatase activity. Our knowledge on bovine and porcine PGCs is too limited to conclude that these cells are similar to or fundamentally different from murine PGCs.

Spermatogenesis

After migration through the hindgut, male PGCs colonize the genital ridges where they become gonocytes and after temporal mitotic activity enter a dormant stage in the G_0 phase of the cell cycle [54]. In mouse, a short burst of activity in somatic cells of a single gene on the Y chromosome, *Sex-determining region of the Y-chromosome* (*Sry*), results in testis development and from E12.5 the first morphological signs of sexual differentiation are visible by the appearance of seminiferous cords [55]. After birth, mouse gonocytes resume the cell cycle and give rise to spermatogonial stem cells (SSCs) that reside at the basal membrane of seminiferous tubules [54].

Recently, mammalian spermatogonial stem cells (SSCs) have joined PGCs and cells from the epiblast as a source of pluripotent cells [56-60]. While female germ cells stop proliferation before birth, male spermatogonial stem cells display self-renewal throughout adult life until senescence. Transplantation of SSCs to a host testis that has been depleted of stem cells by chemical treatment or irradiation can restore fertility of infertile mouse similar to how bone-marrow derived hematopoietic stem cells can restore function when production of blood cells is impaired. An important difference, however, is that haematopoietic stem cells are multipotent and can develop into multiple cell types, whereas SSCs are unipotent and can only differentiate into sperm cells. The group of Shinohara was the first to describe a method for the long-term culture of unmodified mouse SSCs that maintained the capacity to colonize a testis [61]. Additionally, the same group were the first to derive multipotent germline stem cells from their spermatogonial stem cell cultures [58]. Colonies of mGS cells occasionally arose under standard SSC culture conditions and these colonies displayed long term self renewal when transferred to ES-cell culture conditions. Moreover, cells of these colonies proved to be pluripotent, as demonstrated by their somatic and germline contribution to chimaeric embryos [58]. SSC colonies and mGS colonies can be derived from a single spermatogonial stem cell [59], however, the mechanism that causes SSCs to switch to a pluripotent state remains to be elucidated.

There is a strong connection between the testis and pluripotency. First of all, the testis can harbor malignant tumors called teratocarcinomas that are composed of pluripotent cells and differentiated progeny of numerous cell types [62]. In fact, the first pluripotent cell lines were derived from teratocarcinomas and are called embryonal carcinoma (EC) cell lines.

The second association of the testis with high plasticity of cells is more straightforward; i.e. in a process known as spermatogenesis the testis produces sperm cells that can fertilize oocytes and thereby contribute to the formation of a whole new organism. Mammalian spermatogenesis is a lengthy, highly orchestrated, intricate process of differentiation that takes place in the tubular compartment of the adult testis. Three distinct consecutive phases in spermatogenesis can be recognized: mitosis, meiosis and cellular differentiation. Here, the mouse model is used to briefly illustrate the principles of spermatogenesis. In the mouse, SSCs are called $A_{s\ (single)}$ spermatogonia that, upon differentiation, first go through a number of successive spermatogonial stages. In consecutive order, these stages are as follows: type A_s, $A_{pr\ (pair)}$, $A_{al4\ (4\ cells\ aligned)}$, A_{al8}, $A_{al16,}$ A1, A2, A3, A4, In (Intermediate), and type B spermatogonia.

Type A_{pr} and A_{al} spermatogonia are two and more cells respectively that are connected by cytoplasmic bridges. From type A_s to type B spermatogonia, nuclear material progressively

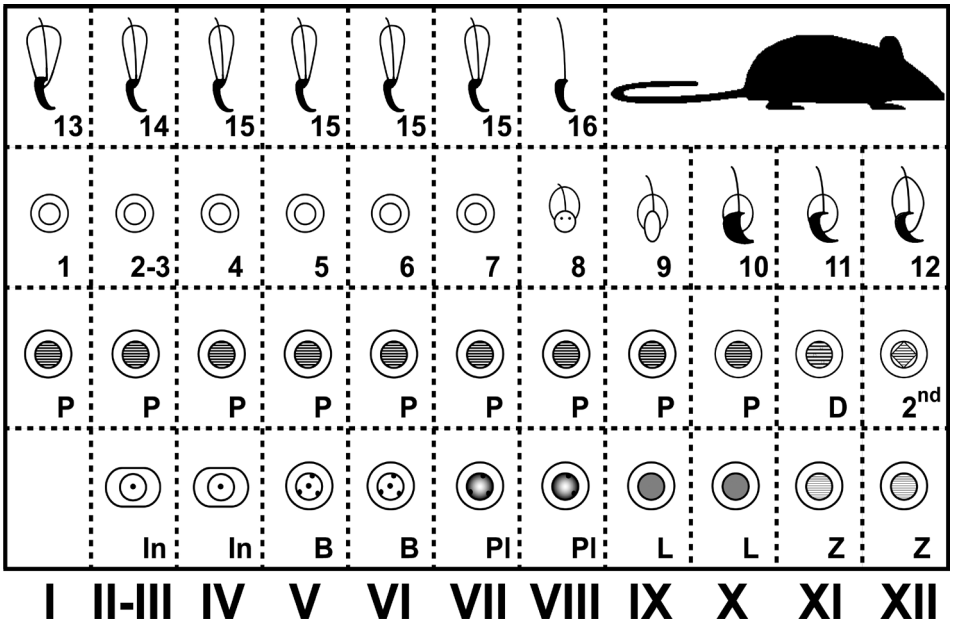

Figure 3: The seminiferous epithelial cycle of murine spermatogenesis.
Each column represents the combination of different cell types that are present in seminiferous tubules that are at that specific stage. Roman figures = stage of the epithelial cycle, In = intermediate spermatogonia, B = type B spermatogonia, Pl = pre-leptotene stage, L = leptotene stage, Z = zygotene stage, P = pachytene stage, D = diplotene stage, 2^{nd} = generation of secondary spermatocytes,1-16 = steps in spermiogenesis.

condenses from a loose euchromatic state to a dense heterochromatic state and, as the name suggests, type In spermatogonia have a chromatic state in between. Transitions from one stage of type A spermatogonia to the next are marked by mitotic events, with the exception of the transition from A_{al16} to A1. Together, these stages represent the proliferative phase of spermatogenesis [54, 63]. Next, Type B spermatogonia leave the basal membrane and develop into primary spermatocytes, which marks the transition from the proliferative phase of spermatogenesis to the meiotic phase of spermatogenesis [54].

An estimated 90% of male meiosis is consumed by prophase of the first meiotic division [64], in which distinct phases can be recognized. At preleptotene, spermatocytes synthesize DNA resulting in a cell with double the somatic number of chromosomes (4n) [65] that will subsequently condensate at leptotene. At zygotene, homologous chromosomes pair through so-called synaptonemal complexes, which are completed at pachytene. Separation of chromosomes is then initiated in the diplotene phase of meiosis followed by the first meiotic division, which results in two secondary spermatocytes (2n). Shortly thereafter, both spermatocytes go through the second meiotic division and 4 haploid (n) round spermatids are produced [64].

With the establishment of spermatids, spermatogenesis enters the phase of cellular differentiation called spermiogenesis. Cellular and morphological modifications lead to the gradual maturation of round spermatids to highly specialized elongated spermatozoa that can fertilize oocytes and contribute to totipotent embryos. Formation of the acrosome, tight packing of DNA in protamines, and the development of a flagellum are some of the processes that are

involved [64].

In cross-sections of seminiferous tubules, spermatogonia, spermatocytes, and spermatids are organized in concentric layers, with the spermatids nearest to the lumen [65]. Routine microscope techniques have revealed that certain steps in spermiogenesis are always closely associated with particular phases in meiosis and also with specific stages of spermatogenesis. For example, in mouse spermatogenesis, intermediate spermatogonia are associated with pachytene spermatocytes and spermiogenic steps 2-4 and 14-15. As such, 12 consecutive stages in mouse spermatogenesis can be identified that are denoted with roman figures and which collectively are referred to as the cycle of the epithelium (Fig.3).

Xeno-transplantation experiments have revealed that spermatogonia from most mammals are able to colonize mouse testes. However, only when closely related donor species are used, can transplanted spermatogonia participate in spermatogenesis. This indicates that the mechanism of spermatogonial stem cell self-renewal is conserved and the mechanism of spermatogenesis diverges between mammalian species. Consequently, culture systems that support self-renewal of mouse SSCs probably support self-renewal of SSCs from other species.

The generation of SSC lines from other species than the mouse, such as pigs and cows, could offer an alternative route to pluripotent cell lines in these species. Moreover, porcine and bovine SSC cultures could be used to create transgenic livestock by targeting genes followed by the transplantation assay. Furthermore, SSC cultures provide an excellent *in vitro* model to study the biology of these cells, such as the mechanism of self-renewal and spermatogenesis.

Thesis outline

The main themes of this thesis are pluripotency of cells, the molecular mechanisms that determine pluripotency, and interspecies similarities or differences in these molecular mechanisms. The practical work described in this thesis covers the next five chapters and focuses on preimplantation embryos, SSCs, and testis function in the light of pluripotency. Chapter 2 describes the identification of a set of reference genes that can be used to normalize gene expression in early porcine development. Through this set of reference genes, gene expression levels can be compared between different porcine developmental stages ranging from germinal vesicle stage oocytes up until the expanded blastocyst stage. In chapter 3, it is described how key factors that are involved in early mouse lineage segregation events show dissimilar expression patterns in porcine and bovine embryos, which suggests that the mechanisms of the first lineage segregations are not conserved between mammals. In the next chapter, a study is presented on the isolation and culture of porcine male germline stem cells. A characterization is presented of the different cell types and colonies that were derived from these cultures as well as an analysis of the effect of different growth factors on newly initiated cultures of porcine testis cells. The following chapter describes an RNAi study on cultures of mouse germline stem cells, which was performed to gain more insight in the mechanisms that insulate male germ cells from pluripotency. Finally, in chapter 6, the findings of a comparative study are presented on the expression of pluripotency factor NANOG in testes of mouse, dog, pig, and human. Primordial germ cells are not the principal subjects of investigation in the experiments that are described in this thesis. Nevertheless, primordial germ cells are discussed in this

introduction and in the discussion section, because of the significant contributions these cell types have made to our understanding of pluripotency.

Chapter II

Validation of reference genes for quantitative RT-PCR studies in porcine oocytes and preimplantation embryos.

Ewart W. Kuijk[1], Leonie du Puy[1,2], Helena T.A. van Tol[1], Henk P. Haagsman[2], Ben Colenbrander[1], Bernard A.J. Roelen[1]

[1]Department of Farm Animal Health, [2]Department of Infectious Diseases and Immunology, Faculty of Veterinary Medicine, Utrecht University, The Netherlands

Adapted from *BMC Developmental Biology* 2007, 7:58.

Validation of reference genes for quantitative RT-PCR studies in porcine oocytes and preimplantation embryos.

Abstract

In the developing embryo, total RNA abundance fluctuates caused by functional RNA degradation and zygotic genome activation. These variations in the transcriptome in early development complicate the choice of good reference genes for gene expression studies by quantitative real time polymerase chain reaction.

In order to identify stably expressed genes for normalisation of quantitative data, within early stages of development, transcription levels were examined of 7 frequently used reference genes (*B2M*, *BACT*, *GAPDH*, *H2A*, *PGK1*, *S18*, and *UBC*) at different stages of early porcine embryonic development (germinal vesicle, metaphase-2, 2-cell, 4-cell, early blastocyst, expanded blastocyst). Analysis of transcription profiling by geNorm software revealed that *GAPDH*, *PGK1*, *S18*, and *UBC* showed high stability in early porcine embryonic development, while transcription levels of *B2M*, *BACT*, and *H2A* were highly regulated.

Good reference genes that reflect total RNA content were identified in early embryonic development from oocyte to blastocyst. A selection of either *GAPDH* or *PGK1*, together with *S18*, and *UBC* is proposed as reference genes, but the use of *B2M*, *BACT*, or *H2A* is discouraged.

Background

Preimplantation development is a highly dynamic process including phenomena such as oogenesis, oocyte maturation, fertilization and lineage segregation. Not surprisingly, early embryonic development is characterized by dramatic changes in transcription. To start with, at the diplotene stage of an oocyte's first meiotic prophase, numerous genes are transcribed and translated, resulting in storage of mRNA and proteins that support early embryonic development. After completion of maturation, oocytes arrest at the metaphase of the second meiotic division, where transcription is halted and translation of mRNA is reduced [1]. Transcription is restored after fertilization, which can be detected by incorporation of labelled nucleotides in mRNA of embryos [2,3]. In mammals, the start of zygotic genome activation varies between 1- and 8-cell stage embryos, dependent on the species [4].

The main part of our knowledge on the transition from maternal to zygotic transcipts has been derived from studies in mouse, but also from studies in rabbits, cattle and pigs. In the mouse, early embryonic development shows wave-like gene activation patterns and two major transitions in gene expression can be recognized. The first major wave of gene activation peaks at the 2- to 4-cell stage. This corresponds to the well-known zygotic genome activation, by which embryonic transcripts replace maternally inherited transcripts. The second major wave of gene activation, the so-called mid-preimplantation genome activation, peaks at the 8-cell stage and precedes the obvious morphological changes in subsequent stages: compac-

tion and blastocyst formation. These major waves of activation are followed by two minor waves, one at the morula stage and another at the blastocyst stage [5]. In addition to these bursts in transcription, maternal mRNA is actively degraded during early embryonic development, restricting the time window in which these transcripts can function. In the mouse, the amount of total RNA at the 2-cell stage is reduced to ~10% compared to that of an unfertilised oocyte [5-7]. These temporal changes in transcriptome are considered to fulfil the need of the embryo for particular classes of proteins at the appropriate phases in development. Minor genome activations, prior to the major zygotic genome activation, have been observed during the first cleavage stages of rabbit, human, and bovine embryos, which suggests a conserved mechanism of sequential acquisition of transcriptional control in mammals [8-13].

Dynamic changes in the transcriptome take place in the developing porcine embryo as well. In this species, loss of maternal transcripts in zygotes is demonstrated by decreasing levels of *CYCLIN B1* and *CDC25C* in early embryonic development [14,15]. At the 4- cell stage of porcine embryos the first synthesis of extra-nucleolar RNA was observed by using uridine-3H labelling techniques, which is an indication that from the third cell cycle onwards the porcine embryonic genome is reactivated. [16]. Activation of the porcine embryonic genome at this stage of development is also confirmed by fluorescent in situ hybridisation of rRNA transcripts at the 4-cell stage but not in earlier embryonic stages [17]. *CDC25C* transcription is also observed in 4-cell stage pig embryos [14], another indication that the porcine embryonic genome is active in these embryos. In other words, early porcine embryonic development is characterized by significant changes in the transcriptome.

Studying alterations in gene expression is essential to understand the processes that are important for preimplantation development. Presently, the method of choice to quantify mRNA levels is quantitative Reverse Transcription Polymerase Chain Reaction (qRT-PCR), particularly when small amounts of mRNA are present [18]. In gene expression studies, there are several sources of variation, such as the amount of starting material, enzymatic efficiencies, and differences between tissues or cells in overall transcriptional activity. In an ideal situation, transcript numbers are standardized to the number of cells [19]. However, during preimplantation development, cell numbers and cell sizes are constantly changing. Alternatively, gene expression is normalized by the amount of starting material, but RNA yield from preimplantation embryos is too low for reliable quantification and variation in its reverse transcription cannot be excluded. Also for proper use of external controls, quantification of starting material is indispensable [20], and therefore not the preferred method when using small amounts of material. An elegant way to control for all variables, including the amount of input material, is normalization against internal control genes, on the condition that these internal control genes are stably expressed [19]. Traditionally, mRNA levels in Northern blots and RNAse protection assays have been quantified by normalisation to a reference gene that shows constant expression levels between samples with similar RNA content. In the present study, a similar line is followed; a stably expressed gene is defined as a gene of which its quantity is an indication of the total amount of RNA. In other words, a good reference gene for early embryonic development reflects the fluctuating transcriptomes by its expression. Commonly used reference genes are beta-actin (*BACT*), glyceraldehyde-3-phosphate dehydrogenase (*GAPDH*), and 18S ribosomal RNA (*S18*). However, it is unknown whether these genes are stably expressed in early

developmental stages ranging from immature oocytes to expanded blastocyst stage embryos.

Most gene expression studies in preimplantation development have focused on murine models, but where mouse embryos form an egg cylinder, human and porcine embryos have a planar morphology [21], and where human and murine embryos show invasive implantation at the blastocyst stage, porcine embryos have a loose diffuse non-invasive placenta [22]. There are also some clear differences between preimplantation embryos at the molecular level. Human embryos differ in surface specific antigens expression compared to mouse [23], and in pigs, expression of the pluripotency marker *OCT4* is, contrarily to human and mouse, not restricted to the inner cell mass [24]. These clear differences in mammalian early embryonic development could also have an effect on the validity of reference genes between species. Such species dependency of good reference genes has lately been demonstrated in differentiating mouse and human embryonic stem cells, cells that are closely related to preimplantation embryos [25]. To validate candidate reference genes in a non-mouse model, the potential of seven genes to be used as internal controls during early porcine embryonic development was investigated, using three separate pools of developmental stages ranging from germinal vesicle stage oocytes to blastocyst stage embryos.

Results

RT-PCR

For each developmental stage, porcine oocytes and embryos with good morphology [26] were collected from three independent *in vitro* cultures (Fig. 1), and RNA was isolated separately from these biological replicates . β-2-microglobulin (*B2M*), beta-actin (*BACT*), glyceraldehyde-3-phosphate dehydrogenase (*GAPDH*), histone 2α (*H2A*), phosphoglycerate kinase 1 (*PGK1*), 18S ribosomal RNA (*S18*), and ubiquitin (*UBC*) were chosen as candidate reference genes and used for RT-PCR on oocytes. These genes are regularly used to normalise mRNA transcript levels and at least five of the genes have previously been used as reference genes in early development (*BACT* [27], *GAPDH* [28], *H2A* [29], *S18* and *UBC* [30]). Amplicons were of the expected sizes (Figure 2) and their specificity was confirmed by sequence analysis (data not shown). Optimal annealing temperature was determined using a temperature gradient ranging from 50 to 65 ºC (Table 1). For each biological replicate, three technical replicates were run in all qRT-PCR experiments, and all samples for one gene product were run on one 96-well plate to minimize inter-experimental variation. Dilution curves of all candidate reference genes showed an average amplification ef-

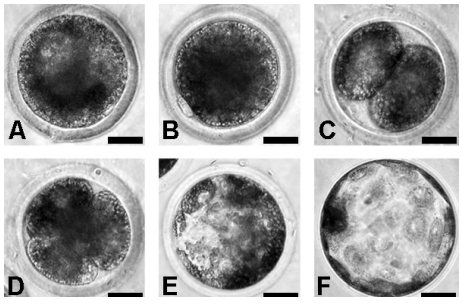

Figure 1: Representative pictures of porcine oocytes and embryos collected for qRT-PCR.
(A) Germinal vesicle stage, (B) metaphase-2 stage, (C) 2-cell stage, (D) 4-cell stage, (E) early (cavitating) blastocyst, (F) expanded blastocyst. Scale bar = 50μm.

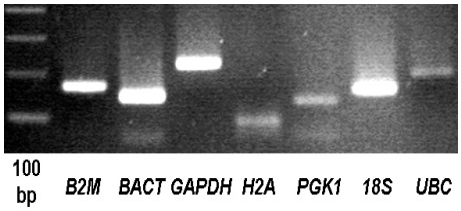

Figure 2: PCR results of candidate reference genes.
Amplicons were of the expected sizes (*B2M* 166 bp, *BACT* 141 bp, *GAPDH* 219 bp, *H2A* 83 bp, *PGK1* 126 bp, *S18* 149 bp, *UBC* 186 bp). 100 bp = 100 base pair ladder.

ficiency of 100.2% (min. 86%, max 113.3%) and an average coefficient of determination (R^2) of 0.992. Single distinctive peaks in the melt curves confirmed specific amplification of the gene of interest. All reference genes were consistently detected in all samples except one metaphase-2 sample, which was excluded from further analysis. This reliable detection indicates integrity of the cDNA samples. Starting quantities were based on the gene specific standard curves and calculated with MyIQ software. The –RT levels of *B2M*, *BACT*, *GAPDH,* and *PGK1*, were below detectable levels. *S18* was detected at an average level of 0.05% in –RT samples, *UBC* was detected at an average of 0.007% and *H2A* was detected at an average of 1.27% compared to their RT counterparts. The –RT values were subtracted from their RT counterparts.

GeNorm analysis

Several statistical tools are available to identify stably expressed genes, but since studies have not found large differences between statistical tools such as geNorm, NormFinder, and Bestkeeper [25,31], only one of these applications was used here to calculate gene expression stability [19]. For each gene, Ct values of unknown samples were transformed into the log of the starting quantities with the formula obtained from the standard curve, thereby taking into account the efficiency of the PCR reaction. Raw starting quantities were analysed with geNorm

Table 1: Primer details used for qRT-PCR

F = forward, R = Reverse, Ta = optimal annealing temperature

Gene	Genbank Accession	Primer Sequences	Ta (ºC)
B2M	NM_213978	F: 5'-TTCACACCGCTCCAGTAG-3' R: 5'-CCAGATACATAGCAGTTCAGG-3'	59.5
BACT	AY550069	F: 5'-CATCACCATCGGCAACGAGC-3' R: 5'-TAGAGGTCCTTGCGGATGTC-3'	55.8
GAPDH	AF017079	F: 5'-TCGGAGTGAACGGATTTG-3' R: 5'-CCTGGAAGATGGTGATGG-3'	51.1
H2A	BX921568	F: 5'-GCTGTTGGGCAAAGTCAC-3' R: 5'-GGCTCTCCGTCTTCTTGG-3'	54.3
PGK1	AY677198	F: 5'-AGATAACGAACAACCAGAGG-3' R: 5'-TGTCAGGCATAGGGATACC-3'	56.4
S18	NR_002170	F: 5'-GGCTACCACATCCAAGGAAG-3' R: 5'-TCCAATGGATCCTCGCGGAA-3'	58.7
UBC	M18159	F: 5'-TTCGTGAAGACCTTGACTG-3' R: 5'-GGACTCCTTCTGGATGTTG-3'	51.1

to determine gene expression stability over the different developmental stages, which resulted in a gene expression stability measure *M* for each gene (Table 2). Stepwise exclusion of unstable genes and subsequent recalculation of the average *M*-values, results in a ranking of the genes based on their *M*-values, with the two most stable genes, with the lowest *M*-values, leading the ranking (Fig. 3)[19]. This stepwise elimination of the least stable genes revealed that *GAPDH*, *PGK1*, *S18,* and *UBC* were the 4 most stable genes.

Table 2: Ranking of genes by expression stability; less stable genes have higher M-values.

Gene	M
1: *GAPDH*	1.278
2: *UBC*	1.300
3: *PGK1*	1.312
4: *S18*	1.352
5: *H2A*	1.650
6: *BACT*	1.912
7: *B2M*	2.540

The geometric mean of the expression levels of the 2 best reference genes, *GAPDH* and *UBC*, was used to calculate normalisation factors. To reveal the optimum number of reference genes, it was determined whether stepwise inclusion of less stable genes significantly affected the normalisation factors. This pair wise variation (*V*) showed that inclusion of a fourth reference gene had a significant effect on the normalisation factors, but including a fifth gene did not improve the normalisation factors (Fig. 4). Therefore, the least stable genes *B2M*, *BACT*, and *H2A* were not very suitable for normalisation. *GAPDH* and *PGK1* play important roles in the glycolytic pathway and are potentially co regulated, but removal of either of these genes from the analysis did not affect the ranking of the genes by stability (Table 3). *In vitro* produced porcine embryos are vulnerable to polyspermy. In this study, the susceptibility to polyspermy was minimized by using sow oocytes instead of those from pre-pubertal gilts, [32,33] and by addition of porcine fol-

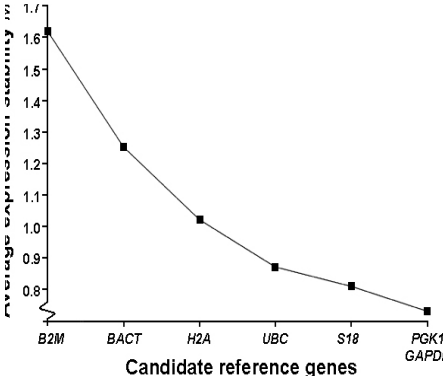

Figure 3: Average expression stability M after stepwise exclusion of the least stable gene.
On the left-most side is the average expression stability M for all genes, with the least stable gene within that group on the x-axis. Exclusion of this gene from the analysis generates the next data point. After stepwise exclusion of the least stable genes, the two best genes, which cannot be further ranked, remain and are depicted on the rightmost side of the graph.

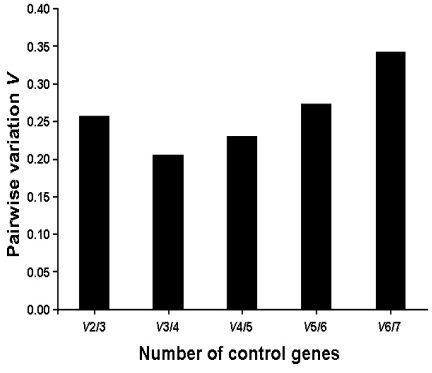

Figure 4: Optimal number of reference genes.
Pair wise variation of normalization factors after successive inclusion of less stable genes determined the optimal number of reference genes. On the left-most side is the pair wise variation when the number of genes is enlarged from 2 to 3 (V2/3). Stepwise inclusion of less stable genes generates the next data points. Inclusion of a 4th gene has a significant effect on the normalization factors. Inclusion of a 5th, 6th, or 7th gene has a negative effect on the pair wise variation value and reflects the average expression stability M of these genes.

Table 3: Ranking of genes by expression stability.

All genes included	Minus *GAPDH*	Minus *PGK1*	Minus *H2A*	Minus Blastocysts
1: *GAPDH*	2: *UBC*	2: *UBC*	1: *GAPDH*	1: *GAPDH*
2: *UBC*	3: *PGK1*	1: *GAPDH*	3: *PGK1*	3: *PGK1*
3: *PGK1*	4: *S18*	4: *S18*	4: *S18*	2: *UBC*
4: *S18*	5: *H2A*	5: *H2A*	2: *UBC*	4: *S18*
5: *H2A*	6: *BACT*	6: *BACT*	6: *BACT*	5: *H2A*
6: *BACT*	7: *B2M*	7: *B2M*	7: *B2M*	7: *B2M*
7: *B2M*	X	X	X	6: *BACT*

In the first column, all genes and developmental stages were included in the analysis, and in the following columns the genes GAPDH, PGK1, or H2A were excluded, and in the last column, blastocyst stage embryos were excluded. The numbers represent ranking position of that gene when all genes are included

licular fluid to the in vitro maturation medium [34]. Exclusion of the transcriptionally active blastocyst stages from the analysis resulted in merely minor influences on gene ranking (Table 3). Therefore, the same panel of reference genes can be used to normalize gene expression from the germinal vesicle stage oocyte to the 4-cell stage embryo, with *GAPDH*, *PGK1*, *UBC*, and S*18* as the best four genes for normalisation, to be preferred over *H2A*, B2M, and *BACT*. Amplification of a large product might influence PCR efficiency and the final ranking of a gene. In this study however, there was not a correlation between product size and *M*-value or between product size and efficiency (Fig. 5), indicating that the ranking of genes by stability was not a methodological artefact. Since the –RT levels for *H2A* were relatively high in some samples, the ranking of reference genes was also calculated when this gene was excluded, but exclusion of this gene left the ranking intact except for *UBC*, which was repositioned from first to fourth in rank (Table 3).

Gene expression patterns

In porcine early developmental stages *B2M*, *BACT*, and *H2A*, were not expressed at consistent levels. The expression pattern of these genes was studied by normalising the qRT-PCR data of these genes with the normalisation factors calculated by geNorm and based on the four most stable genes (Figure 6, top row). *B2M* expression levels in GV, M2, 2-cell, and 4-cell stage embryos were similar. Early blastocysts showed an increase in *B2M* expression, and highest expression levels were seen in expanded blastocysts. *BACT* showed stable expression in the oocyte stages, was downregulated at the 2-cell stage, showed up regulation at the 4-cell stage and was downregulated again in the blastocyst stages. *H2A* expression was upregulated in the M2 stage compared to the GV stage. The M2 and the 2-cell stage showed similar levels of *H2A* expression, and at the 4-cell stage, *H2A* expression was downregulated. Early blastocysts showed increased expression and expression was highest in expanded blastocyst stage embryos. Expression patterns of stably expressed genes are also presented (Figure 6, bottom row).

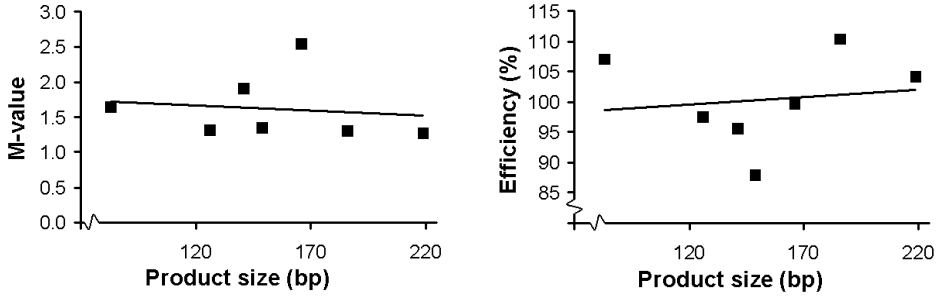

Figure 5: No correlation was found between product size and M-value or between product size and amplification efficiencies of the PCR-reactions; left: Product size is plotted against the stability factor M. M-values of the genes are not correlated to the product size of the PCR reactions (R2 = 0.0196). **right:** Product size is plotted against efficiency of the PCR reaction as an the average of the plus RT and the minus RT run. Average efficiencies are not correlated to the product size (R2 = 0.0199).

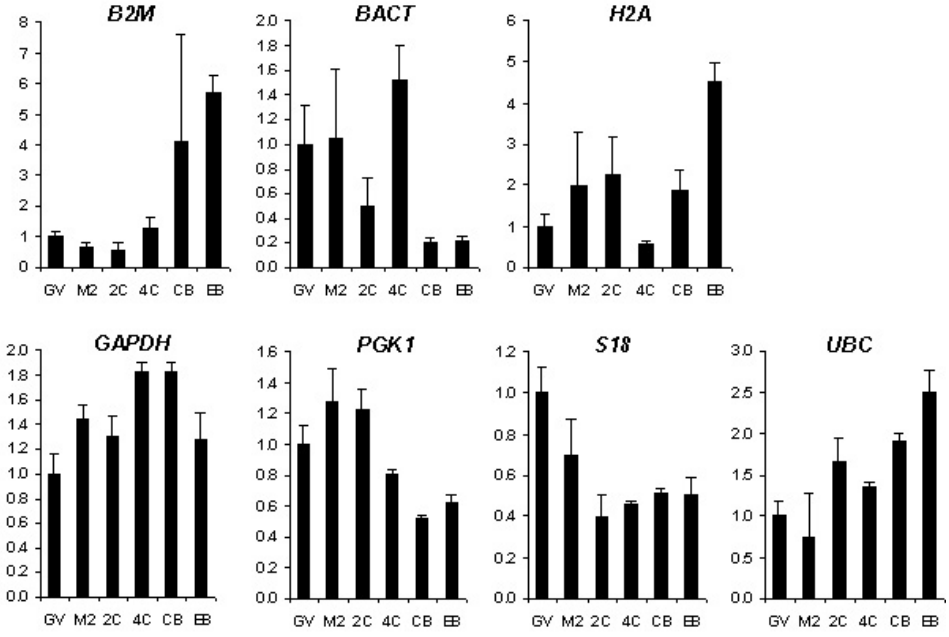

Figure 6: Relative expression of BACT, H2A, B2M, GAPDH, PGK1, S18, and UBC at different stages of porcine embryonic development; Top row: regulated genes; bottom row: stably expressed genes; X-axis: developmental stage (GV = germinal vesicle stage, M2 = metaphase-2 stage, 2C = 2-cell stage, 4C = 4-cell stage, CB = early cavitating blastocyst, EB = expanded blastocyst). Y-axis: normalized relative expression. Data was normalized to the geometric mean of 4 stably expressed genes (18S, PGK1, GAPDH, UBC) as determined by geNorm analysis. For each developmental stage, the normalized expression value was subsequently divided by the normalized expression value of the germinal vesicle stage. Error bars represent SEM.

Discussion

Gene expression studies often rely on an internal standard that shows stable expression in the cell types or tissues examined, independent of the differentiation or biological state of the cell. Identifying a good reference gene in preimplantation embryonic development is however hindered by significant fluctuations in the transcriptomes. Moreover, within mammals there is clear morphological and molecular biological variation between embryos of different species such as mouse, pig and human. In the present study, the usefulness of genes as reference genes in early porcine development was tested. *GAPDH* and *PGK1* were identified as the genes with the most stable expression, followed by *S18* and *UBC*, whereas *B2M*, *BACT*, and *H2A* demonstrated to be inferior reference genes in this non-mouse model. *In vitro* produced porcine embryos are susceptible to polyspermy. In this study, sow oocytes were used instead of those from pre-pubertal gilts, in order to minimize the generation of polyspermic embryos [32,33]. Moreover, exclusion of the transcriptionally active blastocyst stages from the analysis resulted in merely minor influences on gene ranking. There was not a correlation between product size and *M*-value, or between product size and PCR efficiency, indicating that the ranking of genes by expression stability is not a methodological artefact, as described previously for amplicons below 200 base pairs [35].

Several studies have attempted to identify good reference genes in mammalian oocytes and preimplantation embryos [36-39]. Goossens et al. used geNorm to test reference genes in bovine preimplantation embryos, but unfortunately this study excludes oocytes and starts the developmental range from the 2-cell stage onwards [36]. Other studies have included oocytes in their ranges of developmental stages, and in those studies, the approaches were highly similar in that the numbers of oocytes/embryos were kept equal in RNA isolations. The RNA was subsequently used as a template for cDNA synthesis, and a fixed volume of cDNA was used in each PCR reaction. The best reference genes were considered those genes that showed least variation between developmental stages [37-39]. However, due to the nature of preimplantation development the quantity of RNA differs between stages. For example, 2-cell stage mouse embryos have less total RNA than germinal vesicle stage oocytes, since ~90% of maternal RNA will be degraded and the embryonic genome is mostly inactive. Genes that show constant expression throughout all stages are genes that somehow escape mRNA degradation from the GV stage to the 2-cell stage and are barely transcribed at later stages. Normalisation with such a gene will result in the absolute value that a gene is up- or downregulated. However, it is unclear whether this up- or downregulation is biologically significant, because the entire transcriptome might show a similar up- or downregulation. Therefore, in this study, appropriate reference genes were defined as those genes that represent the total RNA content, which is in line with methods such as Northern Blotting and RNAse protection assays. This difference in method partly explains the discrepancy in findings between previous studies and the current one. For example, *H2A* has previously been advocated as a good reference gene in bovine and murine preimplantation development, because of its unaffected mRNA levels during preimplantation development [37,38]. In contrast, in this study, the average expression stability *M* of *H2A* was high and this gene was therefore excluded from the set of reference genes on which the normalisation factors were based. Moreover, *GAPDH*, *PGK1*, *S18*, and *UBC* have previously been rejected as good reference genes for the reason that their gene

products show high fluctuations in absolute copy numbers in early development [37-39]. In this study, however, these genes are advocated as reference genes, because their fluctuations reflect the fluctuations in the transcriptomes. With this method, it should be kept in mind that apparent up- or downregulation of a certain gene might be caused by changes in total RNA abundance and not reflect increased or decreased transcription.

The four best candidate reference genes *GAPDH*, *PGK1*, *S18*, and *UBC* were stably expressed in spontaneously differentiating human embryonic stem cells as well. Moreover, these genes showed stable expression in differentiating mouse embryonic stem cells, with the exception of *S18* [25]. Although thorough testing of reference genes in any new experimental set-up is advocated, it is not unlikely that these genes can also be used to normalise gene expression data of preimplantation embryos and embryonic stem cells, enabling a comparison between these two closely related systems. In mouse peri-implantation embryos ranging from 3.5 days post coitum (dpc) blastocysts to 9.5 dpc neurulating embryos *GAPDH*, *PGK1*, and *S18* show unstable expression [25], which is an indication that these genes should not be used to study post-implantation development.

By pair wise variation the optimal number of reference genes was determined at four. Therefore, normalisation factors were derived from the best four reference genes and these factors were subsequently used to calculate the gene expression patterns of regulated genes. *B2M* plays a role in expression of MHC class I antigen on cells. *B2M* showed increased expression in blastocyst stages, which is consistent with the role that *B2M* has in the proper expression of blastocyst Major Histocompatibility Complex, to protect fetal trophoblast cells from maternal NK cells [40]. Expression of *BACT*, a major component of microfilaments of the cytoskeleton of eukaryotic cells, was downregulated at 2-cell stage embryos compared to the oocyte stages, indicating that *BACT* mRNA is actively degraded or translated between these stages. *BACT* mRNA peaked at the 4-cell stage, which coincides with the porcine embryonic genome activation and might reflect the cytoskeletal changes when embryos switch from cleavage divisions to cell proliferation in later stages. *H2A* is one of the 5 main histone proteins, which are involved in the structure of chromatin. Chromatin structure has an important role in epigenetic gene regulation and is probably involved in coordinating gene activity in early embryonic stages [41]. *H2A* expression increased in expanded blastocyst stages, which suggests changes in chromatin structure and possibly nuclear reprogramming at that stage of development. In summary, mRNA abundance of *B2M*, *BACT*, and *H2A* showed distinct temporal regulation from oocyte maturation to early embryo development.

Analysis of transcription profiles of 7 candidate reference genes in early porcine embryonic development revealed that *GAPDH*, *PGK1*, *S18*, and *UBC* showed stable expression and can therefore be used as reference genes. Since *GAPDH* and *PGK1* both have roles in glycolysis, it is advised not to use both genes for normalisation, unless independent stability of these genes is made clear. Therefore, a selection of either *GAPDH* or *PGK1* together with *S18* and *UBC* is proposed. To our knowledge, this is the first evaluation of reference genes that reflect total RNA content in early mammalian embryonic development from oocyte to blastocyst.

Materials and Methods

Oocyte maturation, IVF, embryo culture

All incubations described below took place in a humidified atmosphere of 38.5ºC and 5% CO_2. Recovery, *in vitro* maturation and fertilization of porcine oocytes and subsequent *in vitro* culture of porcine embryos proceeded as previously described [42]. In short, sow ovaries were collected from a regional slaughterhouse and cumulus oocyte complexes (COCs) were aspirated from antral follicles of 2-6 mm. Oocytes of equal size and three or more layers of compact cumulus were selected and transferred to maturation medium, containing NCSU-23 medium [43], supplemented with 10% porcine follicular fluid, 0.57 mM cysteine, 25 mM β-mercaptoethanol, 10 IU/ml eCG (Chorulon, Intervet, Boxmeer, the Netherlands) and 10 IU/ml hCG (Folligonan, Intervet). After 24 hr culture, the COCs were transferred to maturation medium excluding eCG and hCG and cultured for an additional 18 hr. After culture, COCs were denuded and transferred to Tris-buffered IVF-medium, containing 113.1 mM NaCl, 3 mM KCl, 20 mM Tris, 11 mM D-glucose, 1 mM caffeine, 5 mM sodium pyruvate, 7.5 mM $CaCl_2$, 0.1% (w/v) bovine serum albumine (BSA; Sigma-Aldrich Chemie, Zwijndrecht, the Netherlands) and 1% pen/strep. IVF was performed with fresh semen from two randomly selected boars at a concentration of 1000 cells/oocyte. Next day, the presumptive zygotes were cultured in IVC medium, which contained NCSU-23 and 0.4% BSA.

RNA extraction and reverse transcription

Total RNA was isolated from denuded germinal vesicle stage oocytes, denuded metaphase 2 stage oocytes (as confirmed by the presence of one polar body), 2-cell stage embryos, 4-cell stage embryos, early blastocysts and expanded blastocysts, using the RNeasy minikit (Qiagen, Venlo, the Netherlands). RNA yield is lower in oocytes and cleavage stage embryos compared to blastocyst stage embryos and therefore, 40 oocytes/embryos per sample were collected for the early stages and 10 blastocysts were pooled for every sample. First-strand cDNA was synthesised with Superscript II (Invitrogen, Groningen, the Netherlands) and random primers were used to prime reverse transcription of RNA. As negative controls, mixtures were prepared without reverse transcriptase. Reaction mixtures with samples were incubated for 1 hr at 42ºC and subsequently for 5 min at 80ºC, chilled on ice and stored at -20ºC.

Quantitative RT-PCR

Preceding qRT-PCR amplification, primers were designed using Primer Select software (DNAstar, Madison, WI, USA) and Beacon Designer 4 (PREMIER Biosoft International, Palo Alto, CA, USA)(Table 1). Primers were tested on cDNA of *in vitro* produced embryos. The amplicons were run on a 2% agarose gel and products were sequenced to test the specificity of the primers. Subsequent PCR was performed in a Bio-Rad iCycler (Bio-Rad, Veenendaal, the Netherlands). Gene transcripts were quantified using iQ SYBR Green supermix (Bio-Rad). The optimal annealing temperature of the primers was tested experimentally with a temperature gradient. A separate reaction was run for each gene and a standard curve of tenfold dilution ranging from 10pg to 1ag supplemented each run. All points of the standard curve and all samples were run in triplets as technical replicates. In each run 1 µl of cDNA was used as template for amplification per reaction. The sample was added to 24 µl of reaction mixture, containing 12.5 µl H_2O, 11.25 µl iQ SYBR Green supermix (Bio-Rad), and 0.5mM of both forward and reverse primers (Isogen, Maarssen, the Netherlands). The thermal cycling profile started with a 3-min dwell temperature of 94ºC, followed by 40 cycles of 30 sec at 94ºC, 30 sec at the primer specific annealing temperature, 30 sec at 72ºC, and a final step at which fluorescence was acquired. After 40 cycles, the program continued with a post-dwell of 1 min at 94ºC. Finally, a melt curve was generated by temperature increments of 0.1ºC starting from 65 to 100ºC, with fluorescence acquisition after each step. Data was analysed with My-IQ software (Bio-Rad), which for all samples calculated the starting quantities of all candidate reference genes, based on the standard curves for these genes.

Chapter III

Differences in early lineage segregation between mammals

Ewart W. Kuijk[1], Leonie du Puy[1,2], Helena T.A. van Tol[1], Christine H.Y. Oei[1], Henk P. Haagsman[2], Ben Colenbrander[1], Bernard A.J. Roelen[1]

[1]Department of Farm Animal Health, [2]Department of Infectious Diseases and Immunology, Faculty of Veterinary Medicine, Utrecht University, The Netherlands

Adapted from *Developmental Dynamics* 2008, 237: 918-927.

Differences in early lineage segregation between mammals

Abstract

Two lineage segregation events in mammalian development form the trophectoderm, primitive endoderm, and pluripotent primitive ectoderm. In mouse embryos, *Oct4*, *Cdx2*, *Nanog*, and *Gata6* govern these events, but it is unknown whether this is conserved between mammals. Here, the expression patterns of these genes and their products were determined in porcine oocytes and embryos and in bovine embryos. *CDX2* and *GATA6* expression in porcine and bovine blastocysts resembled that of mouse indicating conserved functions. However, *NANOG* expression was undetectable in porcine oocytes and embryos. Some inner cell mass cells in bovine blastocysts expressed NANOG protein. OCT4 protein was undetectable in porcine morulae, but present in both the trophectoderm and the inner cell mass of blastocysts, suggesting that downregulation of OCT4 in the trophectoderm does not precede trophectoderm formation. Combined, the results indicate differences in lineage segregation between mammals.

Background

In the mouse, there is considerable knowledge on the molecular mechanisms of early development, with the transcription factors *Oct4*, *Cdx2*, *Nanog* and *Gata6* as key players. Two successive differentiation events in early embryonic development result in the segregation of three committed lineages that together form the blastocyst. The first segregation occurs at the compacted morula stage with the outer layer of cells forming the epithelial trophectoderm (TE), which becomes the embryonic part of the placenta, and the inner layer of cells forming the inner cell mass (ICM), which produces embryonic cells and the extra-embryonic mesoderm and primitive endoderm. Embryos that lack *Oct4* fail to form an ICM that can differentiate along embryonic lineages and cells are restricted to differentiation along the extraembryonic trophoblast lineage [13], whereas embryos that lack *Cdx2* are unable to maintain the TE lineage [17]. Furthermore, *Oct4* and *Cdx2* mutually inhibit each other's expression and both transcription factors are detected in all nuclei of 8-cell stage embryos [20]. These findings have resulted in a model in which mutual repression of these transcription factors in early morulae results in *Cdx2* expressing- and *Oct4* expressing- cells, with loss of *Cdx2* expression in the ICM as primary event, and with segregation of the inner cell mass and trophectoderm lineages as a consequence [17, 20, 21].

The second segregation of lineages divides the inner cell mass into the primitive ectoderm, which gives rise to the embryo proper and the primitive endoderm (PE) that forms the extra-embryonic endoderm layer of the visceral yolk sac and in rodents also the parietal endoderm. Before the PE is formed, its precursors can already be detected by expression of Nanog and Gata6, which shows a so-called ´pepper-and-salt' distribution, with Nanog positive cells destined to become epiblast and Gata6 positive cells destined to become PE [30]. The mosaic distribution of these precursors is considered to depend on Grb2-Ras-MAP kinase signaling, because inactivation of *Grb2* results in *Nanog* expression in all cells of the ICM and loss of

Gata6 expression [30]. Embryonic stem (ES) cells in which *Gata6* or a close family member *Gata4* are over-expressed develop into PE cells [22], whereas ES cells that lack *Gata6* or *Gata4* fail to develop visceral endoderm in *in vitro* differentiation experiments such as embryoid body cultures [23, 66]. Mouse embryos that lack *Nanog* develop TE and PE, but fail to form an epiblast and loss of *Nanog* in ES cells results in extra-embryonic endoderm-like cells [26]. As a consequence, the murine epiblast is defined by two segregation events that depend on expression of respectively *Oct4* and *Nanog*, whereas *Cdx2* specifies the trophectoderm, and *Gata6* the primitive endoderm.

Stem cells can be derived from all three lineages [21]. Only ES cells derived from the ICM of blastocysts that express *Oct4* [14] and *Nanog* [25] are pluripotent, which means they have the potential to become any specialized cell of all three embryonic germ layers even after prolonged culture. Therefore, these cells are important for differentiation studies and future regenerative medicine [1]. Thus the mechanism of early lineage segregation also defines the pluripotent cell population in blastocysts.

Recently, it was demonstrated that fibroblasts can be reprogrammed to a pluripotent state by retroviral induction of just four factors, that is *Oct4*, *c-Myc*, *Klf4*, and *Sox2* [67]. If these cells were selected for expression of *Nanog*, these induced pluripotent stem cells could colonize the germline, thereby unraveling an important part of the mechanism behind pluripotency [68, 69]. Still, the efficiency of reprogramming was rather low and it is unclear why only some cells were reprogrammed to the pluripotent state. Interestingly, an oocyte has the same capacity to reprogram differentiated cells to the pluripotent state, as made evident by cloning through somatic cell nuclear transfer [70]. Therefore, it is important to study the dynamics of oocyte and early embryo development, to increase our knowledge on processes that contribute to pluripotency of cells.

Preimplantation development in mammals shows remarkable differences between species, possibly influencing the mechanism responsible for the formation of a pluripotent cell population. For instance, mouse embryos form an egg cylinder after implantation, whereas human, bovine, and porcine embryos have a planar morphology [35]. Furthermore, mouse and human embryos invasively implant at the blastocyst stage, which results in a haemochorial placenta. However, porcine and bovine blastocysts elongate before implantation, transforming from a sphere of a few mm diameter to a long thin filament that in pigs can reach up to 100 cm in length at the time of implantation. This results in a loose diffuse non-invasive epitheliochorial placenta [36]. Moreover, *OCT4* expression in bovine and porcine embryos is not limited to the ICM [37, 38], which suggests a difference in mechanism of the earliest lineage segregation between species. As a consequence, species differ in the factors that contribute to the establishment of the pluripotent cell population in embryos, which could explain why ES cell lines from species such as cow and pig have not been established yet [10]. Therefore, a better understanding of the mechanisms underlying pluripotency in these species is needed [71]. In order to obtain more insight in early lineage segregation events and the establishment of the pluripotent cell population in these species, the expression patterns of *NANOG*, *OCT4*, *CDX2*, *GATA4*, and *GATA6* were studied during early porcine and bovine embryonic development. The expression patterns of porcine and bovine orthologs of key genes in lineage segregation indicate diversity in early lineage segregation between mammals.

Results

Gene expression patterns

Porcine oocytes and embryos with good morphology [72], ranging from germinal vesicle stage oocytes to blastocysts, were collected from three independent porcine *in vitro* cultures. These samples were used to study gene expression patterns using quantitative RT-PCR (QPCR) of genes important for pluripotency (*NANOG* and *OCT4*), for the development of the TE (*CDX2*), and for the development of the primitive endoderm (*GATA4* and *GATA6*). PCR products were of the anticipated sizes (Fig. 1) and sequenceanalysis confirmed amplification of the desired product (data not shown).

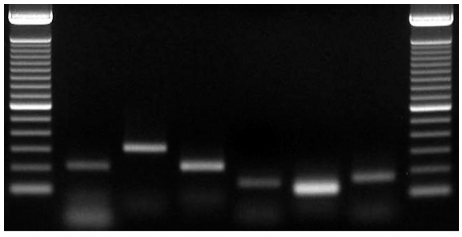

Figure 1: PCR results on cDNA of porcine oocytes and embryos of genes that were used in the QPCR study. Genomic DNA served as template for Nanog primers. Amplicons were of the expected sizes (see also Table 1). *GATA6* product is not shown, because the primers have been described previously by Gillio-Meina *et al.* [91]. 100 bp = 100 base pair ladder.

In the case of *NANOG*, genomic DNA served as a positive control. All samples, except for one 4-cell stage embryo, showed very late threshold cycles, which indicates low starting quantities. In 9 samples, expression levels did not exceed background levels from their corresponding –RTs, which surprisingly included all expanded blastocysts. This suggests that *NANOG* does not play an important role in porcine embryos at this time of development. Therefore, *NANOG* was excluded from the quantitative PCR analysis. For all other genes, expression levels were normalized to the geometric mean of *GAPDH*, *PGK1*, *S18*, and *UBC*. These reference genes allow direct comparison of gene expression levels in early porcine developmental stages ranging from oocytes to blastocysts [73]

OCT4 expression showed a 5-fold up-regulation from the germinal vesicle (GV) stage to the metaphase 2 (M2) stage (Fig. 2), indicating that *OCT4* could be involved in oocyte maturation. At the 2-cell stage *OCT4* expression had dropped drastically and at the 4-cell stage *OCT4* expression was restored to GV stage levels. *OCT4* expression was significantly higher in blastocysts than in cleavage stage embryos, which indicates a more prominent role for *OCT4* at these stages. *CDX2* expression was upregulated more than 10-fold in blastocysts when compared with GV stage oocytes.

Of those genes that in mouse embryos are important for PE formation, *GATA4* expression showed a 4-fold higher expression in M2 stage oocytes than in GV stage oocytes, which suggests that *GATA4* plays a role in oocyte maturation. Blastocysts showed significantly less *GATA4* expression than cleavage stage embryos. *GATA6* expression was more than 20-fold upregulated in blastocysts when compared with 4-cell embryos and expression of this gene was significantly higher in blastocysts than at earlier stages.

Additionally, the expression pattern of *UTF1*, which is a protein correlated with pluripotency in mouse embryos [74, 75] and the expression pattern of *CK18*, an intermediate filament protein highly expressed in blastocysts [76, 77], were investigated by QPCR in porcine oocytes and embryos (Fig. 2). *UTF1* expression was comparatively low in both oocytes and

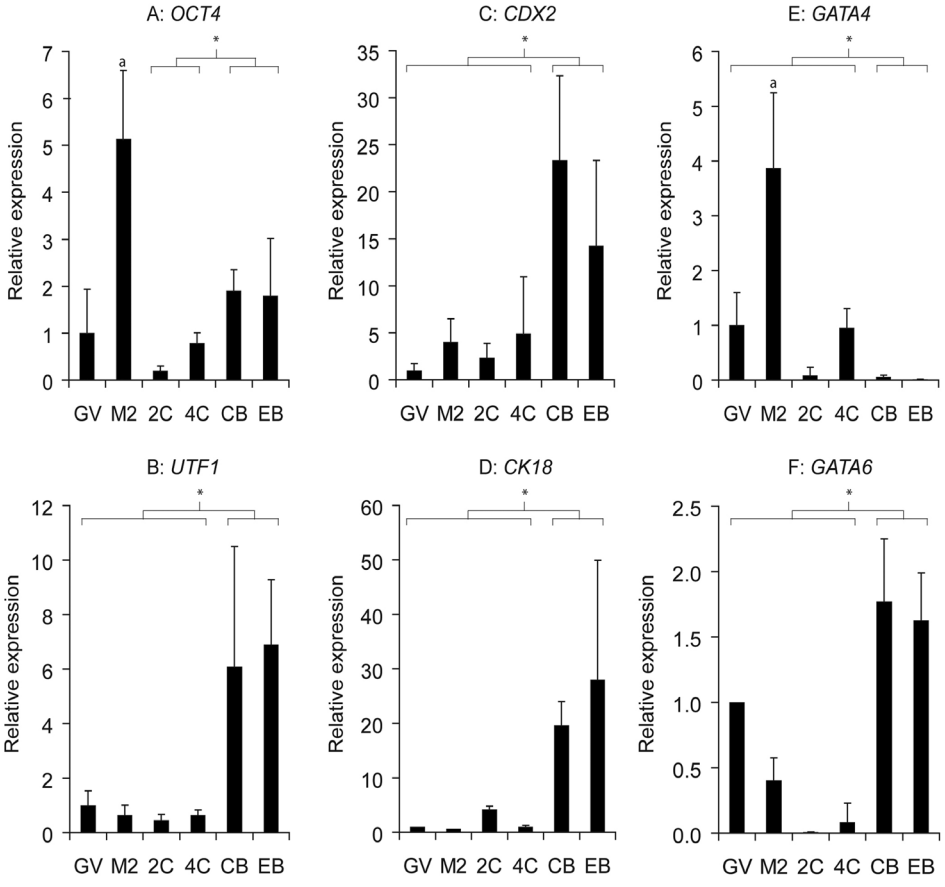

Figure 2: Relative expression of genes specific for the ICM, TE, or PE in porcine oocytes and preimplantation embryos.
X-axis: developmental stage (GV = germinal vesicle stage, M2 = metaphase-2 stage, 2C = 2-cell stage, 4C = 4-cell stage, CB = early cavitating blastocyst, EB = expanded blastocyst). Y-axis: normalized relative expression. For each developmental stage, the normalized expression value was divided by the normalized expression value of the germinal vesicle stage. Asterisks denote significant differences between the stages that are within the brackets. **a** denotes significant differences between GV stage and M2 stage oocytes. Error bars represent standard deviation.

cleavage stages and was significantly higher in both blastocyst stages, with more than six-fold up-regulation compared to GV stage oocytes (Fig. 2). This induction in expression correlates with previously observed specific expression of *UTF1* in cells of the ICM of mouse blastocysts [74]. The expression of *CK18* showed more than 10-fold higher expression in blastocyst stage embryos.

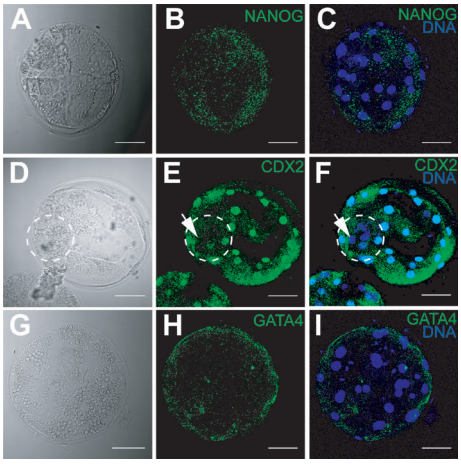

Figure 3: Immunofluorescence results on *in vitro* produced porcine blastocysts.
(A-C) embryo, NANOG stain, and overlay of NANOG with DNA stain respectively; (D-F) embryo, CDX2 stain, and overlay of CDX2 with DNA stain respectively. Dashed line denotes ICM. Arrow = CDX2 negative ICM cell; (G-I) embryo, GATA4 stain, and overlay of GATA4 with DNA stain respectively. Scale bar = 50μm.

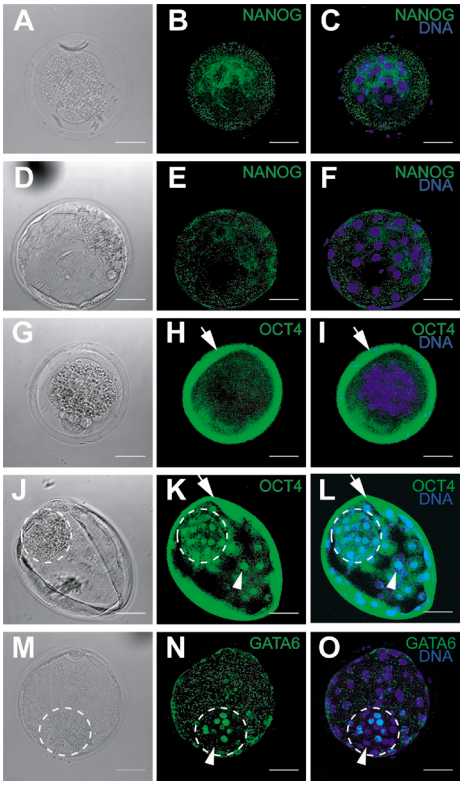

Figure 4: Immunofluorescence results on *in vivo* produced porcine morulae and blastocysts.
(A-C) morula, NANOG stain, and overlay of NANOG with DNA stain respectively; (D-F) blastocyst, NANOG stain, and overlay of NANOG with DNA stain respectively; (G-I) morula, OCT4 stain, and overlay of OCT4 with DNA stain respectively. Arrow denotes aspecific binding of antibody to zona pelucida; (J-L) blastocyst, OCT4 stain, and overlay of OCT4 with DNA stain respectively. Arrow denotes aspecific binding of antibody to zona pelucida. Arrowhead denotes OCT4 positive TE cell; (M-O) blastocyst, GATA6 stain, and overlay of GATA6 with DNA stain respectively. Dashed line denotes ICM. Arrowhead = GATA6 negative ICM cell. Scale bar = 50μm.

Whole Mount Immunofluorescence

Porcine embryos: *In vitro* and *in vivo* produced porcine embryos were used in immunofluorescence studies to examine the expression and localization of factors associated with lineage segregation. Of those proteins that are involved in formation of pluripotent primitive ectoderm cells in the mouse, NANOG was neither detectable in *in vitro* produced porcine blastocysts (Fig. 3), nor in *in vivo* produced morulae and blastocysts (Fig. 4). This is compatible with the QPCR data and suggests a lack of NANOG contribution to lineage segregation processes at these stages. In concordance with previous findings [37] and in line with the gene expression levels, OCT4 was expressed in all cells of *in vitro* (Fig. 5) and *in vivo* produced blastocysts, whereas *in vivo* produced morulae lacked OCT4 expression (Fig. 4).

Expression of CDX2, a transcription factor involved in the development of murine TE, was also restricted to TE cells of *in vitro* produced porcine embryos, which is in agreement with its mRNA levels and suggests that CDX2 contributes to the formation of porcine TE.

Of those proteins that are associated with mouse PE, GATA4 was not detected in *in vitro*

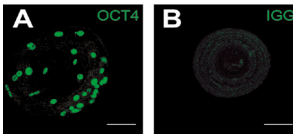

Fig. 5: Immuno-fluorescence results on *in vitro* produced porcine blastocysts; (A) OCT4 stain; (B) Mouse IgG isotype control (MIGG). Scale bar = 50µm.

produced porcine blastocysts, whereas sections of paraffin embedded testicular tissue, which served as a positive control, showed positive staining for GATA4 in Sertoli cells (Fig. 6)[78]. This is in line with its mRNA expression and suggests *GATA4* is not involved in PE formation in pigs. In contrast to mRNA expression levels, GATA6 protein could not be detected in *in vitro*-produced blastocysts (data not shown), which suggests that transcripts are not translated yet. On the other hand, some cells of the ICM of *in vivo* produced blastocysts expressed GATA6 (Fig. 4), what indicates that this factor is involved in establishing porcine PE. All signals were detected above background levels of isotype controls (Fig. 6).

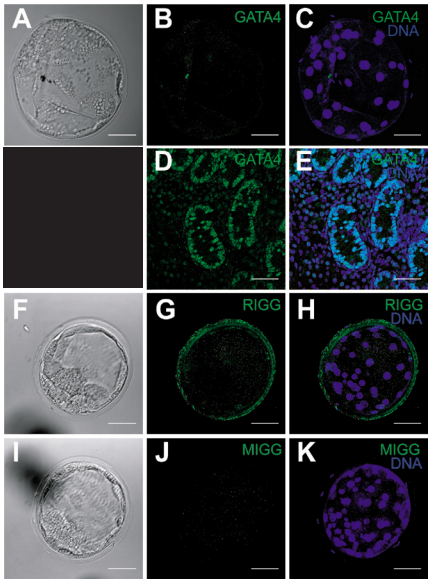

Figure 6: Immunofluorescence results on porcine blastocysts and paraffin embedded testicular tissue. (A-C) blastocyst, GATA4 stain, and overlay of GATA4 with DNA stain respectively. Embryos were processed according to the paraffin embedded tissue protocol; (D-E) GATA4 stain, and overlay of GATA4 with DNA stain respectively on paraffin embedded testicular tissue. (F-H) Blastocyst, rabbit IgG isotype control (RIGG), and overlay of rabbit IgG isotype control with DNA stain respectively. (I-K) Blastocyst, mouse IgG isotype control (MIGG), and overlay of mouse IgG isotype control with DNA stain respectively. Scale bar = 50µm.

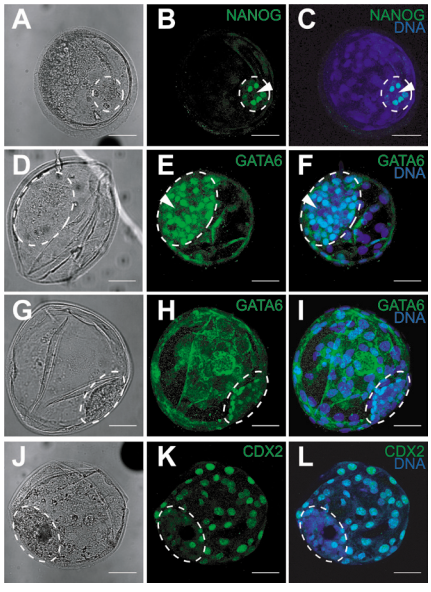

Figure 7: Immunofluorescence results on *in vitro* produced bovine blastocysts.
(A-C) blastocyst, NANOG stain, and overlay of NANOG with DNA stain respectively; dashed line denotes ICM. Arrowhead denotes NANOG negative ICM cell (D-F) blastocyst, GATA6 stain, and overlay of GATA6 with DNA stain respectively; dashed line denotes ICM. Arrowhead denotes GATA6 negative ICM cell; (G-I) blastocyst, GATA6 stain, and overlay of GATA6 with DNA stain respectively; dashed line denotes ICM with GATA6 positive cells aligning the ICM; (J-L) blastocyst, CDX2 stain, and overlay of CDX2 with DNA stain respectively. Dashed line denotes CDX2 negative ICM. Scale bar = 50µm.

Bovine embryos: In order to determine whether the expression patterns of key players in murine early lineage segregation behave differently in other mammals, the spatial expression of these proteins was also studied in blastocysts of another ungulate species, the cow. As in mouse embryos but contrary to pig embryos, several cells of the ICM of *in vitro* produced bovine blastocysts were positive for NANOG expression, while others were negative (Fig. 7), which indicates NANOG is expressed in cells of the ICM that will contribute to the primitive ectoderm. CDX2 was detected in TE cells of bovine blastocysts, but it was not detected in cells of the ICM, which suggests a role of this factor in the formation of the bovine TE. Also in line with mouse development, GATA6 displayed a mottled expression pattern in the ICM of bovine blastocysts (Fig. 7). Occasionally, GATA6 positive cells aligned the ICM in a PE like fashion (Fig. 7). This suggests a role for GATA6 in PE development in cows. All signals were detected above background levels of isotype controls (Fig. 8).

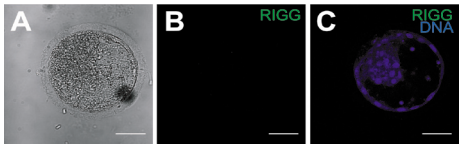

Figure 8: Immunofluorescence results on bovine blastocysts; (A-C) blastocyst, rabbit IgG isotype control (RIGG), and overlay of rabbit IgG isotype control with DNA stain respectively. Scale bar = 50μm.

Discussion

Most of our molecular knowledge on early embryonic development comes from studies on mouse embryos and ES cells. These studies have resulted in a model for the first two differentiation events: firstly, segregation of the TE from the ICM as a consequence of reciprocal inhibition of *Oct4* and *Cdx2* [17, 20, 21] and secondly, *Grb2* mediated mosaic expression of *Nanog* and *Gata6* in the ICM which causes subsequent segregation of the primitive ectoderm from the primitive endoderm [30]. These events define the embryonic pluripotent cell population that in the case of mouse [79] and human [1] can be isolated and cultured without loss of pluripotency. A somatic cell that is not pluripotent, but can obtain such a trait by transfer of its nucleus into an enucleated oocyte by which the genome is reprogrammed to a pluripotent state [70]. Knowledge on oocytes and early lineage segregation events will help to resolve the mechanism of pluripotency. Embryonic differences between mammals indicate that the pluripotent cell population is established differentially between species. For example, expression of OCT4 in TE of pigs and cows demonstrates that this factor is not involved in the segregation of TE and ICM in these species [37, 38].

In vitro fertilized oocytes are susceptible to polyspermy leading to abnormal embryo formation. In this study, sow oocytes were used instead of those from pre-pubertal gilts, in order to minimize the occurrence of polyspermy [80, 81]. Of those factors that play a part in formation of the primitive ectoderm, *NANOG* mRNA levels did not exceed background levels in *in vitro*-produced porcine embryos. In support of the mRNA expression levels in the current study, NANOG protein was also not detected in *in vitro*- and *in vivo*-produced porcine embryos, even though the antibody used in this study was able to detect porcine NANOG protein in gonocytes of neonatal pig testis (data not shown). Some cells of the ICM of bovine blastocysts expressed NANOG. A recent study described detection of NANOG mRNA in isolated ICM from *in vivo*-derived day 8 pig embryos [71]. However, the author's used RNA

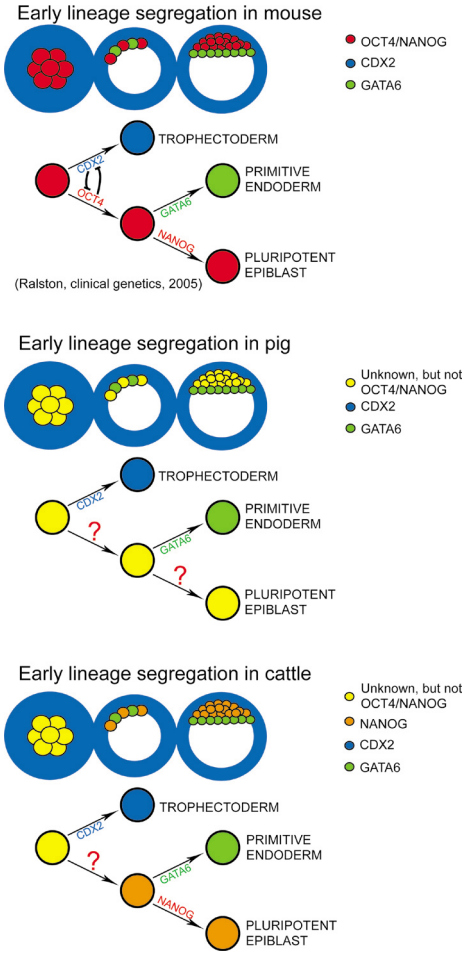

Figure 5: Early lineage segregation in mouse, pig, and cattle; See text for details.

amplification and the relative quantity was significantly less than in isolated ICMs after 24 hrs of culture [71]. In another study, low levels of *NANOG* mRNA have been detected in *in vitro*-produced porcine embryos, whereas *in vivo*-produced embryos and embryos produced by nuclear transfer showed higher expression levels [82]. However, in the same study, NANOG mRNA levels in *in vivo*-derived blastocysts were approximately equal to *in vivo* derived 4 cell stage embryos. Moreover, differences in mRNA levels were less than 2-fold between all in vivo derived stages, which included 4-cell stage embryos, 8-cell stage embryos, morulae, and blastocysts. These observations, in combination with those from the present study, do not support a large role for *NANOG* in early lineage segregation events or in defining the pluripotent cell population in pig embryos. On the other hand, the heterogeneous distribution observed in ICMs of bovine blastocysts, which resembles that of mouse [30], suggests a conserved function of this gene between these species.

From germinal vesicle- to metaphase 2-stage oocytes, *OCT4* showed up regulation, but at the 2-cell stage mRNA levels were reduced again below those of the germinal vesicle stage. *Oct4* is one of the four factors that can reprogram somatic nuclei [67]. Moreover, the peak observed in its expression profile coincides with the stage at which oocytes can reprogram a somatic nucleus [83]. Possibly high levels of OCT4 in metaphase 2-stage oocytes indicate a role for OCT4 in oocyte maturation, preparing the oocyte for totipotency. An alternative explanation could be the building up of maternal mRNA stores. The potential role of OCT4 at these early stages can be studied by interfering with OCT4 expression in oocytes. Do this affect the ability of oocytes to reprogram somatic nuclei and what is the effect on the epigenetic status of the maternal genome?

Porcine blastocysts showed increased mRNA expression of *OCT4* and, in line with previous findings [37], *in vitro*- as well as *in vivo*-produced blastocysts expressed OCT4 protein in nuclei of both the ICM and the TE. Remarkably, and in contrast with mouse embryos [12, 20],

in vivo produced porcine morulae lacked such nuclear OCT4 expression, which is another indication that this protein is not involved in inhibition of TE formation as it is in the mouse [14]. Proliferation of TE stem cells depends on fibroblast growth factor 4 (FGF4) [19], the expression of which is under the control of a complex formed by OCT4 and SOX2, a member of the Sry-related Sox factor family [84]. It has been suggested that for species with an epitheliochorial placenta continued OCT4 expression in TE cells is essential to stimulate FGF4 mediated self-renewal of TS stem cells, which allows elongation and prevents premature differentiation of the trophectoderm [85, 86]. This idea is supported by the finding that OCT4 expression is not restricted to the ICM in caprine embryos [85].

CDX2, which is involved in formation of the mouse TE [17, 20], was expressed at higher levels in porcine blastocysts compared to earlier developmental stages, and congruous with this CDX2 was expressed in TE cells of pig blastocysts as well as bovine blastocysts. Therefore, CDX2 is likely to be involved in the formation of the TE in these species.

Surprisingly, expression of GATA4, important for the formation of the PE in mouse, was significantly reduced in pig blastocysts compared with earlier developmental stages, which suggests that it is not involved in major processes that occur in blastocysts. Indeed, GATA4 protein was not detected in porcine blastocysts. *GATA6* on the other hand, was expressed at significant higher levels in blastocysts. In porcine *in vivo* produced blastocysts and in bovine blastocysts GATA6 was localized to a subset of cells of the ICM. As a consequence, GATA6 is expected to play a role in PE formation in porcine and bovine embryos similar to its function in mouse embryos [30]. Absence of GATA6 in *in vitro* produced porcine embryos could indicate differences in embryos as a result of their origin, but could also be a reflection of differences in developmental age.

UTF1 and *CK18* are specifically expressed in blastocyst stages [74, 76, 77]. These genes served as positive controls for the QPCR and conform the expectations, *UTF1* and *CK18* showed significant increased expression in blastocysts.

In summary, *OCT4* and *NANOG* behave differently in pig embryos (Fig. 9) than in mouse embryos, where these factors play a role in the formation of the pluripotent primitive ectoderm. This makes it unlikely that *OCT4* and *NANOG* are involved in the specification of the primitive ectoderm or defining the pluripotent cell population. In bovine embryos however, the protein NANOG showed a similar random-like distribution in the cells of the ICM as in mouse embryos, which indicates a role for NANOG in the development of the PE in bovine embryos. CDX2 expression in porcine and bovine embryos resembled that of mouse embryos, suggesting a conserved role for CDX2 in the formation of the TE between mammals. A random distribution of GATA6 in porcine and bovine cells of the ICM, comparable to that found in mouse, also implies a conserved function of GATA6 in PE formation in mammalian development. From these experiments it can be concluded that mammals differ in early lineage segregation, which potentially influences the formation and characteristics of the pluripotent cell population. Functional studies such as siRNA-mediated knockdown are needed to further elucidate the roles of factors such as OCT4, NANOG, CDX2, GATA4, and GATA6 in other species than the mouse.

Materials and Methods

Oocyte maturation, IVF, embryo culture, and collection of in vivo *produced embryos*

All incubations described below took place in a humidified atmosphere of 38.5ºC and 5% CO_2, unless noted otherwise. Oocyte retrieval, *in vitro* oocyte maturation, *in vitro* fertilization, and subsequent *in vitro* culture of porcine embryos proceeded as previously described [87]. In short, cumulus oocyte complexes (COCs) were aspirated from 2-6 mm antral follicles of sow ovaries, which were collected at a regional slaughterhouse. Equally sized oocytes with at least three layers of compact cumulus were selected and placed in maturation medium, containing NCSU-23 medium [88], supplemented with 10% porcine follicular fluid, 0.57 mM cysteine, 25 mM β-mercaptoethanol, 10 IU/ml eCG (Chorulon, Intervet, Boxmeer, the Netherlands) and 10 IU/ml hCG (Folligonan, Intervet). After 24 hr culture, the COCs were transferred to hormone free maturation medium and cultured for an additional 18 hr. After culture, denuded oocytes were placed in Tris-buffered IVF-medium, containing 113.1 mM NaCl, 3 mM KCl, 20 mM Tris, 11 mM D-glucose, 1 mM caffeine, 5 mM sodium pyruvate, 7.5 mM $CaCl_2$, 0.1% (w/v) bovine serum albumine (BSA; Sigma-Aldrich Chemie, Zwijndrecht, the Netherlands) and 1% pen/strep. Oocytes were fertilized *in vitro* with fresh semen from two randomly selected boars at a concentration of 1000 cells/oocyte. From one day after IVF onward, presumptive zygotes were cultured in IVC medium, which contained NCSU-23 and 0.4% BSA.

An estrous sow was artificially inseminated 5 days after weaning and sacrificed at day 5 of pregnancy. Subsequently, the genital tract was removed and flushed with PBS to collect *in vivo*-derived embryos. The Institutional Animal Care and Use Committee of Utrecht University approved of this animal experiment.

Bovine embryos were retrieved from *in vitro* cultures, using the following methods. COCs were retrieved from 3 to 8 mm follicles of ovaries that were supplied by a local slaughterhouse. Groups of 35 COCs with an intact cumulus oophorus were incubated in 500 µl M199 (Gibco BRL, Paisley, UK) supplemented with 10% fetal calf serum (Gibco BRL), 0.2 IU/ml bovine FSH (Sioux Biochemical Inc., Sioux Center, IA, USA), 0.2 IU/ml bovine LH (Sioux Biochemical Inc.), 15.42 µg/ml cysteamine (Sigma-Aldrich), and 1% (v/v) penicillin-streptomycin (Gibco-BRL). *In vitro* fertilization was performed 23 hr after oocyte maturation according to the procedure previously described by Parrish et al. [89] with a few modifications [90]. In short, oocytes were transferred to fertilization medium (Fert-Talp) supplemented with 1.8 IU/ml heparin (Sigma-Aldrich), 20 µM d-penicillamine (Sigma-Aldrich), 10 µM hypotaurine (Sigma-Aldrich), and 1 µM epinephrine (Sigma-Aldrich). Frozen-thawed semen from a fertile bull was centrifuged over a Percoll gradient and sperm cells were added to a final concentration of $5x10^5$ spermatozoa/ml. After 20 h of incubation, presumptive zygotes were denuded by vortexing for 3 min and subsequently placed in synthetic oviduct fluid (SOF) medium. Incubation took place at 39ºC in a humidified atmosphere with 7% O_2 and 5% CO_2. On day 5 of embryo culture cleaved embryos were transferred to fresh SOF medium and blastocysts were collected on day 8.

RNA extraction and reverse transcription

Total RNA was isolated from denuded germinal vesicle stage oocytes, denuded metaphase 2 stage oocytes (as confirmed by the presence of one polar body), 2-cell stage embryos, 4-cell stage embryos, early blastocysts and expanded blastocysts, using the RNeasy minikit (Qiagen, Venlo, the Netherlands). RNA yield is higher in blastocyst stage embryos compared to oocytes and cleavage stage embryos and therefore, 40 oocytes/embryos per sample were collected for the early stages and 10 blastocysts were pooled for every sample. Primed with random primers, RNA was reverse transcribed to first-strand cDNA with Superscript II (Invitrogen, Groningen, the Netherlands). For each sample, mixtures were also prepared without reverse transcriptase to serve as negative controls. Synthesis of cDNA was carried out for 1 hr at 42ºC, after which samples were placed at 80ºC for 5 min, chilled on ice, and stored at –20ºC.

Quantitative RT-PCR

Prior to quantitative reverse transcription-polymerase chain reaction (QPCR) amplification, primers were designed using Primer Select software (DNAstar, Madison, WI, USA) and Beacon Designer 4 (PREMIER Biosoft International, Palo Alto, CA, USA) (Table 1). Primers were tested on genomic DNA, cDNA of porcine oocytes, and *in vitro* produced embryos. The amplicons were run on 2% agarose gels and primer specificity was confirmed by sequencing of the products. Subsequent PCR was executed in a Bio-Rad iCycler (Bio-Rad, Veenendaal, the Netherlands). The reaction and quantification of the transcripts was performed with iQ SYBR Green supermix (Bio-Rad). With a temperature gradient, the optimal annealing temperature of each primer pair was determined. Every gene was run separately and a standard curve of tenfold dilutions ranging from 10 pg to 1 ag supplemented each run. Three technical replicates were run of all points of the standard curve and all samples, and 1 µl/ reaction of cDNA was used as template. This sample was added to 24 µl of reaction mixture, containing 12.5 µl H_2O, 11.25 µl iQ SYBR Green supermix (Bio-Rad), and 0.5mM of both forward and reverse primers (Isogen, Maarssen, the Netherlands). The thermal cycling profile started with a 3-min dwell temperature of 94ºC, which was followed by 40 cycles with 4 steps/cycle; 30 sec at 94ºC, 30 sec at the primer specific annealing temperature, 30 sec at 72ºC, and finally a step at which fluorescence was acquired. These cycles were followed by a post-dwell of 1 min at 94ºC and finally, a melt curve was generated by temperature increments of 0.5ºC starting from 65 to 100ºC, with fluorescence acquisition after each step.

Data was analyzed with IQ5 software (Bio-Rad), with which the starting quantities of all candidate genes were calculated, based on their standard curves. QPCR data was normalized to *GAPDH*, *PGK1*, *S18*, and *UBC*, which have been demonstrated as a good set of reference genes for QPCR studies in porcine oocytes and preimplantation embryos [73].

Dilution curves of all candidate reference genes showed an average amplification efficiency of 93.6% ± 10.3 and an average coefficient of determination (R^2) of 0.986 ± 0.013. Single distinctive peaks

Table 1: Primers used for RT-PCR and Q-PCR
F = Forward, R = Reverse, bp = base pairs

Gene	Primers	Ta (°C)	Size (bp)
NANOG (AY596464)	F: 5'-CCTCCATGGATCTGCTTATTC-3' R: 5'-CATCTGCTGGAGGCTGAGGT-3'	63.0	210
OCT4 (AJ251914)	F: 5'-GTTCTCTTTGGGAAGGTGTT-3' R: 5'-ACACGCGGACCACATCCTTC-3'	55.4	313
UTF1 (CN028152)	F: 5'-CCGCGGGCCCGACCTCACG-3' R: 5'-GAACGCCGCCCTCCTGCAGACCTT-3'	66.0	216
CDX2 (EU137688)	F: 5'-GTCACCAGAGCTTCTCTGGG-3' R: 5'-AGACCAACAACCCAAACAGC-3'	52.9	144
CK18 (EU131884)	F: 5'-ATGAAGAAGAACCACGAGGAGGAA-3' R: 5'-TGTCTGCCATGATCTTGCTGAGG-3'	54.8	118
GATA4 (NM_214293)	F: 5'-ATGAAGCTCCATGGTGTCCC-3' R: 5'- ACTGCTGGAGTTGCTGGAAG -3'	55.8	162
GATA6 (NM_214328)	F: 5'-GAGCAGCCGGAGGAGATGTACCAGAC-3' R: 5'-GGCTCAGGCCAGGGCCAGGGCGCACC-3'	59.5	110

OCT4 primers were based on primers specific for bovine *OCT4,* which has been previously described by Van Eijk *et al.*[38]. The sequence of this gene was blasted against porcine nucleotide sequences, which resulted in one sequence with high query coverage. After alignment of this porcine with the bovine sequence, bovine specific primers were redesigned by nucleotide substitution of any mismatching nucleotides. *UTF1* primers were designed on a pig sequence that has 91% coverage with the coding sequence of *Homo sapiens* mRNA for *UTF1*. *CDX2* was detected with E-PCR primers from the UniSTS database on the NCBI website (UniSTS code: RH48331). *GATA6* primers have been described by Gillio-Meina *et al.* [91].

Table 2: Antibodies used for immunofluorescence. AA = Amino Acids.

Immunogen	Source	Concentration	Description
Full length mouse NANOG fusion protein	AB21603 (Abcam)	2 ug/ml	Rabbit polyclonal
AA 1-134 of human Oct4	SC5279 (Santa Cruz)	4 ug/ml	Mouse monoclonal
Synthetic peptide (AA 234-248) of human CDX2	AB4123 (Chemicon)	2 ug/ml	Rabbit polyclonal
C-terminal AA 328-439 of human GATA-4	SC9053 (Santa Cruz)	4 ug/ml	Rabbit polyclonal
C-terminal AA 358-449 of human GATA-6	SC9055 (Santa Cruz)	4 ug/ml	Rabbit polyclonal
Rabbit IgG control	SC2027 (Santa Cruz)	4 ug/ml	Rabbit
Mouse IgG control	SC2025 (Santa Cruz)	4 ug/ml	Mouse

in the melt curves verified specific amplification of the gene of interest. Integrity of the cDNA samples was confirmed by consistent detection of all reference genes in all samples, except for one metaphase-2 sample, which was excluded from further analysis. Genomic DNA contributions, as determined by –RT levels, were 0 in the case of *OCT4*, and detected at an average level of 0.44% for *CDX2*, 0.63% for *CK18*, 0.012% for *GATA4*, 0.033% for *GATA6*, and 0.64% for *UTF1*. If –RT levels were higher than 5% of the +RT levels, samples were excluded from the analysis for that particular gene, which resulted in exclusion of 5 samples for *CDX2*, 3 samples for *CK18* and 3 samples for *GATA6*, without loss of a developmental stage for any of these genes.

For each developmental stage, normalized values were divided by the normalized value of the germinal vesicle stage for that particular gene. As a consequence, gene expression levels are relative to the amount of expression in oocytes. Values for blastocyst stages were compared with the mean expression level and corrected standard deviation of all earlier stages. For OCT4, blastocyst stages were compared with cleavage stages. Statistical differences between both groups were tested by Students' t-test and a probability value <0.05 was considered significant. For OCT4 and GATA4, a Bonferroni correction was applied for multiple comparisons and for these genes a probability value of <0.025 was considered significant.

Whole mount immunofluorescence

In vitro and *in vivo* derived embryos were fixed overnight with 4% paraformaldehyde in PBS with 0.2% Tween (ICN biomedicals, Aurora, USA). Subsequently, embryos were permeabilised in methanol at –20ºC overnight and Tris buffered saline with 0.05% Tween (TBST) and 0.1% TritonX (Sigma-Aldrich) for 10 min, after which the embryos were blocked for 1 hr in TBST with 0.5% BSA. Next, the embryos were incubated in primary antibody 3-4 days, followed by another 2 days of incubation in the secondary antibody. Antibodies were diluted in blocking solution and rabbit and mouse isotypes served as negative control. Embryos were counterstained with ToPro (Invitrogen) and mounted in Vectashield (Vectorlab, Burlingame, CA, USA) before observation. Fluorescent signals were visualized using a Confocal Laser Scanning Microscope (Bio-Rad) and on an Olympus BH2 epifluorescence microscope.

Chapter IV

Isolation, culture, and characterization of porcine germ cells

Ewart W. Kuijk, Ben Colenbrander, Bernard A.J. Roelen

Department of Farm Animal Health, Faculty of Veterinary Medicine, Utrecht University, The Netherlands

Submitted

Isolation, culture, and characterization of porcine germ cells

Abstract

In this study, cell lines from neonate porcine testis were cultured and characterized, and the effects of growth factors were investigated, in order to determine the requirements for the establishment of porcine spermatogonial stem cell (SSC) lines. In the isolated cells, germ cells could be identified by the detection of NANOG and by reactivity of cells to DBA-lectin. In primary cultures, three different colony types with distinctive morphologies could be recognized. From SSC-like colonies, two cell lines were derived and maintained for 9 passages after which proliferation stopped. Growth of these cell lines depended on the growth factors LIF, EGF, GDNF, and FGF. In both cell lines *NANOG*, *PLZF*, and *EPCAM*, were expressed at higher levels and *GFRα1*, *INTEGRINα6*, and *THY1* were expressed at lower levels than in neonate porcine testis. Furthermore, primary cultures of neonate pig testis were subjected to a factorial design of the growth factors LIF, GDNF, EGF, and FGF. Addition of EGF and FGF to primary cell cultures of neonate pig testis affected the expression of *NANOG*, *OCT4*, and *GATA4*, whereas an effect of LIF or GDNF could not be detected. FGF decreased the expression levels of *NANOG*, a marker for pluripotency also expressed in porcine gonocytes. FGF enhanced the expression levels of Sertoli cell marker *GATA4* and pluripotency-related gene *OCT4*. EGF counteracted the positive effect of FGF on *GATA4* expression. These results suggest that FGF can impede successful derivation of porcine SSCs from neonate pig testis.

Background

In developing mouse embryos, primordial germ cells (PGCs) originate from the proximal epiblast. PGCs concentrate at the base of the allantois and migrate via the hindgut mesentery towards the genital ridges [92]. After colonizing the genital ridges, male germ cells become gonocytes and, after birth, gonocytes migrate to the basement membrane and differentiate into spermatogonial stem cells [93]. Spermatogonial stem cells (SSCs) have a capacity of self-renewal and the potential to give rise to cell types that are committed to differentiate to spermatozoa in a complex process called spermatogenesis [93]. In mammals, SSCs are unique because they are the only adult stem cells that can contribute to the next generation. Recent developments have shown that mouse SSCs can be isolated from pre-pubertal and adult testes, and cultured long-term *in vitro* without losing the capacity to restore fertility of infertile mice by transplantation into testes depleted of germ cells [61, 94]. It has also been demonstrated that in these cells, prior to transplantation, genes can be targeted through homologous recombination, which is an alternative to embryonic stem (ES)-cell-based gene targeting for directed genetic modification in mice [95]. In mammalian species other than mouse and human, where ample attempts to generate ES cell lines have had limited success, SSC based gene targeting is a promising technique for the production of transgenic offspring. Gene targeting would particularly mean a highly valuable tool in pigs because of their importance in agriculture and because the organ sizes and life span make pigs valuable model organisms for medical

purposes.

Another interesting aspect of mouse SSC cultures is that in these cell lines ES-like cells are formed spontaneously. Pluripotency of these ES-like cells has been demonstrated by their capacity to contribute to germ-line chimaeras [56, 58]. Potentially, a similar approach could result in pluripotent ES-like cells from other species, such as pigs, from which pluripotent cell lines are not available yet.

Xenografting of testicular cells from a diversity of species has shown that porcine and other alien SSCs can colonize a recipient mouse testis [96]. This suggests a conserved mechanism of self-renewal for these cell types between mammals [96]. In the adult testis, Sertoli cells, Leydig cells, and peritubular myoid cells define a major part of the niche of spermatogonial stem cells. This microenvironment supports SSCs by providing essential external stimuli such as growth factor stimulation [63]. In the testis, FSH stimulates Sertoli cells to produce glial derived neurotrophic factor (GDNF), an essential growth factor that supports SSC function [97, 98]. In mice, spermatogonial stem cell self-renewal depends on GDNF signaling through the RET tyrosine kinase/GFRA1 receptor complex [98]. Self-renewal of SSCs in *in vitro* cultures depends on GDNF in combination with either basic fibroblast growth factor (FGF) or epidermal growth factor (EGF) [99]. Leukemia inhibitory factor (LIF), an important growth factor in mouse embryonic stem cells, has also been reported to be an essential growth factor that supports SSC-self renewal [56]. Proliferation of SSCs in vitro cultures is enhanced by the addition of FGF [94]. For these reasons, SSCs are generally cultured in presence of LIF, GDNF, EGF, and FGF. However, the presence of FGF, EGF, and LIF for the initial culture of testicular cells may also result in the overgrowth of somatic cells, such as fibroblasts, endothelial cells and Sertoli cells [56]. Furthermore, little is known about the contribution of these factors to stem cell function in other species than the mouse, and if the presence of these factors in primary cell cultures enhances the success in establishing spermatogonial stem cell lines.

The aim of the current study was to culture and characterize porcine SSCs and to increase our knowledge on the growth factors required for the successful establishment of porcine SSC lines. Neonate porcine testis cells were cultured for 9 passages and expression of SSC-specific and somatic genes and proteins were analyzed by quantitative PCR and immunofluorescence. A factorial design of in which the presence of commonly used growth factors was tested on primary cell cultures revealed that basic FGF had considerable influence on the gene expression patterns and its presence potentially impedes successful derivation of porcine SSC lines.

Results

It has been demonstrated that, after transplantation, porcine gonocytes from neonate testis can colonize a mouse testis that has been depleted of spermatogonia by busulphan treatment [100]. This demonstrates the stem cell potential of porcine gonocytes and therefore neonate testes were regarded as a valid source for the current study. Seminiferous tubules from neonatal pig testes were dissociated and Nomarski-microscopy revealed the presence of gonocytes in the cell suspension, which could be recognized by their high nuclear to cytoplasm ratio and the presence of prominent nucleoli (Fig. 1 A,B). Cells were then cultured under conditions that have previously been shown to be suitable for the establishment and long term culture of

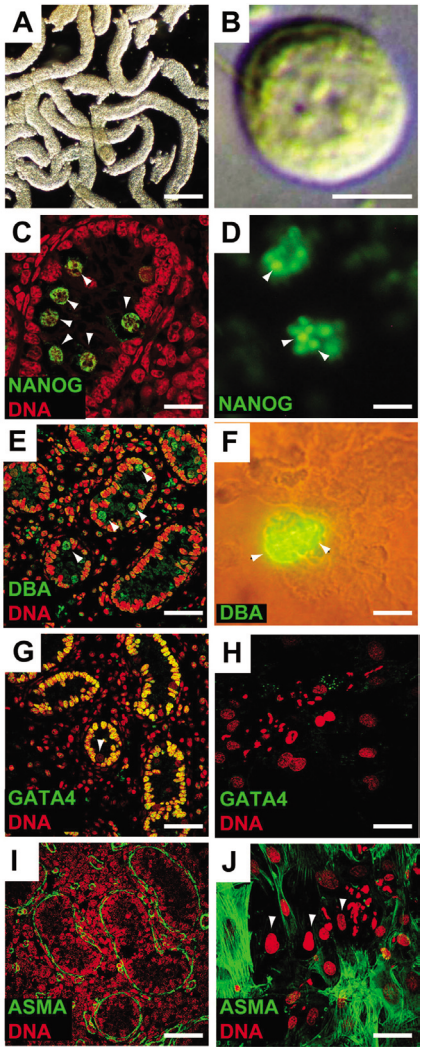

Figure 1: Isolation, culture, and characterization of primary cell cultures of porcine neonate testis. (A) seminiferous tubules from neonate pig testis after isolation by two-step enzymatic digestion; (B) gonocyte in single cell suspension after enzymatic treatment of seminiferous tubules; (C) expression of NANOG in gonocytes of porcine neonate testis, arrowheads denote NANOG-positive gonocytes; (D) expression of NANOG in a group of cells in cell culture of neonate porcine testis, arrowheads denote NANOG-positive cells; (E) specific binding of DBA lectin to gonocytes in neonate porcine testis, arrowheads denote DBA-lectin-positive gonocytes; (F) specific binding of DBA lectin to cells in culture, arrowheads denote DBA-lectin-positive gonocytes; (G) expression of GATA4 in Sertoli cells in neonate porcine testis, arrowhead denotes GATA4-negative gonocyte; (H) expression of GATA4 in cell culture of neonate porcine testis, most cells were negative; (I) expression of alpha smooth muscle actin (ASMA) in peritubular myoid cells in porcine neonate testis; (J) expression of ASMA in cell culture of neonate porcine testis, arrowheads denote ASMA negative-cells. Scale bars represent: 250 µm (A), 5 µm (B), 50 µm (C,D,F,H,J), 100 µm (E).

mouse SSC lines [61, 99]. Porcine cell cultures were characterized by investigating the expression of germ cell markers and somatic cell markers of which the expression patterns in testis were known. Porcine gonocytes of the neonate testis express the pluripotency-related transcription factor NANOG (Fig. 1C)[100]. In the current study, cells that expressed NANOG were also observed in primary cell cultures that originated from neonate testis (Fig. 1D). *Dolichos biflorus* agglutinin (DBA) is a lectin with carbohydrate specificity towards α-linked N-acetyl-galactosamine and is known to bind specifically to porcine gonocytes and primitive spermatogonia in neonatal pig testis (Fig. 1E)[52, 101]. Primary cultures of porcine neonate testis cells also contained DBA lectin positive cells (Fig. 1 F). Contrary to gonocytes, Sertoli cells express transcription factor GATA4 (Fig. 1G)[78, 102], but most cells in the culture were negative for GATA4 (Fig. 1 H), which suggests that these cells are not Sertoli cells. Peritubular myoid cells express Alpha Smooth Muscle Actin (ASMA) (Fig. 1I)[103], expression of which was also observed in primary cultures of porcine neonate testis cells, but cells that did not express ASMA were also observed (Fig. 1 J). These results demonstrate heterogeneity in the cell culture, which was also demonstrated by the presence of three different types of cell colonies, each with distinct morphology that could be

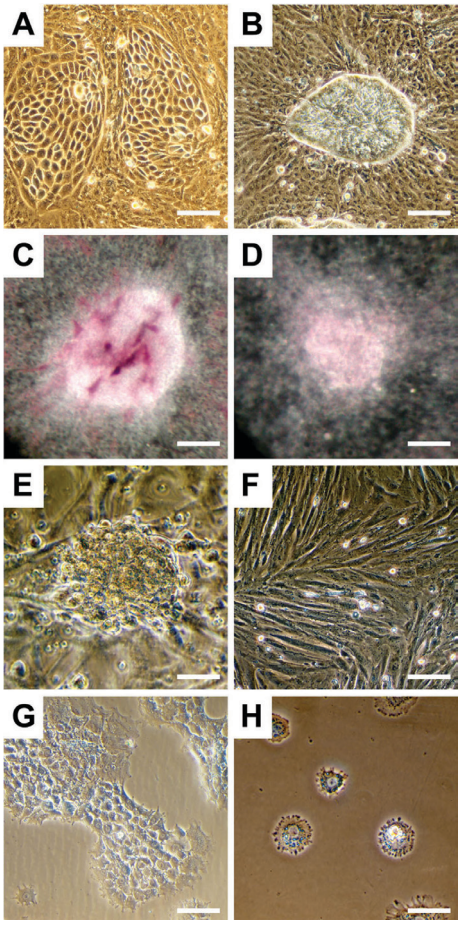

Figure 2: Morphology and characterization of colonies in primary cell cultures of porcine neonate testis. (A) Morphology of polygonal cells growing in a monolayer reminiscent of Sertoli cells; (B) primordial germ cell-like colony in cultures of neonate porcine testis cells; (C) alkaline phosphatase activity in primordial germ cell-like colony; (D) negative control (with 5 mM levamisol) for alkaline phosphatase activity in primordial germ cell-like colony; (E) morphology of SSC-like colony in primary cultures of neonate pig testis; (F) morphology of primary neonate porcine testis cells, cultured in ES medium with a high serum concentration, colonies were not observed; (G) morphology of cells of individually picked colonies after growth on laminin-coated plates; (H) morphology of cells of individually picked colonies after growth on laminin-coated plates in absence of growth factors. Scale bars represent: 100 µm (A,B,G), 50 µm (C,E,F,H), 75 µm (D)

observed after approximately 8 to 14 days of culture (Fig. 2 A, B, E). These colonies were not observed when cells were cultured in ES medium, which in contrast with the SSC medium contains a high serum concentration (Fig. 2 F) or when the cells were cultured on mitomycin C treated mouse embryonic fibroblasts (data not shown). One type of colonies consisted of polygonal cells growing in a monolayer reminiscent of Sertoli cells (Fig. 2A)[104]. Cells of these colonies stopped proliferating shortly after transplantation of the colonies to new plates and could not be cultured further (data not shown). It was more difficult to recognize individual cells in another type of cell colony, which grew as compact structures that were morphologically comparable to colonies derived from primordial germ cells (Fig. 2 B). However, most cells of these colonies did not have alkaline phosphatase activity, which suggests that cells of these colonies are not equivalent to cell cultures derived from PGCs (Fig. 2 C, D). The morphology of yet another colony type of round proliferating cells on top of a monolayer of cells (Fig. 2 E) most closely resembled that of previously described SSC lines [61, 94] and these colonies were individually picked, dissociated, and cultured on laminin-coated plates (Fig. 2 G). Two of such colonies, which originated from different isolations, were both subsequently cultured for 9 passages, and were referred to as pGS4 (#4) and pGS6 (#6). Every 4-6 days, approximately 1/3 of the cells were transferred to new laminin-coated plates when cultures reached 50-70% confluency. After 9 passages, proliferation was reduced and cell culture was stopped.

The cell lines were further characterized by their gene expression patterns using quantitative RT-PCR. Both cell lines expressed genes that are also expressed by porcine

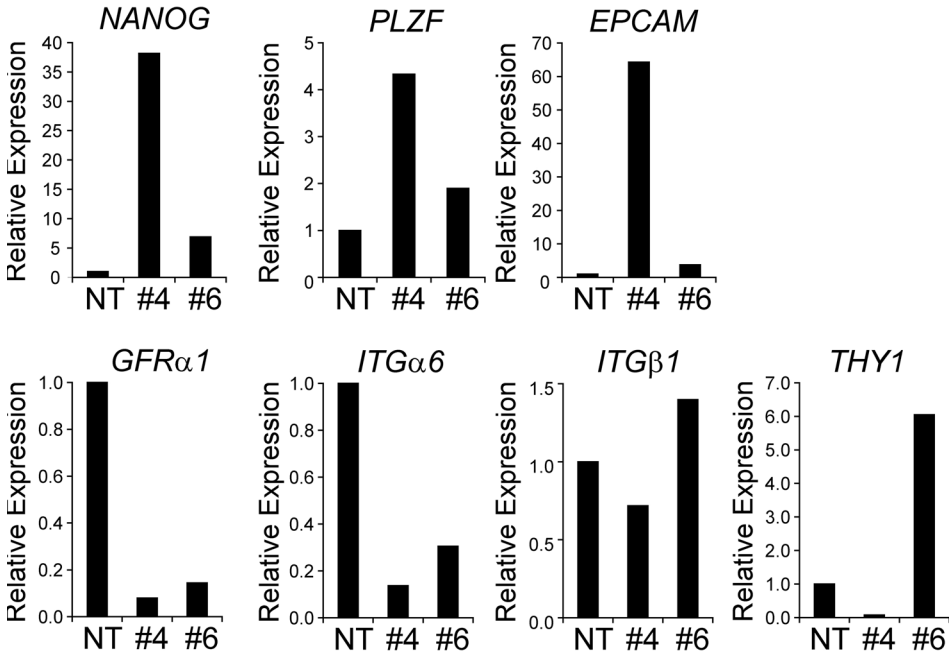

Figure 3: Relative mRNA expression levels of genes (known to be expressed in mouse male germ cells) in two cell lines (#4 and #6) derived from neonate porcine testis.
For each gene, relative expression in neonate testis (NT) was set to 1.

gonocytes and spermatogonial stem cells (Fig. 3). NANOG is a transcription factor important for pluripotency of cells and expression has been demonstrated in gonocytes of neonate porcine testis [25, 26, 28, 100]. *NANOG*, expression levels were higher in PGS4 and PGS6 than in whole neonate testis as determined by quantitative RT-PCR (Fig. 3). Promyelocytic leukemia zinc-finger (PLZF) is a transcriptional repressor expressed in gonocytes and undifferentiated spermatogonia with a role in stem cell self renewal and maintenance of the stem cell pool [105]. PGS4 and PGS6 expressed *PLZF* at higher levels than whole neonate testis (Fig. 3). *EP-CAM* is a homophilic adhesion molecule expressed by undifferentiated germ cells [106]. *EP-CAM* expression levels were higher in PGS4 and PGS6 than in whole neonate testis (Fig. 3). In the mouse, GDNF signaling through the receptor *GFRα1* mediates self-renewal *of* SSCs [98]. Expression levels of *GFRα1* were lower in PGS4 and PGS6 than in whole neonate testis. *ITGα6, ITGβ1*, and *THY1* are cell surface markers that can be used to enrich for SSCs [107, 108]. *ITGα6* expression levels were lower in PGS4 and PGS6 than in neonate pig testis and *ITGβ1-expression* levels were approximately equal between testis and cell cultures. In PGS6, *THY1* expression was higher than in testis but in PGS4, *THY1* expression was lower (Fig. 3).

When cells were transferred to medium without the growth factors LIF, FGF, EGF, and GDNF, these cells attached, but proliferation was not observed (Fig. 2 H). To further determine the effects of different commonly used growth factors in primary cell cultures of porcine testis cells a factorial design experiment was performed. For LIF, GDNF, EGF, and FGF (16 combinations; Table 1) the effects were determined on the expression of pluripotency gene

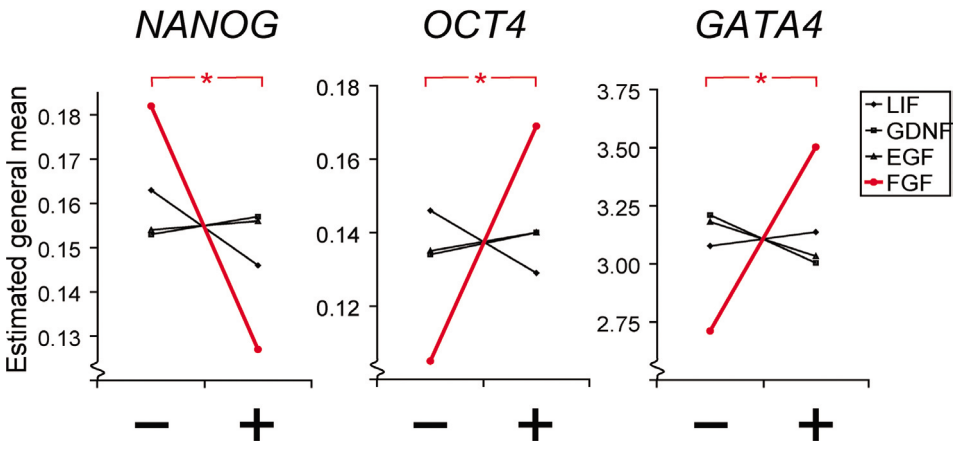

Figure 4: Effects (in estimated marginal means) of the growth factors LIG, GDNF, EGF, and FGF on the expression of *NANOG*, *GATA6* and *OCT4* in primary cell cultures from neonate porcine testis.
- = absence of growth factor, + = presence of growth factor, asterisks denote significant differences between absence or presence of the growth factor on the expression of that particular gene.

NANOG, which was used as an indication of gonocyte proliferation. In pigs, the expression of *OCT4*, which is commonly used as marker for pluripotency, is absent in gonocytes [100]. Therefore, the expression of this gene was used to determine if a combination of growth factors would establish a pluripotency program in porcine germ cells. Expression levels of GATA4 were determined and used as indicator for Sertoli cell proliferation. Morphology of the cells was also examined, but no correlation was found between the combinations of growth factors and cell morphology. Basic FGF had a significant negative effect on the expression of the pluripotency gene and pig gonocyte marker *NANOG* ($p<0.001$). Remarkably, expression of pluripotency related *OCT4* was enhanced by FGF ($p<0.001$) (Fig. 4). FGF also had strong positive effects on the expression of Sertoli cell marker *GATA4* ($p<0.001$). A two-way interactive effect was detected between EGF and FGF on the expression of GATA4, with EGF counteracting the positive influence of FGF on the expression of this gene ($p<0.05$; Fig. 5). No other interactive effects of the four growth factors on the expression levels of *NANOG*, *GATA4*, and *OCT4* were observed. Rather surprising-

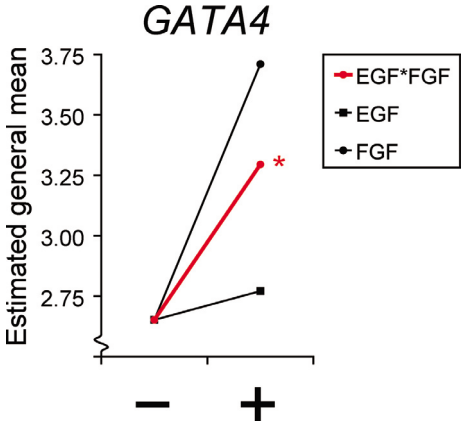

Figure 5: Two way interactive effect (in estimated marginal means) between EGF and FGF on the expression of GATA4 in primary cell cultures from neonate porcine testis.
- = absence of growth factor, + = presence of growth factor, asterisk denotes significant effect on the expression of GATA4 of EGF in combination with FGF when compared with separate presence of EGF or FGF.

ly, LIF, GDNF, and EGF did not have detectable effects on the expression levels of *NANOG*, *GATA4*, and *OCT4* (Fig.5).

Discussion

In mammals, gene targeting is largely restricted to rodents, for the reason that in these species germline stem cell lines are available such as embryonic and spermatogonial stem cell lines. If germline stem cell lines could be established from non-rodent mammals that would greatly facilitate gene targeting in these species. Particularly in pigs, targeted mutagenesis would open up manifold opportunities, because of the evident importance of pigs in agriculture but also since pigs are valuable model organisms. However, currently embryonic or spermatogonial stem cell lines are not available from this species.

Here, neonate porcine testis cells were cultured under several conditions and characterized. Based on the expression of germ and somatic cell markers it can be concluded that primary cell cultures were composed of mixtures of germ cells and somatic cells. Mouse SSC cultures are also characterized by their heterogeneity. Even though several surface markers have been identified in the mouse that can be used to enrich the number of spermatogonial stem cells using FACS or MACS, e.g. *ITGα6, ITGβ1*, and *THY1* [107, 108], none of these markers are restricted to SSCs. As a result, pure populations of SSCs have not yet been described [63].

From two independent primary cell cultures, spermatogonial stem cell like colonies gave rise to two morphologically similar cell lines. These lines were cultured for 9 passages on laminin-coated plates and expressed various spermatogonial stem cell markers. Especially in PGS4, expression levels of *NANOG*, *PLZF*, and *EP-CAM* were markedly higher than in testis, which indicates that this culture was relatively enriched for germ cells. On the other hand, *GFRα1* was expressed at lower levels in both cell lines when compared with the expression levels in neonate testis. In mouse SSCs, it is known that GFRα1 mediates GDNF signaling and thereby supports SSC self-renewal [98]. The relatively low expression levels of *GFRα1* in the porcine cell cultures could indicate that stem cell numbers are low. However, expression of GFRα1 is not restricted to the stem cell population in rat testis [109]. The expression pattern of *GFRα1* in pig testis is unknown and therefore it is necessary to cautiously use of this gene as a marker for SSCs in pigs.

Cells from neonate mouse testes can give rise to SSCs and to pluripotent ES-like cells [58, 59]. Successful derivation of such cell lines will greatly depend on the culture conditions. However, the effect of various growth factors on germ cells and somatic cells of heterogeneous primary cultures is largely unknown. Therefore, a factorial design experiment was performed to test the effect of commonly used growth factors on primary cell cultures derived from neonate pig testis. As determined by this factorial design experiment, FGF had a positive effect on the expression of *OCT4* in cell lines derived from neonate pig testes. FGF is an essential ingredient for the establishment of pluripotent EG cell lines from primordial germ cells [110]. Furthermore, recent developments have shown that various combinations of the factors C-MYC, SOX2, KLF4, OCT4, LIN28, and NANOG, can reprogram somatic cells to a pluripotent state. OCT4 has been a key ingredient for this reprogramming to occur

[67-69, 111-113]. The effect of FGF on the levels of OCT4 expression in primary cell cultures of neonate porcine testis indicates that the threshold for germ cells to make the transition to pluripotent ES-like cells is lowered.

In the current study, FGF had a negative effect on the expression levels of *NANOG*, a gene that is expressed in porcine gonocytes. This suggests that FGF impairs self-renewal of gonocytes in primary cell cultures of neonate pig testis. The decrease in expression could be a reflection of the progressive loss of *NANOG* in gonocytes with increasing age [100], even though germ cell numbers increase. Alternatively, it could indicate that proliferation of male germ cells is not supported by FGF and that decreasing *NANOG* levels are a reflection of a decrease in the proportion of germ cells. However, the latter possibility is less likely, because in primary cultures of neonate testis cells from the rat, FGF had a positive effect on gonocyte proliferation [114].

Although NANOG was used as a marker for gonocytes in this study, in the mouse, *Nanog* is not expressed in gonocytes, but closely associated to pluripotent cell populations [25, 26, 28]. If NANOG plays a similar role in pluripotency of porcine cells remains to be determined, because in contrast with embryos from the mouse, NANOG does not seem to be expressed in the pluripotent inner cell mass of early porcine blastocysts [115]. Furthermore, NANOG expressing porcine gonocytes can colonize a recipient mouse testis without formation of teratocarcinomas, which is another indication that expression of NANOG in porcine cells does not necessarily reflect pluripotency of these cells [100]. Nevertheless, the observed decrease in expression levels of *NANOG* in primary cell cultures with FGF indicates that an expression program related to pluripotency is abandoned upon FGF signaling.

FGF also enhanced the expression of Sertoli cell marker *GATA4*. In a previous study, FGF has been identified as a potent mitogen of Sertoli cells [114, 116]. Therefore, the enhanced levels of *GATA4* expression are most likely caused by increased proliferation of Sertoli cells. EGF has also been described as a weak mitogen of Sertoli cells [116]. In the current study, a one-way effect of EGF on *GATA4* expression was not detected. Cells cultured in the presence of EGF and FGF expressed lower levels of *GATA4* than cells cultured with FGF alone. In other words, EGF partially eliminated the positive influence of FGF on *GATA4* expression. These findings suggests that for the isolation and culture of germ cells in the presence of FGF, addition of EGF can partially prevent the mitogenic effect of FGF on Sertoli cells, thereby limiting the contribution of this somatic cell type to the culture.

Remarkably, despite the power of using factorial designs in determining possible effects, GDNF did not affect the expression of *NANOG*, *OCT4*, and *GATA4* in primary cell cultures of pig neonate testis. This is rather surprising, because *GFRα1*, the receptor that mediates GDNF signaling, is expressed in neonate testis. The lack of effect suggests that the initial increase of germ cells and Sertoli cells that can be observed in pig testis from birth onwards [117], does not depend on GDNF signaling. Porcine gonocytes express PLZF and NANOG and are positive for DBA lectin shortly after birth, but expression of PLZF and NANOG and DBA lectin affinity are progressively lost within the first few weeks after birth [100, 101]. The correlation between age and the expression of PLZF and NANOG demonstrates that porcine germ cells experience dynamic changes between birth and puberty. Likewise, the responsiveness of male porcine germ cells towards GDNF might also increase between birth and puberty. A recent

report describes the positive effects of GDNF on germ cell numbers in bovine SSC cultures. [118]. The sources of these bovine SSC cultures were testes from calves aged 4-6 months. Given the close relationship between cow and pig, it would be interesting to determine if GDNF has an effect on porcine germ cells that are derived from animals of an older age than used in the current study.

In conclusion, if the aim of the cell culture is to establish pluripotent ES-like cells from porcine neonate testis, it could be advantageous to add EGF and FGF. However, if the goal is to establish porcine SSC lines, FGF could have negative effect on the proliferation of porcine gonocytes.

Materials and Methods

Cell isolation and cell culture

Pig (*Sus scrofa*) testes of a mixed breed were obtained from neonate piglets that underwent routine castration under local anesthesia at the farm 'De Tolakker' of the Faculty of Veterinary Medicine, Utrecht University. After collection in Hank's Balanced Salt Solution (HBSS; Invitrogen, Groningen, The Netherlands), the tunica was removed and minced testis sections were treated for 15-30 min with 1mg/ml hyaluronidase, 1mg/ml collagenase type IV, and 1.4 mg/ml DNAse (all from Sigma-Aldrich, Zwijndrecht, The Netherlands) in HBSS at 37°C. After washing with HBSS, the cells were treated for an additional 15 min with 1mg/ml collagenase type IV and 1.4 mg/ml DNAse at 37°C. Again, the cells were washed with HBSS and subsequently treated for 4 min with trypsin EDTA (Invitrogen) supplemented with 1.4 mg/ml DNAse. Next, enzymatic activity was blocked by addition of Iscove's modified Dulbecco's medium (Sigma) with 0.5% bovine serum albumin (BSA; Sigma-Aldrich). The resulting cell suspension was filtered with a 40µm filter (BD Falcon, Erembodegem, Belgium) before culture. Cells were cultured in previously described culture medium, which contained 1% bovine serum and the growth factors murine LIF (10^3 U/ml), GDNF (10 ng/ml), EGF (20 ng/ml), and bFGF (10 ng/ml)[61] on autologous feeders, MEFs or laminin-coated plates [99]. Porcine cells from neonate testes were also cultured in mouse embryonic stem cell medium, which consisted of GMEM (Invitrogen), supplemented with 2mM L-glutamine, 1x non-essential amino-acids (Invitrogen), 0.1mM β-mercaptoethanol, 1mM sodium pyruvate, 10% fetal bovine serum and LIF.

Table 1: Factorial design: 16 combinations of growth factors were used in primary cell cultures of neonate pig testis.

	condition	a	b	c	d
1	0	0	0	0	0
2	a	a	0	0	0
3	b	0	b	0	0
4	ab	a	b	0	0
5	c	0	0	c	0
6	ac	a	0	c	0
7	bc	0	b	c	0
8	abc	a	b	c	0
9	d	0	0	0	d
10	ad	a	0	0	d
11	bd	0	b	0	d
12	abd	a	b	0	d
13	cd	0	0	c	d
14	acd	a	0	c	d
15	bcd	0	b	c	d
16	abcd	a	b	c	d

In this study the factorial design was as follows: a = LIF; b = GDNF; c = EGF; d = FGF; 0 = growth factor not added.

Table 2: Antibodies used for immunofluorescence on porcine cells. AA = Amino Acids.

Immunogen	Source	Dilution	Description
Full length mouse NANOG fusion protein	Abcam, AB21603	1:100	Rabbit polyclonal
AA328-439 of human GATA4	Santa Cruz, sc-9053	1:100	Rabbit polyclonal
N-terminal human ASMA	DAKO, M0851	1:70	Mouse monoclonal

For the factorial design experiment, freshly isolated cells were plated on gelatin-coated plates in standard SSC medium without growth factors or with any combination of LIF, GDNF, EGF, or FGF (Table 1). The following day, unattached cells were transferred to uncoated plates. Every other day, half of the medium was replaced by fresh medium supplemented with the same combination of growth factors. After ten days, cultures were terminated and RNA was isolated with Trizol as described below. The entire factorial design experiment was repeated once.

Immunohistochemistry, Immunofluorescence, Confocal Laser Scanning Microscopy, and AP staining

For immunofluorescence on testis sections, testis tissue was fixed overnight (o/n) in 4% PFA and embedded in paraffin the following day. Sections were cut at 5-7 µm and mounted on superfrost plus slides (Menzel, Braunschweig, Germany), which were dried o/n at 37°C. For immunofluorescence, slides were

Table 3: Primers used for RT-PCR and Q-PCR on porcine cells

Gene	Primers	Optimal Annealing T
NANOG	F: 5'-CCTCCATGGATCTGCTTATTC-3' R: 5'-CATCTGCTGGAGGCTGAGGT-3'	63.0
PLZF	F: 5'-AAAGCGGTTCCTGGATAGTTTG-3' R: 5'-GGTCTGCCTGTGTGTCTCC-3'	54.4
EPCAM	F: 5'-ACCAGAGAATGCTATCCAGAAC-3' R: 5'-CTCACTCGCTCCAAACAGG-3'	53.0
GFRα1	F: 5'-ATAGACTCTAGTAGCCTCAG-3' R: 5'-AGGGACTTGTTCTTGACC-3'	53.8
ITGα6	F: 5'-AAACGAGAAATTGCTGAAAGAC-3' R: 5'-CACTAGAATGATCCACCAAGG-3'	54.5
ITGβ1	F: 5'-ATGAGGAGGATTACTTCAGACTTC-3' R: 5'-GCAGCCGTGTCACATTCC-3'	53.2
THY1	F: 5'-TCTCTTGCTAACAGTCTTG-3' R: 5'-GGTAGTGAAGCCTGATAAG-3'	54.4
B2M	F: 5'-TTCACACCGCTCCAGTAG-3' R: 5'-CCAGATACATAGCAGTTCAGG-3'	59.5
BACT	F: 5'-CATCACCATCGGCAACGAGC-3' R: 5'-TAGAGGTCCTTGCGGATGTC-3'	55.8
GAPDH	F: 5'-TCGGAGTGAACGGATTTG-3' R: 5'-CCTGGAAGATGGTGATGG-3'	51.1
PGK1	F: 5'-AGATAACGAACAACCAGAGG-3' R: 5'-TGTCAGGCATAGGGATACC-3'	56.4

Primers for NANOG, B2M, BACT, GAPDH, and PGK1 have also been used in previous studies [73, 115]; F = forward primer, R = reverse primer.

deparaffinized in xylol and subjected to antigen retrieval by boiling the slides for 10 min in citrate buffer at pH6. Following antigen retrieval, slides were permeabilized in TBS with 0.05% tween (TBST) and with TritonX100 (0.1%). Permeabilized slides were blocked for 1 hr in TBST with 0.5% BSA (Sigma-Aldrich) followed by o/n incubation with the primary antibody (Table 2) in blocking solution at 4°C. The following day, slides were incubated in the secondary antibody in blocking solution for 1hr at 4°C, after which the slides were counterstained with TOPRO-3 (Invitrogen) and mounted in Vectashield. Cells were cultured on chamberslides (LabTek/Nunc, Roskilde, Denmark) and subsequently fixed in cold methanol for 5 min, washed for 5 min in ice-cold acetone, and from there on, the above described staining procedure was continued from the permeabilization step onwards. Fluorescent images were retrieved with a digital camera mounted on an epifluorescence microscope and with a Confocal Laser Scanning Microscope (Bio-Rad).

The presence of cells reactive to DBA lectin was determined by incubating slides with FITC-labeled DBA lectin (Sigma) immediately after antigen retrieval. Cultured cells were incubated in FITC-labeled DBA lectin immediately after fixation with 4% PFA. For alkaline phosphatase activity detection, cells were fixed for 30 min in 4% PFA and subsequently incubated in 2% NBT/BCIP (Roche, Mannheim, Germany) diluted in 0.1M Tris-HCl (pH 9.5) with 0.1M NaCl. As negative controls, cells were incubated in 2% NBT/BCIP diluted in 0.1M Tris-HCl (pH 9.5) with 0.1M NaCl and 5 mM levamisole (Sigma).

RNA extraction, reverse transcription, and Quantitative RT-PCR

RNA from neonate testis and cell cultures was isolated with Trizol (Invitrogen, Groningen, The Netherlands), according to the manufacturer's instructions. In an additional purification step immediately following phase separation, one volume of phenol:chloroform:isoamyl alcohol (Fluka, Sigma-Aldrich, Zwijndrecht, The Netherlands) was added to the aqueous phase. Subsequently, samples were mixed, incubated at room temperature (RT) for 5 min, centrifuged and incubated at RT for an additional 5 min. The aqueous phase was transferred to a new tube and put on ice. From here, the Trizol RNA isolation procedure was resumed, from the RNA precipitation step onwards. RNA was treated with 2 µl DNAse (2.75 Kunitz units/µl; Qiagen, Venlo, The Netherlands) for 20 min at 37°C, after which the enzyme was inactivated by incubation at 65°C for 10 min. Synthesis of cDNA was primed with random primers and RNA samples were reverse transcribed with Superscript III (Invitrogen) according to the company's instructions. For each RNA sample an equivalent mixture was prepared, from which Superscript III was omitted, to control for genomic DNA contamination. After cDNA synthesis, samples were stored at –20°C before they were used in polymerase chain reactions. Relative quantification of transcript levels was performed as previously described [73]. Primers were designed with Beacon Designer 4 (PREMIER Biosoft International, Palo Alto, CA, USA; Table 3). In all samples, the expression levels of four housekeeping genes (*BACT*, *B2M*, *GAPDH*, and *PGK1*) were examined with geNorm, to determine which of these housekeeping genes were stably expressed in all conditions [119]. *BACT* was the least stable gene and *B2M* and *PGK1* were the most stable genes. Therefore, these latter two genes were used as reference genes for the normalization of quantitative PCR data. For each sample, -RT negative controls were used in all reactions to exclude the possibility of mistaking genomic DNA for transcripts. The amplicons (10 µl) were run on 1% agarose gels and primer specificity was confirmed by sequencing of the products.

Statistical Analysis

Data obtained with the factorial design were analyzed with SPSS. A square root transformation was carried out on the expression data of NANOG, GATA4, and OCT4, after which these values displayed a normal distribution. Subsequently, a mixed model analysis determined the effects of the different growth factors on the expression levels of the different genes. The effects were visualized by displaying the estimated marginal means for the absence and presence of each growth factor.

Chapter V

PTEN and TRP53 independently suppress *Nanog* in spermatogonial stem cells

Ewart W. Kuijk[1], Alain van Mil[1], Bas Brinkhof[2], Louis C. Penning[2], Ben Colenbrander[1], Bernard A.J. Roelen[1]

[1]Department of Farm Animal Health and [2]Department of Clinical Sciences of Companion Animals, Faculty of Veterinary Medicine, Utrecht University, The Netherlands

Submitted

PTEN and TRP53 independently suppress *Nanog* in spermatogonial stem cells

Abstract

Mammalian spermatogonial stem cells (SSCs) are the only adult stem cells that can contribute to the next generation. Knock-out studies have indicated a role for TRP53 and PTEN in insulating male germ cells from pluripotency, but the mechanism by which this is achieved is largely unknown. To get more insight in these processes, an RNAi experiment was performed on the mouse spermatogonial stem cell line GSDG1. Lipofectamine-mediated transfection of siRNAs directed against *Trp53* and *Pten* resulted in decreased mRNA expression levels of these genes, as determined by quantitative RT-PCR. A decrease in TRP53 protein levels because of the knockdown was also observed, using immunoblotting. The effects of knockdown were examined by determining the expression levels of genes that are involved in reprogramming and pluripotency of cells, specifically *Nanog*, *Eras*, *c-Myc*, *Klf4*, *Oct4*, and *Sox2*. Additionally, the effect of TRP53- or PTEN-knockdown on *Plzf* expression was measured, which is a SSC-associated transcription factor required for stem cell maintenance. An effect of TRP53 and PTEN knockdown on the expression level of *Ddx4*, expressed in primordial germ cells, spermatogonia, and at high levels in differentiating male germ cells, was also analyzed. The main finding of this study is that knockdown of TRP53 and PTEN independently resulted in significant higher expression levels of the pluripotency-associated gene *Nanog*. The findings of this study demonstrate that *Nanog* is independently suppressed by TRP53 and PTEN, suggesting that this TRP53- and PTEN-mediated repression is important for the insulation of male germ cells from pluripotency.

Background

In mammals, spermatogonial stem cells (SSCs) are the only adult stem cells that can contribute to the next generation. In the seminiferous tubules of the adult testis, SSCs display self-renewal or differentiation by the complex process of spermatogenesis [54]. SSCs are unipotent, which means that their developmental potential is limited to one cell type: spermatozoa. Despite the highly restricted developmental potential of SSCs, spermatozoa can contribute to the formation of a totipotent zygote that can differentiate to all embryonic and extraembryonic tissues. In *in vitro* cultures, mouse SSCs can be maintained long-term while retaining the capacity to restore fertility following transplantation to the testis of infertile mice [61].

In contrast with SSCs, *in vitro* cultured embryonic stem (ES) cells, derived from preimplantation embryos, are pluripotent and can give rise to all the various specialized cell types that make up the body. Subcutaneous injection of these cells in immuno-compromised mice results in the formation of teratomas; tumors that consist of cell types from all three embryonic germ layers. After injection in blastocyst stage embryos, ES cells can participate in host embryonic development and contribute to the formation of all fetal cell types including germ cells. Interestingly, under normal culture conditions, SSCs can spontaneously form ES-like colonies with enhanced expression of pluripotency genes and decreased expression of genes

characteristic of SSCs. Pluripotency of these ES-like cells has been confirmed by their contribution to germline chimaeras following injection into blastocysts [58]. A subsequent study verified that a single lineage-specific spermatogonial stem cell could give rise to pluripotent ES-like daughter cells and to colonies of spermatogonial stem cells [59]. Interestingly, after transplantation these ES-like cells had lost the capacity to restore fertility in testis of infertile mice, but instead formed teratomas, reminiscent of true ES cells that are unable to restore fertility after transplantation [59].

The capacity of SSCs to spontaneously convert from a unipotent to a pluripotent state implies that these cells provide a tool to study the mechanism behind pluripotency and nuclear reprogramming. Moreover, improving our understanding of the mechanism by which SSCs acquire pluripotency and how to induce this could provide new opportunities to obtain pluripotent cells from species such as cow and pig in which attempts to derive ES cell lines have failed [7, 10]. However, it is still unclear what causes the shift from unipotency to pluripotency and how to induce this transition. Interestingly, an increased susceptibility to testicular teratomas has been observed in mice deficient in *Transformation related protein 53* (*Trp53*), that codes for a transcription factor and tumor suppressor that can arrest cells for repair of DNA damage [120]. SSCs isolated from neonatal and adult testis of *Trp53* knockout mice convert more easily to ES-like cells [58, 121]. *Trp53* has also been shown to suppress the pluripotency-associated gene *Nanog* and thereby induces the differentiation of ES cells into cell types that undergo efficient *Trp53* -dependent cell cycle arrest and apoptosis [122]. Moreover, pluripotent embryonic germ cells are more easily established from primordial germ cells of *Trp53*-deficient embryos than from wildtype and heterozygous embryos [123]. These results suggest an involvement of TRP53 in insulating germ cells and SSCs from pluripotency and that loss of this single gene can be sufficient for SSCs to acquire pluripotency.

The association of pluripotency with oncogenic transformation is also seen with loss of *Phosphatase and tensin homolog* (*Pten*), coding for a tumor suppressor and agonist of the PI3K/AKT pathway, which leads to testicular teratoma [124]. Downregulation of PTEN enhances the transformation of primordial germ cells into pluripotent embryonic germ cells and a similar phenotype is observed after hyperactivation of AKT, an effect that is probably exerted by inactivation of *Trp53* [123, 125].

In the current study, the mechanism was investigated by which TRP53 and PTEN insulate SSCs from pluripotency. Therefore, expression levels of TRP53 and PTEN were downregulated in *in vitro* cultured SSCs and changes in expression of candidate target genes were examined. The effect of transient RNAi-mediated knockdown of TRP53 and PTEN was studied by measuring expression levels of factors that play a role in pluripotency of ES cells (*Nanog* [25, 26], *Eras [126]*, *c-Myc*, *Klf4*, *Oct4*, and *Sox2* [67-69, 112, 127]). Furthermore, the effect of TRP53- or PTEN-knockdown was measured on *Plzf* expression*,* a spermatogonia-specific transcription factor required for stem cell maintenance *[105, 128]*) and on *Ddx4* (DEAD (Asp-Glu-Ala-Asp) box polypeptide 4), which is expressed in primordial germ cells, spermatogonia, and at high levels in differentiating male germ cells of the adult testis [129, 130]. In this study, it is demonstrated that independent knockdown of TRP53 and PTEN, leads to a significant increase in the expression of ES marker *Nanog*. The results of this study suggest that TRP53 and PTEN insulate unipotent spermatogonial stem cells from pluripotency primarily

through suppression of *Nanog*.

Results

Expression levels of pluripotency and SSC factors in ES cells and SSCs

In routinely cultured SSCs and ES cells, expression levels were determined for factors related to pluripotency or spermatogonial stem cells by quantitative RT PCR. ES cells showed distinctively higher expression levels of genes involved in pluripotency and reprogramming than SSCs (Fig. 1). *Klf4*, *Sox2*, and *Eras* were approximately 10 times higher expressed in ES cells than in SSCs. The expression level of *Oct4* was approximately 400 times higher in ES cells than in SSCs, and *Nanog* expression level was approximately 500 times higher in ES cells compared with SSCs. An inverse pattern was observed for SSC-marker *Plzf*, of which the expression level was almost 600 times lower in ES cells compared with SSCs. *Ddx4* was expressed at a more than 10-fold lower level in ES cells than in SSCs. It was presumed that RNAi-mediated knockdown of TRP53 or PTEN in SSCs would affect the mechanism by which these cells are insulated from pluripotency, and consequently, enhance the expression levels of pluripotency factors. Before knockdown, *Trp53* expression was approximately equal in ES cells and SSCs and levels of *Pten* expression were 2-fold lower in ES cells than in SSCs (Fig. 1).

Efficiency of Trp53 and Pten knockdown experiments

Transfection efficiency of SSCs was determined with FITC-labeled oligos. Eight hour after transfection, siRNA transfection

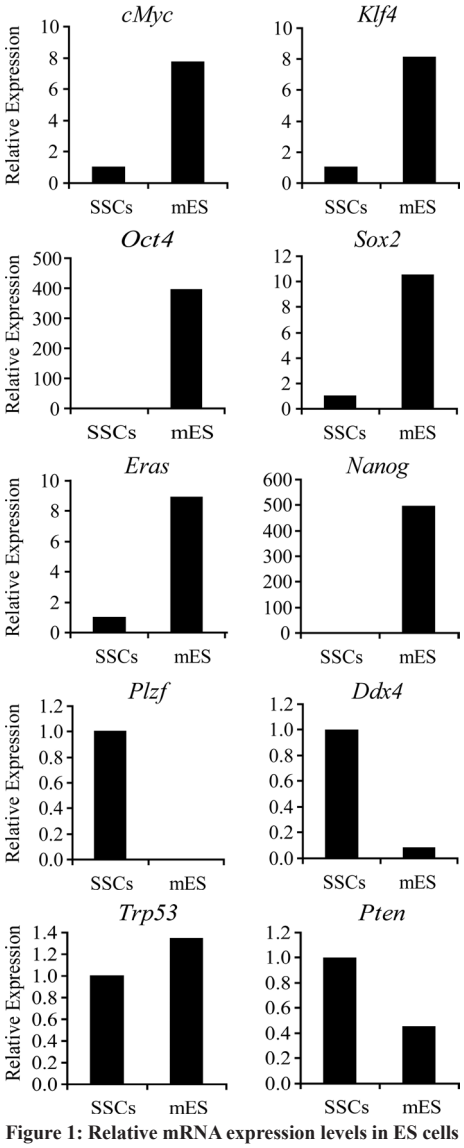

Figure 1: Relative mRNA expression levels in ES cells and SSCs of genes that are characteristic for pluripotent ES cells (*c-Myc*, *Klf4*, *Oct4*, *Sox2*, *Eras*, and *Nanog*), of genes that are characteristic for SSCs (*Plzf*, *Ddx4*), and of the RNAi targets (*Trp53*, *Pten*). SSCs = SSC line GSDG1 [61], mES = mouse ES cells. Relative expression levels in SSCs were set to 1.

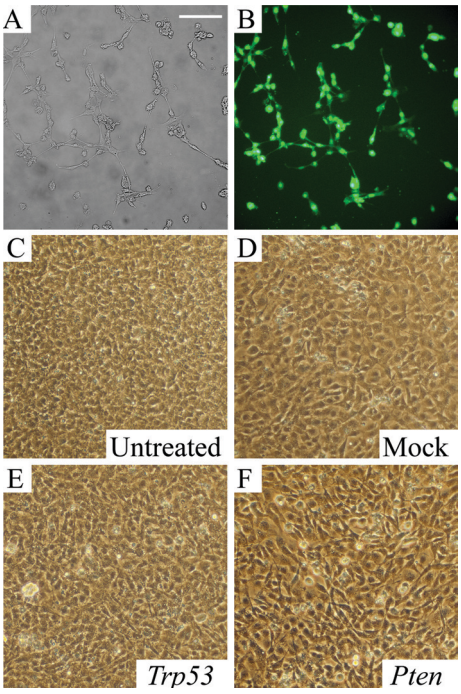

Figure 2: Transfection efficiency and cell morphology after knockdown of *Trp53* and *Pten*.
(A) Bright-field view and (B) fluorescent image of transfected cells; Morphology of (C) untreated cells, (D) negative control (mock transfected) cells, and cells transfected with siRNAs against (E) *Trp53* and (F) *Pten*.

efficiency was estimated between 95 and 100% (Fig. 2) and fluorescent signal could be detected up to four days after transfection. *Trp53* mRNA levels were significantly knocked down at 48 hr, 72 hr, and 96 hr after transfection, as compared to mock transfected controls (Fig. 3) and the efficiency of *Trp53* knockdown was respectively 80%, 70%, and 60%. A significant reduction in *Pten* mRNA levels of 75% and 70% was also achieved at respectively 72 hr and 96 hr after transfection with *Pten*-specific siRNAs (Fig.3). Knockdown of *Trp53* also resulted in a significant reduction of TRP53 protein levels in SSCs, when compared to mock-transfected controls (Fig. 4). Knockdown of *Pten* did however not result in a detectable decline in PTEN protein levels (Fig. 4). Cell morphology was monitored before and after transfection. A change in cell morphology was not observed in siRNA-transfected cells when compared to untreated or mock-transfected cells (Fig. 2).

Effects of TRP53 and PTEN knockdown on expression levels of pluripotency and SSC factors

At 72 hr and 96 hr after transfection, expression levels of pluripotency factors were measured to determine if TRP53 knockdown influenced the insulation of SSCs from pluripotency. Knockdown of TRP53 resulted in elevated levels of *Nanog* at 72 hr after transfection, and an approximately 2-fold increase at 96 hr after transfection, as assessed by RT-PCR (Fig. 5). Expression levels of the ES-specific genes *c-Myc*, *Klf4*, and *Eras* were unaffected by the knockdown. For most samples, expression levels of *Sox2* and *Oct4* did not reach the threshold cycles, which impeded a quantitative assessment of the effect of knockdown on the expression of these genes. However, *Sox2* expression was detected in 4 out of 6 samples (2 at 72 hr and 2 at 96 hr), in which TRP53 was downregulated, and in just 1 out of 6 mock control samples (data not shown). Surprisingly, expression of the SSC factor *Plzf* significantly increased 2-fold at 96 hr after transfection. *Ddx4* expression levels were unaffected by TRP53 knockdown.

At 72 hr after transfection with siRNA oligonucleotides against *Pten*, expression levels of *Nanog* were similar between siRNA treated cells and mock transfected controls (Fig. 6). However, at 96 hr after transfection, *Nanog* was more than 4 times upregulated in cells in which PTEN was knocked down. Expression levels of pluripotency factors *c-Myc*, *Klf4*,

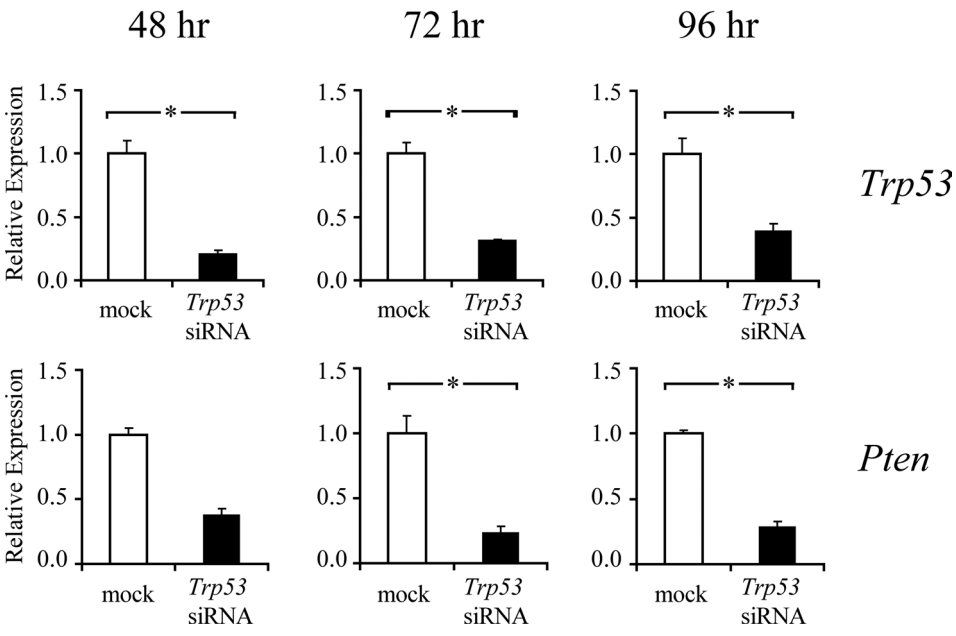

Figure 3: Relative mRNA expression levels of *Trp53* and *Pten* at 48, 72, and 96 hr after transfection with Stealth siRNAs against *Trp53* and *Pten*.
Expression levels in negative controls (mock) were set to 1. Levels are expressed as mean ± s.e.m. (n = 3). Asterisks denote significant differences in expression levels between negative controls (mock transfected cells) and siRNA transfected cells.

and *Eras* were unaffected by the knockdown. The expression levels of pluripotency factors *Sox2* and *Oct4* were below background levels and an effect of knockdown on the expression of these genes could not be determined (data not shown). The level of expression of SSC factor *Plzf* was also unaffected by knockdown of PTEN (Fig.6). However, at 96 hr after transfection, *Ddx4* was expressed at significantly lower levels in cells with decreased *Pten* levels. Important for both experiments is that TRP53 knockdown did not influence *Pten* expression and, *vice versa*, PTEN knockdown did not influence *Trp53* expression in SSCs (Fig. 7).

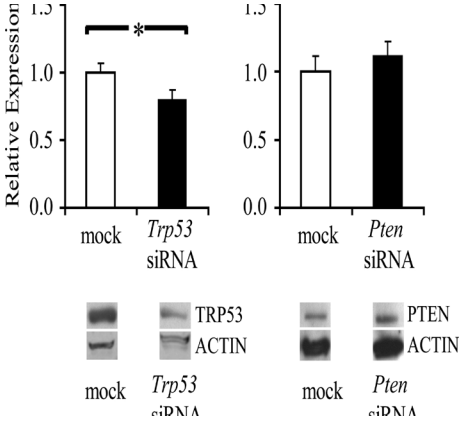

Figure 4: Representative immunoblots (top) and relative protein expression (bottom) of TRP53 and PTEN after transfection with Stealth oligos against *Trp53* and *Pten*.
Expression levels in negative controls (mock) were set to 1. Levels are expressed as mean ± s.e.m. (n = 9). Asterisks denote significant differences in expression levels between negative controls (mock transfected cells) and siRNA transfected cells.

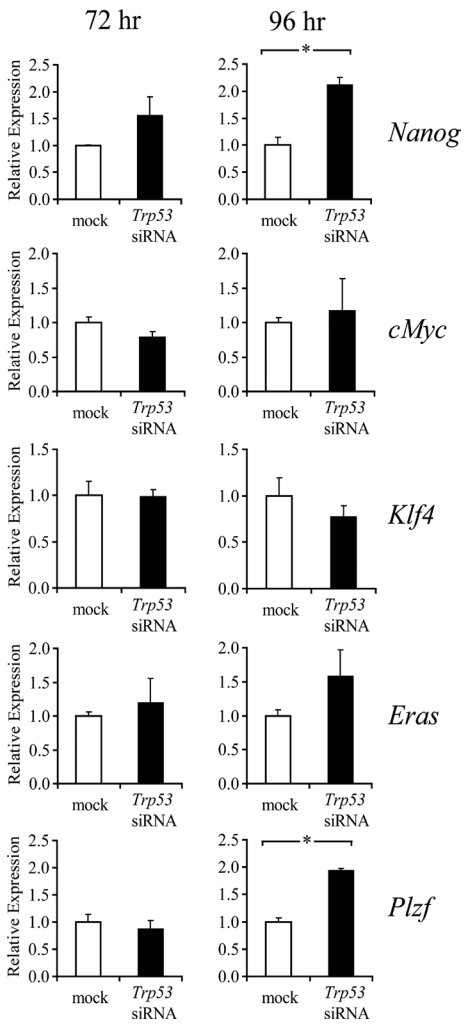

Figure 5: Relative mRNA expression levels of pluripotency genes (*c-Myc*, *Klf4*, *Oct4*, *Sox2*, *Eras*, and *Nanog*) and of genes that are characteristic for SSCs (*Plzf*, *Ddx4*) at 72 hr and 96 hr after transfection with siRNAs against *Trp53*.

Expression levels in negative controls (mock) were set to 1. Levels are expressed as mean ± s.e.m. (n = 3). Asterisks denote significant differences in expression levels between negative controls (mock transfected cells) and siRNA transfected cells.

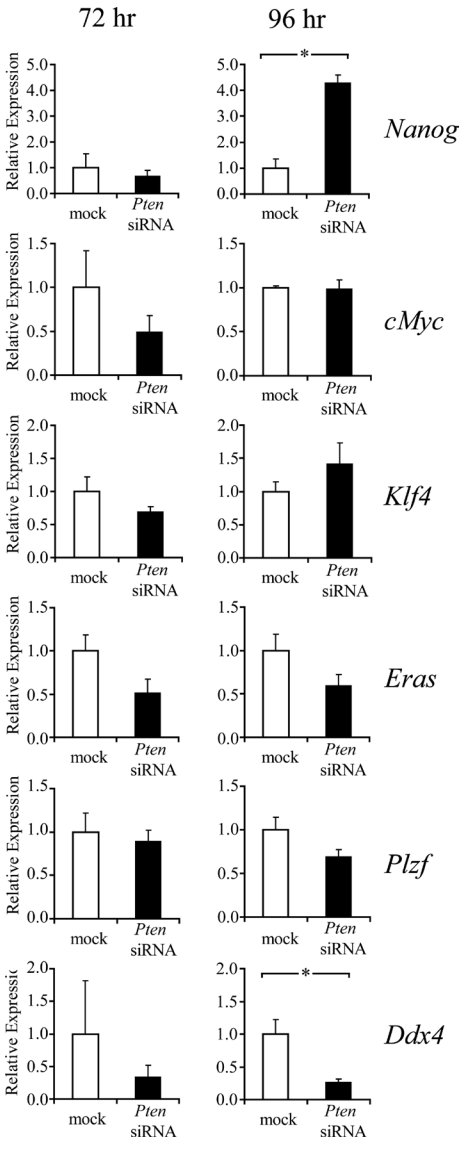

Figure 6: Relative mRNA expression levels of pluripotency genes (*c-Myc*, *Klf4*, *Oct4*, *Sox2*, *Eras*, and *Nanog*) and of genes that are characteristic for SSCs (*Plzf*, *Ddx4*) at 72 hr and 96 hr after transfection with siRNAs against *Pten*.

Expression levels in negative controls (mock) were set to 1. Levels are expressed as mean ± s.e.m. (n = 3). Asterisks denote significant differences in expression levels between negative controls (mock transfected cells) and siRNA transfected cells.

Discussion

Under certain pathogenic or *in vitro* culture conditions, germ cells can acquire pluripotency as demonstrated by teratoma formation in gonads [62] and by the derivation of pluripotent cell lines from primordial germ cells and spermatogonial stem cells [56-58, 60, 110, 131]. Tumor suppressors TRP53 and PTEN and the PI3K-AKT signaling pathway have emerged as key players in refraining germ cells from pluripotency [58, 121, 123, 124]. In the current study, the molecular mechanisms that trigger the conversion of male germ cells towards pluripotency were investigated by RNAi-mediated knockdown of *Trp53* and *Pten* mRNA levels. TRP53 protein levels were significantly reduced by the mRNA-knockdown, but a decline in PTEN protein levels could not be detected. PTEN, which has a similar calculated protein stability as TRP53 [132], showed an approximately 20% less efficient mRNA knockdown at day 2 as compared to *Trp53*, what may have caused the lack of detectable protein knockdown. Lack of detection could also be caused by the limited resolution of immunoblot analysis. Nevertheless, clear specific effects were observed at the gene expression level after the *Pten*-siRNA treatment, as for the *Trp53*-siRNA treatment.

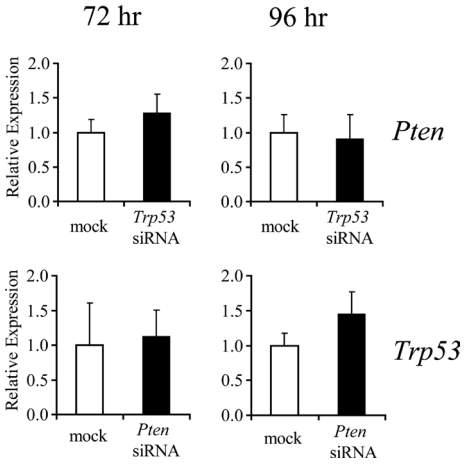

Figure 7: Relative mRNA expression levels of *Pten* and *Trp53* at 72 hr and 96 hr after transfection with siRNAs against *Trp53* and *Pten* respectively.
Expression levels in negative controls (mock) were set to 1. Levels are expressed as mean ± s.e.m. (n = 3).

In this study, is demonstrated that TRP53 and PTEN suppressed expression of the pluripotency factor NANOG in spermatogonial stem cells and that inhibition of either TRP53 or PTEN resulted in significantly elevated *Nanog* expression. It has previously been shown that PTEN protein antagonizes PI3K function and consequently inhibits downstream signaling through AKT [133], leading to the inhibition of TRP53 degradation. Evidently, knockdown of PTEN releases AKT from its inhibition, initiating the degradation of TRP53 via MDM2 [134]. This suggests that the observed increased *Nanog* expression after TRP53 and PTEN down-regulation are part of the same mechanism. However, there are two indications that TRP53 and PTEN suppress *Nanog* in SSCs independently from one another: firstly, knockdown of either gene did not influence the expression of the other, and secondly, different effects were observed on *Ddx4* and *Plzf* expression levels between the TRP53-knockdown and the PTEN-knockdown.

NANOG is also expressed in differentiating male germ cells (manuscript submitted elsewhere) in an expression pattern that is reminiscent of DDX4 expression [130]. DDX4 is an ATP dependent RNA helicase of the DEAD-box protein family, expression of which is restricted to the germ lineage [129, 130, 135, 136]. *Ddx4* expression was unaffected by decreased TRP53 levels, which indicates that elevated *Nanog* levels were not caused by differentiation of germ

cells. Likewise, *Ddx4* expression was expressed at significant lower levels in cells with decreased *Pten* levels, which excludes the possibility that the increase in *Nanog* expression reflects the presence of differentiating male germ cells. A decrease in expression levels of *Ddx4* upon PTEN downregulation is in line with the progressive loss of *Ddx4* expression in primordial germ cells of *Pten* null embryos [124]. Posttranscriptional processing of RNA could be one component of the mechanism by which germ cells are insulated from pluripotency.

The degree of upregulation of *Nanog* after knockdown of TRP53 or PTEN was still much less than the difference in *Nanog* expression between ES cells and GS cells (Fig.1). Moreover, forced expression of *Nanog* or *Sox2* in *Trp53*$^{-/-}$ SSCs is not sufficient to induce the conversion of these cells to pluripotency [59], what suggests that more factors than *Nanog* are necessary for a full conversion. The increase in *Nanog* expression upon TRP53 knockdown is probably a direct effect as TRP53 suppresses the expression of *Nanog* by binding to its promoter [122]. It is therefore remarkable that expression levels of *Nanog* and other pluripotency related genes in *Trp53*$^{-/-}$ SSCs are comparable to wildtype SSCs [59], what could indicate that in these cells other mechanisms are involved in suppression of *Nanog* and insulating SSCs from pluripotency. This is in agreement with the findings of the current study that PTEN suppresses *Nanog* separately from TRP53.

Forced expression of *c-Myc*, *Klf4*, *Oct4*, and *Sox2* can reprogram somatic cells towards a pluripotent state [67-69, 112]. Interestingly, acquisition of *Nanog* expression can be used to distinguish between fully reprogrammed cells and incomplete reprogramming [111], which supports the thought that the observed increase in *Nanog* expression upon knockdown of TRP53 and PTEN is the first step towards reprogramming of SSCs.

In the current study, no major effects were observed of TRP53 or PTEN knockdown on expression of the reprogramming factors *c-Myc*, *Klf4*, and *Oct4*, which suggests that these factors are not involved in the initial transition from unipotent spermatogonial stem cell towards a pluripotent ES-like cell. *Sox2* expression was observed in more samples in which TRP53 was knocked down than in mock control samples. This could indicate that *Sox2* participates as a reprogramming factor in the initial events of the transition of spermatogonial stem cells towards ES-like cells.

A surprising finding was the increase in expression of SSC-marker *Plzf* after TRP53 knockdown. PLZF is a transcriptional repressor that regulates the epigenetic state of undifferentiated cells and is required for self-renewal and maintaining the stem cell pool [105, 128]. Interestingly, a PLZF-RARα (retinoic acid receptor alpha) fusion protein has been shown to inhibit TRP53-dependent transcription and leads to degradation of TRP53 [137]. Consequently, increased *Plzf* expression would further reduce TRP53 protein levels in a feed-forward manner. Little is known about *Plzf* expression in the germline, and therefore it is difficult to interpret what the observed increase in expression implies, but intermediate expression of *Plzf* in the transitional state from SSCs towards ES-like cells is feasible.

In summary, the current study indicates that TRP53 and PTEN are involved in insulating male germ cells from pluripotency. Furthermore, TRP53 and PTEN appear to act separately in the suppression of expression of the pluripotency gene *Nanog* in spermatogonial stem cells.

The results from this study enhance our understanding of the mechanism that insulates pluripotency in spermatogonial stem cells. These findings can be used for the development of

a strategy for the generation of ES-like cells from other species than mice and men, or for the generation of patient specific stem cells in regenerative medicine.

Materials and Methods

Cell culture and transfection

The mouse spermatogonial stem cell line GSDG1 [61], was obtained from the RIKEN BioResource Center Cell Bank in Japan. The cells were cultured under feeder free conditions in 12 well plates coated with 1 ug/cm^2 laminin (Sigma-Aldrich Chemie, Zwijndrecht, The Netherlands), as previously described [61, 99]. Culture medium was supplemented with 0.1% pen/strep (Invitrogen, Breda, The Netherlands) and 0.1% Fungizone (Invitrogen). Cells were routinely cultured from passage 16 up to passage 44 by reseeding every 3 to 4 days at 1.0 x 10^5 cells per well. Mouse ES cells were a kind gift from Stieneke van den Brink of the Hubrecht Laboratory in Utrecht. ES cells were cultured under standard mouse ES cell culture conditions on mitomycin C treated STO cells.

Three different Stealth / siRNA duplex oligoribonucleotides (Invitrogen) against both *Trp53* and *Pten* were tested for their efficiency of knockdown. Quantitative Real Time-PCR (RT-PCR) for *Trp53* and *Pten* expression resulted in the selection of one *Trp53* siRNA (5'-GCCAAGUCUGUUAUGUG-CACGUACU-3') and one *Pten* siRNA (5'-GGAAAUCGAUAGCAUUUGCAGUAUA-3') for the knockdown experiments. Universal Control siRNAs (Invitrogen) with GC contents similar to the specific oligos were used as negative controls. BLOCK-iT Fluorescent (FITC-labeled) oligos (Invitrogen) were used to assess transfection efficiency. One day before transfection, 1.2 x 10^5 cells were plated uniformly across the wells of laminin-coated 12-well plates. On the day of transfection, cells were at 40 to 50% confluence, allowing a long interval between transfection and final assay time, and minimizing the loss of cell viability due to cell overgrowth. All transfections were performed in triplicate with lipofectamin 2000 transfection reagent (Invitrogen) in final siRNA concentrations of 36 nM according to manufacturers instructions. In brief, per well 2 µl lipofectamin was diluted in 48 µl OPTI-MEM-I reduced serum medium (Invitrogen) and incubated for 5 min at room temperature. Next, 2 µl 20 µM siRNA, mock and fluorescent oligos were diluted in 48 µl medium each, added seperately to 50 µl diluted lipofectamin and incubated for 20 min at room temperature. The resulting volume of 0.1 ml transfection solution/well was dispensed into the wells of the culture plates containing 1 ml StemPro-34 SFM (Invitrogen) culture medium supplemented [61, 99] without fetal calf serum and antibiotics. Cells were incubated at 37°C for 6 hr, after which the transfection medium was replaced with 1 ml culture medium with fetal calf serum, and antibiotics. Transfection efficiency was assessed visually by means of FITC-labeled negative control oligos and knockdown efficiency was measured quantitatively by RT-PCR. For fluorescence microscope analysis of FITC-labeled control transfected cells, cells were imaged using an Olympus IMT 2-F inverted microscope.

Quantitative RT-PCR

For quantitative RT-PCR, total RNA was isolated from samples with TRIzol Reagent (Invitrogen), according to manufacturer's instructions, and subsequently treated with RNase-Free DNase (Qiagen, Venlo, The Netherlands) to remove genomic DNA. Next, cDNA was prepared using SuperScript III Reverse Transcriptase (RT; Invitrogen) according to the manufacturer's instructions. In brief, every 40 µl of reaction mix contained 20 µl DNase-treated RNA, 150 ng Random Primers (Invitrogen), 8 µl 5x First Strand Buffer (Invitrogen), 2 µl 0.1M DTT (Invitrogen), 2 µl 10 mM dNTPs, 0,2 µl RNasin Ribonuclease Inhibitor (Promega, Madison, WI), and RNAse/DNAse free water was used to adjust the reaction volume. A cDNA synthesis reaction was also performed without RT to obtain –RT controls for the detection of potential genomic DNA contamination. Amplification and detection was performed with a MyIQ single-color real-time PCR detection system (Bio-Rad, Veenendaal, The Netherlands). PCR primer pairs (Isogen, Maarssen, The Netherlands) were designed using Beacon Designer 4 (PREMIER Biosoft In-

ternational, Palo Alto, CA). Primer nucleotide sequences are provided in Table 1 and sequence analysis confirmed amplification of the genes of interest. Quantitative RT-PCR amplifications were performed with iQ-SYBR Green Supermix (Bio-Rad) and the optimal annealing temperatures of the primer pairs were determined experimentally with a temperature gradient. RT-PCR conditions were: 3 min at 95°C, followed by 40 cycles of 20 sec at 95°C, 30 sec at the specific annealing temperature (Table 1), and 10 sec real time detection at 80-82°C. Finally, a melt curve was generated. For each gene, a separate reaction was performed and standard curves of 10-fold dilutions (10 pg to 1 ag) supplemented each run. The threshold cycle (Ct) was set within the exponential phase of the PCR and standard curve efficiencies were between 90 and 110%. After absolute quantification, expression levels were normalized to the housekeeping genes *Rpl22* and *Rpl27* [138], which showed stable expression between the samples as verified by Genorm analysis [139]. Relative gene expression levels between siRNA transfected cells and mock-transfected cells were determined at 72 hr and 96 hr after transfection and the expression levels are presented as fold increase compared to mock.

Immunoblot Analysis

TRP53 and PTEN protein knockdown in *Trp53* and *Pten* siRNA and mock transfected cells was tested at three time points, which were chosen based on protein half-life predictions (http://www.expasy.org) [132]. Total protein was extracted from each condition 48hr, 72hr, and 96 hr after transfection by lysing the cells with 0.5 ml cold lysis buffer, containing 25 mM MES (2-(N-Morpholino) ethanesulfonic acid), 150 mM NaCl, 1 mM EGTA, 1 tablet/50 ml protease inhibitors (Roche, Almere, The Netherlands) and 1% Triton X-100. The amount of protein was measured by DC protein assay (Bio-Rad), and boiling for 5 min with 0.1 M DTT and 0.5 M β-mercaptoethanol was used to reduce 5 µg of total protein. Reduced protein lysates were separated on 12% Tris–HCl PAGE gels accompanied by a SeeBlue Plus2 Pre-Stained Standard (Invitrogen). Size separated proteins were transferred to a Trans-Blot nitrocellulose transfer membrane (Bio-Rad). Membranes were blocked overnight at 4°C with 2.5% Blotting Grade Blocker non-fat dry milk (Bio-Rad) in 1x PBS-0.1% Tween, and subsequently probed with 1:200 dilution of TRP53 monoclonal anti-mouse IgG_2 (Santa Cruz Biotechnology, Santa Cruz, CA, sc-71817) or PTEN mouse monoclonal IgG_1 antibody (Santa Cruz Biotechnology, sc-7974) in 2.5% non-fat dry milk for 1 hr at room temperature. Membranes were washed in 1x PBS-0.1% Tween, and subsequently probed with 1:5000 dilution of goat anti-mouse IgG secondary antibody, horseradish peroxidase-conjugated (Santa Cruz, sc-2005) in 2.5% non-fat dry milk for 1 hr at room temperature. Subsequently, membranes were washed and signals were visualized using SuperSignal West Dura Extended Duration Substrate (Pierce, Rockford, IL), after which the blots were exposed to film (Kodak). To obtain a quantitative assessment of the protein levels, films were scanned and band intensities were measured using ImageJ software (v1.40; NIH, USA).

Statistical analysis

Data is presented as mean ± s.e.m. of at least three independent experiments and the two-tailed unpaired Student's t test was used to determine the significance of differences. A $p < 0.05$ was considered to be statistically significant.

Table 3: Primers used for Quantitative RT-PCR.

Gene	Primers
c-Myc[*]	5'-TAACTCGAGGAGGAGCTGGA-3' 5'-GCCAAGGTTGTGAGGTTAGG-3'
Eras	5'-TAGCATCTTGGACCTGAG-3' 5'-TCTTTCACGAAGCATTGG-3'
Klf4[*]	5'-AACATGCCCGGACTTACAAA-3' 5'-TTCAAGGGAATCCTGGTCTTC-3'
Nanog	5'-AGATGCGGACTGTGTTCTC-3' 5'-TGCGTTCACCAGATAGCC-3'
Oct4[*]	5'-TAGGTGAGCCGTCTTTCCAC-3' 5'-GCTTAGCCAGGTTCGAGGAT-3'
Plzf	5'-GGTAGAGCAGTGGCAGGAG-3' 5'-CGAAGTTATAGGTTGTGGAGAGG-3'
Pten	5'-GCTGAAGTGGCTGAAGAG-3' 5'-GCTGGAGATGGTGTATGG-3'
Rpl22	5'-CTGGGCTGCTGCTCCTTTG-3' 5'-AATCACCTGTCTGCTTCTGAGG-3'
Rpl27	5'-TCCAACGCCCTCCTTTCCTTTCTG-3' 5'-CCAGGACCAGCACCACTTTCCC-3'
Sox2[*]	5'-AGGGCTGGGAGAAAGAAGAG-3' 5'-CCGCGATTGTTGTGATTAGT-3'
Trp53	5'-GCTGCTCCGATGGTGATG-3' 5'-AGTGTGATGATGGTAAGGATAGG-3'

[*]Primers for *c-Myc*, *Klf4*, *Oct4*, and *Sox2* have been described previously [113].

Chapter VI

NANOG expression in mammalian testes

Ewart W. Kuijk[1], Jeffrey de Gier[2], Susana M. Chuva de Sousa Lopes[3], Ian Chambers[4], Ans M.M. van Pelt[5], Ben Colenbrander[1], Bernard A.J. Roelen[1]

[1] Department of Farm Animal Health, Faculty of Veterinary Medicine, Utrecht University, The Netherlands

[2] Department of Clinical Sciences of Companion Animals, Faculty of Veterinary Medicine, Utrecht University, The Netherlands

[3] Department of Anatomy & Embryology, Leiden University Medical Center, Leiden University, The Netherlands.

[4] Medical Research Council (MRC) Centre for Regenerative Medicine, Institute for Stem Cell Research, School of Biological Sciences, University of Edinburgh, UK.

[5] Center for Reproductive Medicine, Department of Obstetrics and Gynecology, Academic Medical Center, University of Amsterdam, The Netherlands

Submitted

NANOG expression in mammalian testes

Abstract

Expression of the pluripotency transcription factor NANOG is restricted to cells of the ICM, the epiblast and to primordial germ cells, but no definitive expression in other tissues has been described. Spermatogenesis is the process by which spermatogonial stem cells differentiate, complete meiosis, and subsequently develop into highly specialized haploid sperm cells that can contribute to a totipotent embryo. Despite the apparent connection between testis function and pluripotency, a role for NANOG in any of the processes that ultimately lead to a competent sperm cell has not been established yet. In the current study, NANOG expression was examined in testes of mouse dog, pig, and man using RT-PCR, immunoblot analysis, immunohistochemistry, immunofluorescence, and analysis of a *Nanog eGFP* reporter mouse. Here we describe that *Nanog* mRNA and NANOG protein are expressed in maturing gametes in the testis of mouse, dog, pig, and man. Although NANOG has previously mainly been attributed to undifferentiated cells with stem cell potential, expression was observed in pachytene spermatocytes and in the first steps of spermiogenesis. The findings of the present study suggest a conserved role for NANOG in meiotic and post-meiotic stages of male germ cells.

Background

NANOG, named after a mythical Celtic land of the ever young, is a homeobox transcription factor and a key player in pluripotency; i.e. the ability of a cell to differentiate into any other cell type [25, 26]. The role of NANOG in pluripotency is illustrated by expression of NANOG in pluripotent cell lines like embryonic stem (ES) cells and embryonic germ (EG) cells. Loss of NANOG in pluripotent cell lines increases the tendency to differentiate [25, 26, 28]. Moreover, mouse ES cells that constitutively express *Nanog* are less sensitive to differentiation signals and do not require LIF to maintain an ES cell identity [25]. Fusion of somatic cells with ES cells that express elevated levels of NANOG facilitates reprogramming of the restricted somatic genome to a pluripotent state [140].

In vivo expression of NANOG is restricted and essential to the embryonic sources of pluripotent cell lines, namely the pluripotent epiblast and primordial germ cells (PGCs) [25-27]. Cells of the inner cell mass (ICMs) of *Nanog* $^{-/-}$ embryos do not develop to pluripotent epiblast cells and differentiate entirely when put into culture [26]. Remarkably, however, *Nanog*$^{-/-}$ ES cells can participate in chimaeric embryonic development and contribute to all three embryonic germ layers, which demonstrates that NANOG is dispensible for maintenance of somatic pluripotency. However, in these chimaeras, Nanog-/- cells become allocated to the primordial germ cell lineage but do not survive beyond E11.5, indicating that Nanog is indispensable for completion of the embryonic germ cell program [28].

The testis appears to be an important source of cells that are directly linked to pluripotency. Teratocarcinomas, for example, are malignant testicular tumors that are composed of pluripotent cells and differentiated progeny of numerous cell types [62]. Moreover, a number of recent reports describes the derivation of pluripotent cells from neonatal and adult

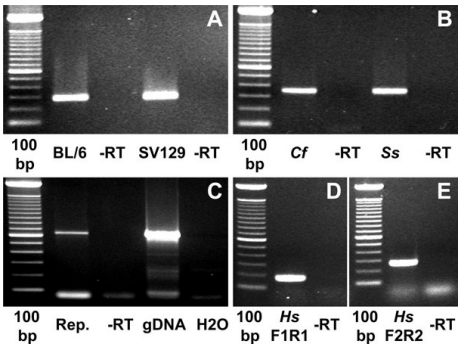

Figure 1: Expression of Nanog in testis of various species as determined by RT-PCR.
(A) Expression of *Nanog* in testis of two different mouse strains, (B) Expression of *NANOG* in dog and pig testes, (C) Expression of *eGFP* in testis of a reporter mouse in which *eGFP* is knocked in to the Nanog locus (D,E) Expression of *NANOG* in human testis as determined by RT-PCR with 2 different primer pairs. In all RT-PCR experiments, amplicons were of the expected sizes (see also Table 1) and products were identified by sequence analysis. Abbreviations: 100 bp = 100 base pair DNA ladder, BL/6 = *Mus musculus* (mouse) Black 6 strain, -RT = minus reverse transcriptase control, SV129 = *Mus musculus* SV129 strain, *Cf* = *Canis familiaris* (dog), *Ss* = *Sus scrofa* (pig), Rep. = reporter mouse, gDNA = genomic DNA from the same reporter mouse, H_20 = water blank, *Hs* = *Homo sapiens* (human), L1R1 = primer pair 1, L2R2 = primer pair 2.

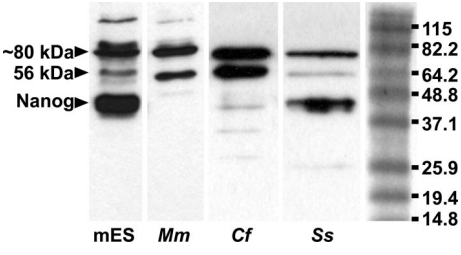

Figure 2: Composite image of immunoblot results for NANOG on testis lysates of mouse, dog, and pig. On the right is a Benchmark protein ladder (Invitrogen) and the indicated molecular weights for each band. Abbreviations: mES = mouse embryonic stem cells, *Mm* = *Mus musculus* (mouse), *Cf* = *Canis familiaris* (dog), *Ss* = *Sus scrofa* (pig).

testes [56-60]. However, the immediate link between testis and pluripotency is evidently spermatogenesis: the production of sperm cells that can fertilize oocytes and thereby contribute to the formation of completely new organisms.

Spermatogonial stem cells (SSCs), that can either self-renew or differentiate, support spermatogenesis throughout adulthood. The differentiation of SSCs to functional sperm cells is a complex process that occurs in the tubular compartment of the adult testis facilitated by somatic Sertoli cells. In rodents, SSCs are called A_{single} spermatogonia that develop through proliferation and differentiation and through multiple consecutive stages of type A spermatogonia into intermediate spermatogonia. Subsequently, intermediate spermatogonia divide into type B spermatogonia. In general, A_{single} spermatogonia have relaxed chromatin whereas type B spermatogonia are characterized by heterochromatin [63]. This initial period in spermatogenesis that is characterized by an increase in cell numbers by mitotic divisions ends with the division of type B spermatogonia into preleptotene spermatocytes.

After the proliferative phase, the newly formed spermatocytes leave the basal membrane and enter meiosis. Prophase of the first meiotic division encompasses an estimated 90% of male meiosis and is subdivided in four components: at leptotene, chromosomes condensate, at zygotene synaptonemal complexes are formed, at pachytene synaptonemal complexes are completed, and at diplotene separation of chromosomes is initiated [141]. When prophase is completed, spermatocytes fulfill the subsequent phases of the first meiotic division. Two secondary spermatocytes (2n) are formed that enter the second meiotic division, thereby producing four haploid (n) spermatids [141]. Meiosis is

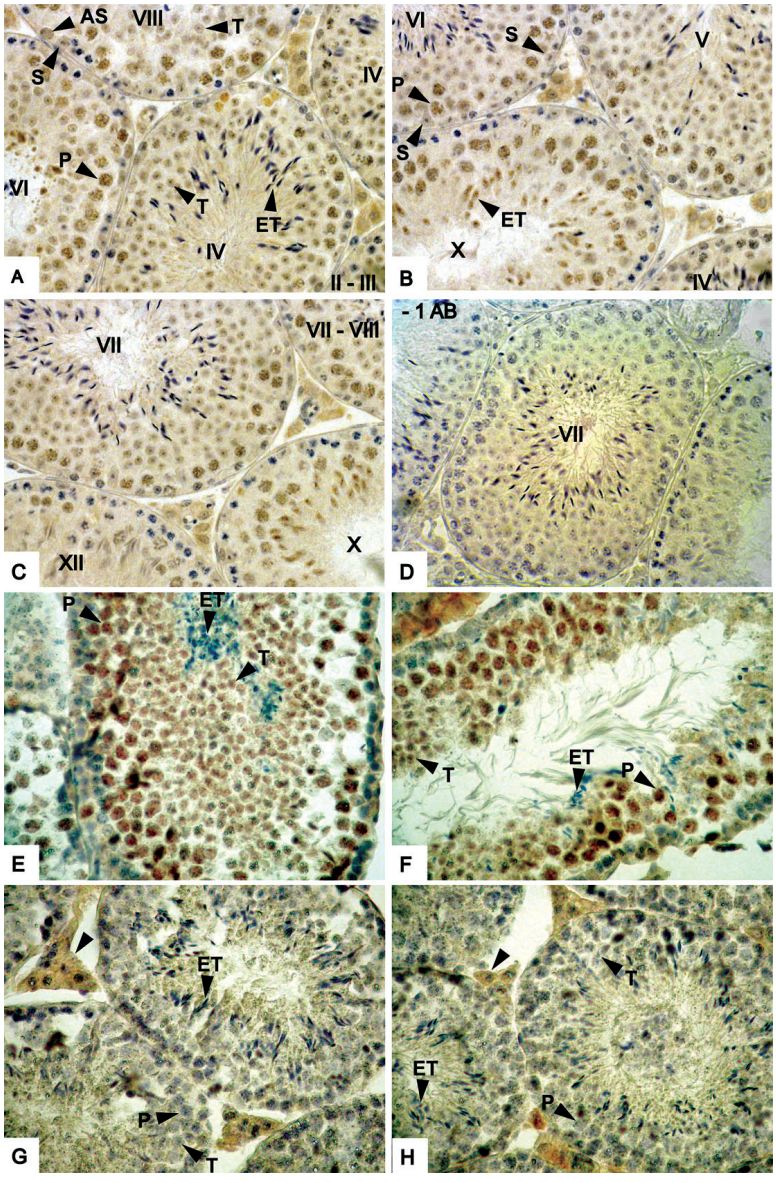

Figure 3: Expression of NANOG and GFP in mouse testes sections as detected by immunohistochemistry.
(A-C) Expression of NANOG in mouse testis at different stages of spermatogenesis. Roman figures in seminiferous tubules represent the stage of the epithelial cycle. Abbreviations: AS = type A spermatogonia, P = Pachytene spermatocyte, T = Spermatid, ET = elongating spermatids, S = Sertoli cell, (D) Negative control section from which the primary antibody was omitted in the staining procedure, (E,F) Expression of eGFP in testis sections of a mouse eGFP reporter, (G,H) eGFP staining on testis sections of a non-transgenic mouse, which served as a negative control for the staining in figures 3 E,F. Arrowheads in panels F,G, and H denote non-specific binding of the antibody to interstitial cells. Sections displayed in panels A-D were fixed in Bouins fixative; sections in panels E-G were fixed in formalin. Formalin fixation impeded accurate staging of the seminiferous tubules.

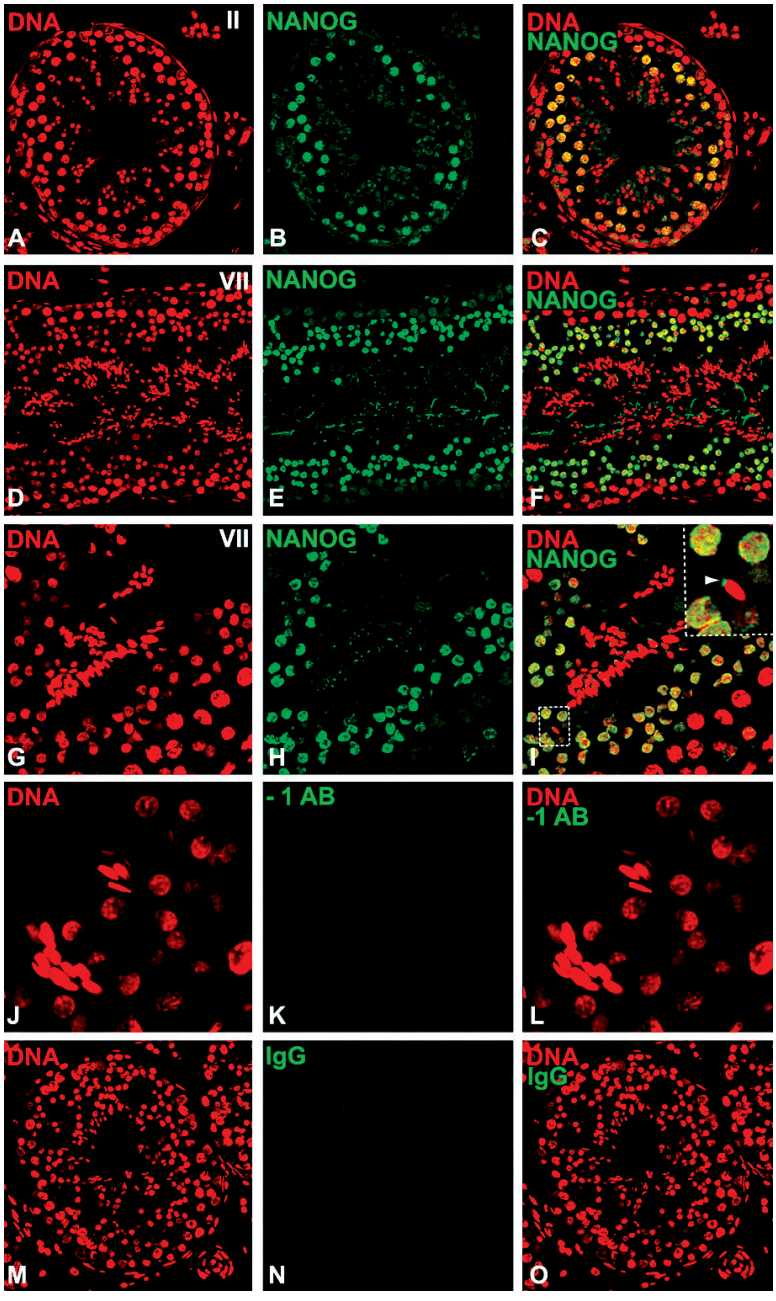

Figure 4: Expression of NANOG in dog testis as determined by immunofluorescence.
(A-I) NANOG expression in differentiating male germ cells; the top right panel of I is an enlargement of the indicated area. Arrowhead in panel I denotes binding of the antibody to the neck region of elongated spermatids, (J-L) high magnification image of section in which the primary antibody was replaced by blocking solution, to control for non-specific binding of the secondary antibody, (M-O) image of testis section that was incubated with a rabbit IgG isotype control, to control for non-specific binding of the primary antibody.

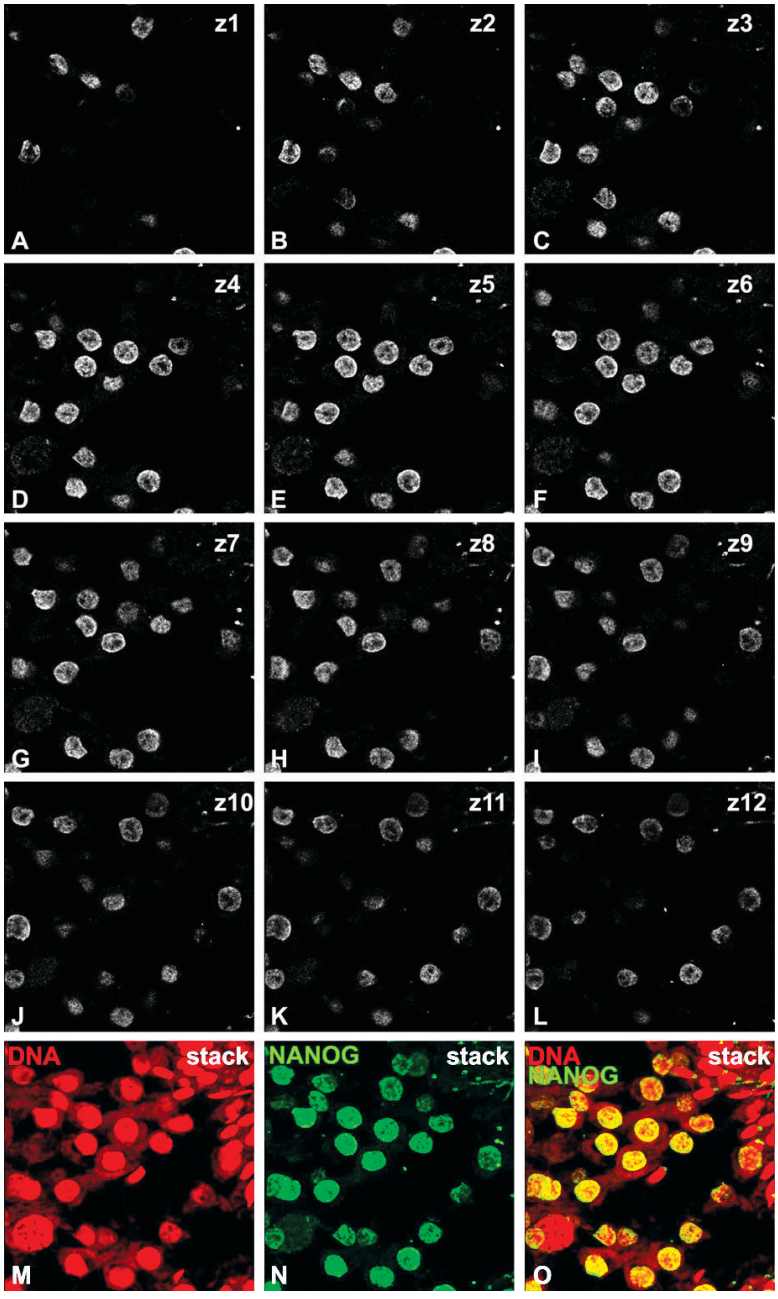

Fig 5: Top to bottom scan through nuclei of canine round spermatids confirms nuclear localization of NANOG. (A-L) grey images for NANOG stain at different heights, z1-z12 = slice number on z-axis, (M-O) stack of z-series.

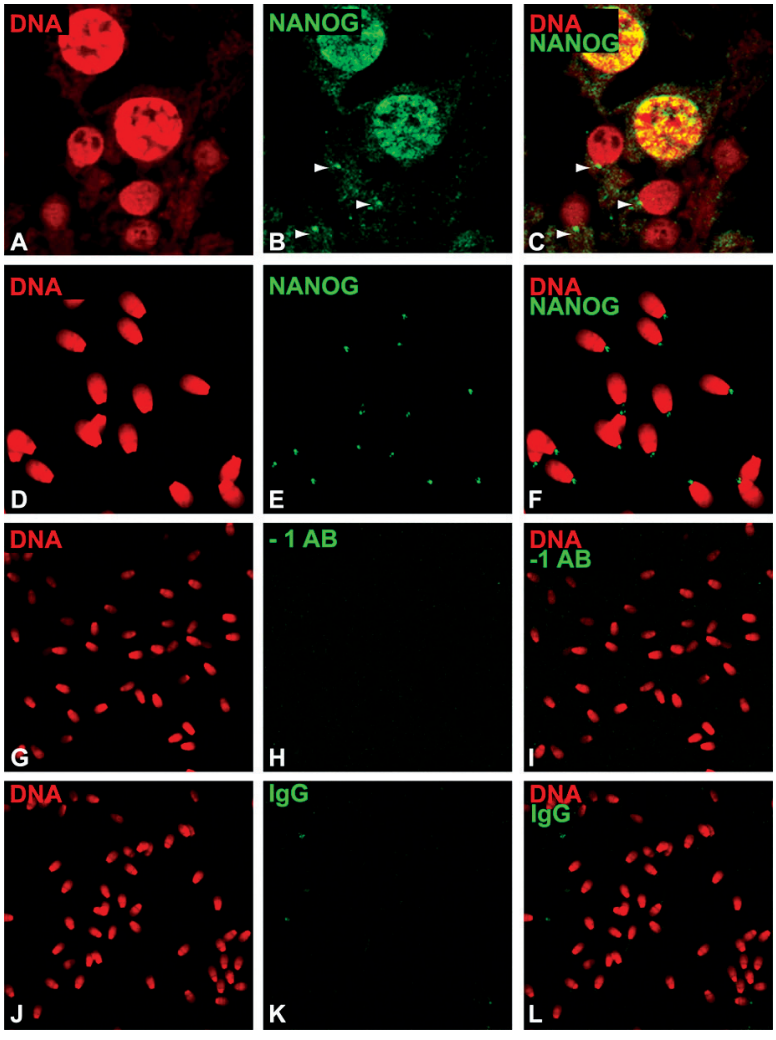

Figure 6: Binding of NANOG antibody to neck region of canine spermatids and sperm cells as determined by immunofluorescence; (A-C) (Enlargement of figure 4 A-C) Arrowheads: binding of NANOG antibody to the neck region of developing dog spermatids, (D-F) Binding of NANOG antibody to neck region of sperm cells from dog ejaculate, (G-I) image from sperm cells in which the primary antibody was replaced by blocking solution in the staining procedure, to control for non-specific binding of the secondary antibody, (J-L) image from sperm cells in which a rabbit IgG isotype control was used to control for non-specific binding of the primary antibody.

followed by spermiogenesis, in which round spermatids mature to highly specialized spermatozoa [54, 141].

Despite the obvious link between testis function and pluripotency, little is known about the involvement of NANOG in any of the processes that ultimately lead to a competent sperm cell. The aim of the current study was to determine if NANOG is expressed in the testis and whether a possible expression pattern of NANOG in the testis is conserved between species.

Therefore, the expression of NANOG was examined in adult testis of mammals ranging from mouse, dog, and pig, to man. *Nanog* transcripts and NANOG protein were detected and expression was mainly observed in pachytene spermatocytes and round and elongating spermatids. The patterns described here, suggest a conserved role for NANOG in male meiosis and spermiogenesis.

Results

Nanog mRNA and NANOG protein are expressed in testes of multiple species

Nanog mRNA transcripts were detected in mouse, dog, and pig whole testes by reverse transcriptase-polymerase chain reaction (RT-PCR; Fig.1). In the mouse, two pseudogenes and two retrotransposed genes have been described for *Nanog* [142, 143]. To determine, for that reason, whether the observed expression in mouse testis originated from the actual *Nanog* gene, expression of *eGFP* in testis tissue of a *Nanog eGFP*-reporter mouse derived from ES cells with GFP targeted to Nanog (TNG cells) [28] was analyzed. Transcripts of *eGFP* were detected by RT-PCR, which confirms that the locus of *Nanog* is transcribed in mouse testis (Fig.1). *NANOG* gene expression was also detected in human testis (Fig.1) and sequence analysis confirmed the authenticity of the *NANOG* transcripts in human testis. Sequences that correspond to pseudogenes *NANOGP4* and *NANOGP8* were also detected in cDNA of human testis.

Subsequently, the presence of NANOG protein in testis was studied by immunoblot analysis (Fig.2). A distinctive band of approximately 40 kDa was observed for mouse embryonic stem (mES) cell lysate and for lysates of dog and pig testes, but not for mouse testis lysate. In the present study, an additional band was observed at approximately 80 kDa in mES cells and in mouse, dog, and pig testes (Fig.2).

NANOG is expressed at pachytene of male meiosis and in the first steps of spermiogenesis

In order to verify the presence of NANOG protein and to get more insight in its localization in mouse testis, immunofluorescence (IF) and immunohistochemistry (IHC) was performed on sections. A distinctive temporal expression pattern in the spermatogenic stages of seminiferous tubules [144] was observed. NANOG was detected in nuclei of pachytene spermatocytes from epithelial stage IV onwards. Expression was maintained throughout meiosis and NANOG was detected until spermiogenic step 10. At sper-

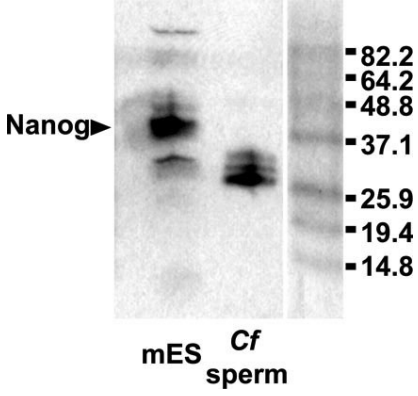

Figure 7: Immunoblot results for NANOG on canine sperm; On the right is a Benchmark protein ladder (Invitrogen) and the indicated molecular weights for each of the bands. mES = mouse embryonic stem cells, *Cf* sperm = *Canis familiaris* sperm.

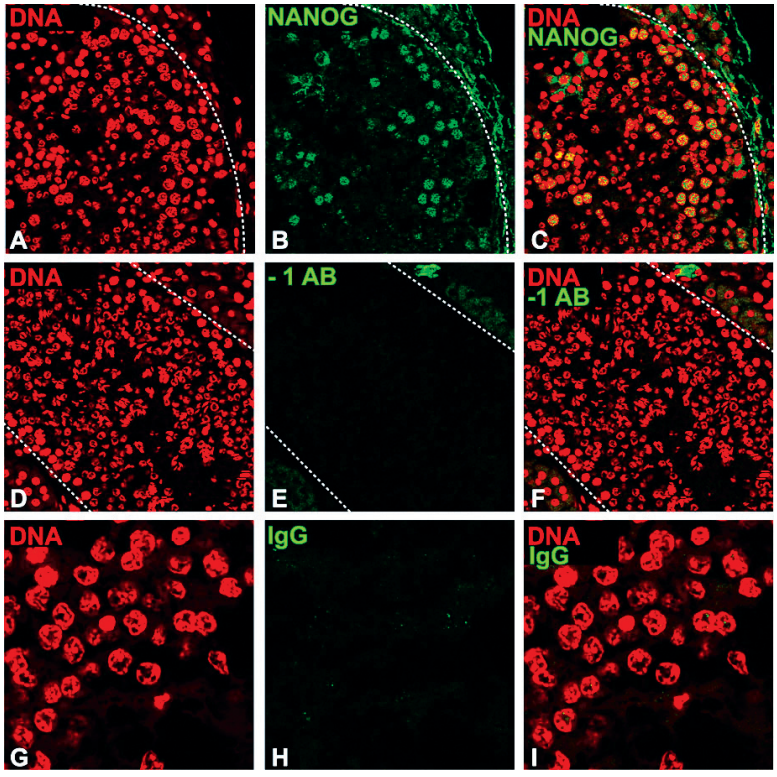

Figure 8: Expression of NANOG in pig testis as determined by immuno- fluorescence.
(A-C) NANOG expression in differentiating male germ cells, (D-F) image of section in which the primary antibody was replaced by blocking solution, to control for non-specific binding of the secondary antibody, (G-I) representative high magnification image of testis section that was incubated with a rabbit IgG isotype control, to control for non-specific binding of the primary antibody. Dashed lines in panels A-F mark the boundaries of the tubules.

miogenic step 10, NANOG expression was distinctly localized to nuclear regions (Fig.3) and from spermiogenic step 10 onwards, expression faded. NANOG was also expressed in type A spermatogonia in all stages of the epithelial cycle (e.g. Fig.3 A), but NANOG was not detected in intermediate spermatogonia (data not shown). Weak staining of Sertoli cells was also observed. Control sections in which the primary antibody solution was replaced by blocking solution did not show these patterns (Fig.3 D). In the testis of a *Nanog eGFP* reporter mouse, eGFP expression was detected in pachytene spermatocytes and round spermatids, as determined by IHC (Fig.3 E-H). The expression pattern of eGFP in the *Nanog eGFP* reporter mouse thus corresponds to the expression of NANOG in mouse testis as determined by IHC (Fig.3 A-C).

Subsequently, NANOG expression was analyzed in dog testis. As in mouse testis, NANOG was mainly detected in maturing gametes (Fig.4). NANOG was specifically expressed in round spermatids and pachytene spermatocytes of dog testis with a dynamic temporal expression pattern in the spermatogenic stages of seminiferous tubules [144]. At canine epithelial stage VI, at which spermatids initiate elongation [144], NANOG was expressed

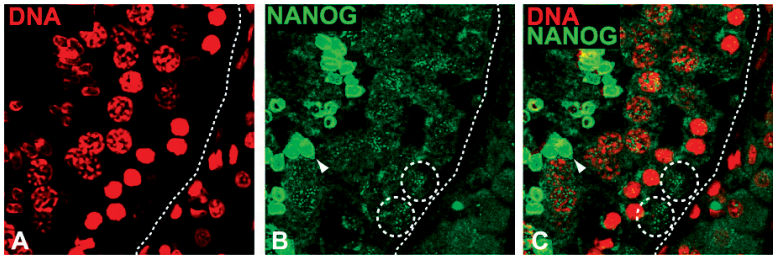

Figure 9: (A-C) Non-specific binding of NANOG antibody to the acrosome of sperm cells in adult pig testis (arrowhead). Dashed circles denote NANOG positive cells located at the basal membrane.

in pachytene spermatocytes, but not in spermatids (Fig.4 A-C). Meiosis in dogs occurs at epithelial stage VIII and metaphase configurations and newly formed round spermatids were positive for NANOG at this stage. NANOG expression was localized to round spermatids until stage V (Fig.4).

Nuclear localization of NANOG in dog testis was confirmed by scanning from top to bottom 12 confocal planes through the nuclei of round spermatids (Fig.5). A strong signal was also observed in the neck and tail region of a subset of elongating spermatids (Fig.4 G-I), which corresponds to the location of the chromatoid body [145], and in the neck region of ejaculated sperm cells (Fig.6). However, NANOG could not be detected in ejaculated sperm cells by immunoblot analysis (Fig.7). Therefore, it was concluded that labeling in the neck and tail region of sperm cells was most likely due to non-specific binding of the primary antibody.

NANOG expression was also detected in maturing gametes in adult porcine testis, as determined by IF on paraffin embedded sections (Fig.8). Expression was detected in pachytene spermatocytes (Fig. 8 A-C) and in a number of cells located at the basal membrane (Fig. 9). The antibody also showed strong non-nuclear and therefore presumably non-specific affinity for the developing acrosome (Fig. 9). The intensity of this non-specific signal impeded careful analysis of the expression in round spermatids.

Finally, NANOG expression was detected in differentiating human male germ cells as determined by IF on paraffin embedded testicular sections (Fig. 10). NANOG was detected in meiotic pachytene spermatocytes. In summary, expression of *Nanog* was observed in mouse, dog, pig, and human testes. *Nanog* transcripts and NANOG protein were detected and expression was primarily localized to differentiating germ cells.

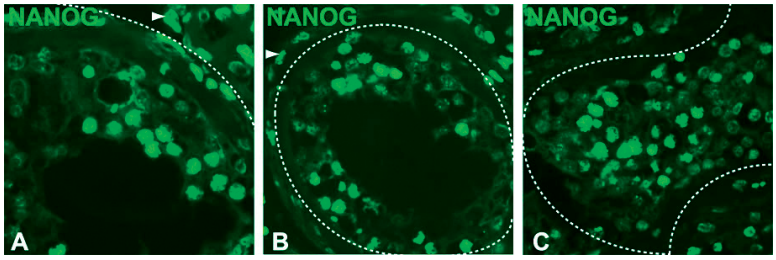

Figure 10: Expression of NANOG in human testis as determined by immuno-fluorescence on paraffin embedded sections; (A-C) NANOG expression in differentiating male germ cells; dashed lines mark the boundaries of tubules. Arrowheads denote non-specific non-nuclear binding to interstitial cells.

Discussion

Epiblast cells and primordial germ cells are important sources of pluripotent cells. This is evident by their *in vivo* behavior: epiblast cells contribute to the formation of an entire embryo, including germ cells, and primordial germ cells have the potential to develop a new organism. Additionally, from both cell types, pluripotent cell lines can be generated. *NANOG* has emerged as a major factor in determining pluripotency and its expression is generally restricted to pluripotent cells such as epiblast cells and PGCs [25-27]. Even though loss of *Nanog* does not prevent ES cells from developing into any somatic cell type, its absence is fatal to the development of germ cells [28].

Although gametes by themselves are not pluripotent, the testis can also harbor pluripotent cells, which is dramatically exemplified by formation of teratomas; tumors, composed of pluripotent cells and numerous differentiated cell types, which have most likely been derived from germ cells that by accident were not insulated from pluripotency [62]. Furthermore, it has recently been described that cultured male germ cells from neonatal and adult mouse testis can gain pluripotency and express *Nanog* [56-60].

In the current study, *Nanog* transcripts were present in whole testis samples of all four investigated mammalian species, as determined by RT-PCR. This is in line with some previous studies, that have also detected *Nanog* transcripts in testis of mouse [146] and man [147]. In the SV129 mouse strain, four retrotransposed copies of *Nanog* have been described [142] and in man a total of eleven *NANOG* pseudogenes have been described [143]. RT-PCR based detection of genes that have a large number of pseudogenes holds a potentially high risk of amplifying genomic DNA or of amplifying pseudogene-derived transcripts [142]. In this study, –RT controls did not amplify products, which excludes the possibility that the observed amplicons were of genomic origin derived from retrotransposed genes or pseudo genes. Furthermore, *eGFP* mRNA was detected in testis of a TNG *Nanog* reporter mouse [28], which is strong evidence that the *Nanog* gene is transcribed in mouse testis. Likewise, sequence analysis of human testis derived transcripts confirmed testicular expression of the human *NANOG* orthologue. Transcripts that correspond to pseudogenes *NANOGP4* and *NANOGP8* were also identified in cDNA of human testis.

In dog and pig testes, NANOG protein could be identified with immunoblot analysis (Fig. 2). A band of approximately 40 kDa was considered specific because mES cell lysate that served as a positive control displayed a band at the same height. In mouse testis lysate, NANOG expression was not detected by immunoblot analysis (Fig.2). Since whole testis lysates were used for immunoblotting, dilution by more abundant proteins could have rendered NANOG undetectable by this method. Remarkably, prominent additional bands of 80 kDa were observed in immunoblots of mouse ES cells and of mouse, dog, and pig testes. These bands do not correspond to NANOG dimers, because similar bands were also observed in samples treated with fresh DTT as reducing agent (data not shown). The origin of these 80-kDa bands is unknown.

In testes of mouse, dog, pig, and man, expression of NANOG was observed in differentiating male germ cells. The expression dynamics of NANOG in mouse and dog testes at the various epithelial stages in spermatogenesis are summarized in figure 11. The observed expression pattern for NANOG in dog testis corresponds well to that observed in mouse testis.

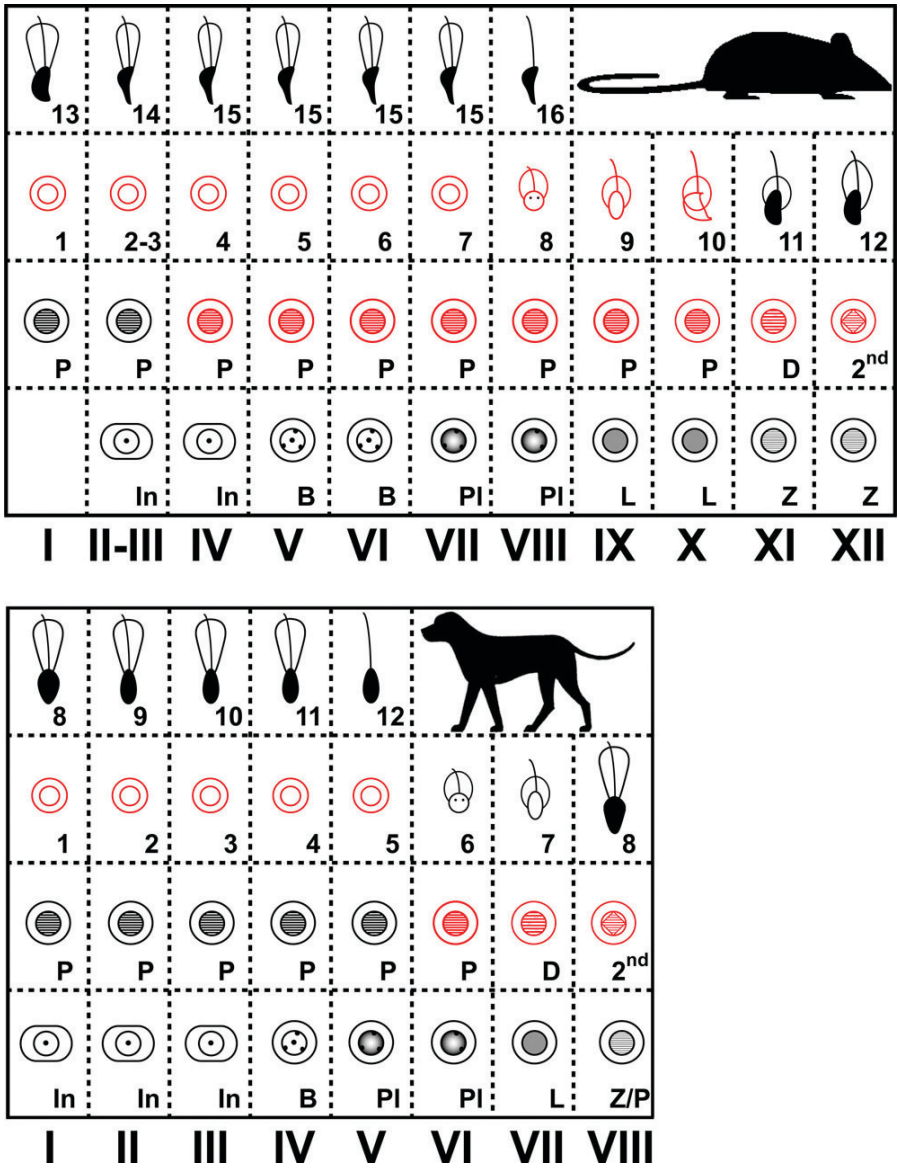

Figure 11: Models for the dynamic expression of NANOG in the epithelial cycle of murine (top) and canine (bottom) spermatogenesis.

Each column represents the combination of different cell types that are present in seminiferous tubules that are at that specific stage. Roman figures = stage of the epithelial cycle, In = intermediate spermatogonia, B = type B spermatogonia, Pl = pre-leptotene stage, L = leptotene stage, Z = zygotene stage, P = pachytene stage, D = diplotene stage, 2^{nd} = generation of secondary spermatocytes,1-16 = steps in spermiogenesis. Cell types that express NANOG are outlined in red and cell types that do not express NANOG have black and grey symbols.

In both species, early pachytene spermatocytes did not express NANOG, but at later stages NANOG expression in pachytene spermatocytes was initiated. Expression was maintained after completion of meiosis and expression was progressively lost in the course of spermiogenesis. Expression of NANOG was also observed in mouse type A spermatogonia throughout the epithelial cycle, but not in intermediate spermatogonia. This could indicate that NANOG is involved in maintaining a transcriptionally active state in type A spermatogonia.

A recent report describes expression of NANOG in porcine testis in spermatocytes, round spermatids, and occasionally in spermatogonia [100]. NANOG expression has also been reported in spermatogonia, spermatocytes, and spermatids of human testis [147]. Importantly, the two latter reports independently describe expression of NANOG in similar cell types as in the current study. Moreover, the antibody that was used by Ezeh et al. was raised against a distinct epitope from those that were used in the present study.

In some previous studies, *Nanog* expression was not detected in testis, even though expression was observed in cells of the ICM, the epiblast, and in primordial germ cells [26, 27], which suggests that expression levels are probably relatively low in differentiating male germ cells. The sensitivity of the various approaches in the current study could have been decisive for the successful detection of NANOG in testis. Multiple antibodies of different origins showed specific staining for NANOG in different species. Consequently, it is unlikely that the signals described here originate from non-specific binding.

Clear immunofluorescent staining for NANOG was observed in the neck region of canine sperm cells, but not in sperm cells of other species. Expression of NANOG protein in canine sperm cells could not be confirmed by immunoblot analysis. Strong reactivity was observed to several low molecular weight proteins, although these could not be identified as truncated forms of NANOG. Therefore, and because of the described function of NANOG as a transcription factor, we do not know the nature of the observed patterns in the neck region of canine sperm cells.

The capacity of cells, e.g. pluripotent or more restricted, is largely determined by epigenetic programs, which are heritable non-genetic alterations that affect cellular phenotypes, such as histone modifications and DNA methylation [148]. NANOG is considered an epigenetic modifier of the germ line [28] and its embryonic expression coincides with two major reprogramming events that are intimately linked with pluripotency. The first event is the formation of the pluripotent epiblast in late blastocysts, a source of ES cells. The second period of reprogramming is established in migrating PGCs, a source of EG cells [149, 150]. *Nanog* null cells can participate in the development of chimaeric embryos, but primordial germ cells that are derived from these cells are lost from embryonic day 11.5 [28]. Therefore, NANOG is considered a key player in setting these epigenetic cell states with minimal epigenetic control [28].

In the course of spermatogenesis, male germ cells undergo vast and critical epigenetic changes intended for successful progression through meiosis, meiotic sex chromosome inactivation, post-meiotic sex-chromosome repression, and chromatin remodeling [141]. The fundamental role of histone and DNA methyltransferases and other epigenetic modifiers in male meiosis is exemplified by various knockout studies that result in arrest and/or apoptosis of early to late pachytene spermatocytes [141, 150].

A candidate epigenetic event in spermatogenesis that NANOG could be involved in is histone deacetylation. NANOG is known to interact with histone deacetylases [151, 152] and inhibition of histone deacetylase-1 results in male infertility through apoptosis in spermatogonia and spermatocytes [153]. The different techniques and the rigorous controls that were used in the present study clearly demonstrate that *Nanog* is expressed in differentiating male germ cells of mouse, dog, pig, and man. The reported meiotic and spermiogenic association of NANOG in male germ line cells, which seems to be conserved between species, suggests a role for NANOG as epigenetic modifier in spermatogenic reprogramming.

Materials and Methods

Sources of testes

Bl/6 mouse testes were surplus material left over from fertile mice that were offered for an experiment that was approved of by the Institutional Animal Care and Use Committee of Utrecht University. Testes from reporter mice with *eGFP* driven by the *Nanog* promoter were obtained from MRC Center Development in Stem Cell Biology, Institute for Stem Cell Research, School of Biological Sciences, University of Edinburgh, and had Bl/6 and SV129 backgrounds. Canine testes were obtained from healthy dogs that underwent elective gonadectomy at the clinic of the Department of Clinical Sciences of Companion Animals, Faculty of Veterinary Medicine, Utrecht University. Adult pig testes were collected at a local slaughterhouse. Human testis samples for RNA isolation were obtained at the Center for Reproductive Medicine, Academic Medical Center, Amsterdam, from 2 patients undergoing bilateral castration as part of prostate cancer treatment in the Academic Medical Center, Amsterdam. Spermatogenesis in both patients was normal as determined by testis morphology. Sections embedded in paraffin of human testes were obtained from the Biobank at the Department of Pathology of the University Medical Center in Utrecht. There were no indications that this material was derived from infertile men or men suffering from testicular diseases as determined by testis morphology.

RNA extraction, reverse transcription, and PCR

From human testes, mRNA was extracted using the MagNA Pure LC (Roche, Basel, Switzerland) according to the manufacturer's protocol. For cDNA synthesis 0.03 µg of mRNA of human testis tissue was used in a reverse transcriptase reaction with random primers and M-MLV reverse transcriptase (Invitrogen, Groningen, The Netherlands). For mouse, dog, and pig, total RNA was isolated from 50-100 mg testis sections with Trizol (Invitrogen), according to the manufacturer's protocol with an additional purification step immediately following phase separation. In this extra step, one volume of phenol:chloroform:isoamyl alcohol (Fluka, Sigma-Aldrich, Zwijndrecht, The Netherlands) was added to the aqueous phase and samples were mixed, incubated at room temperature (RT) for 5 min, and centrifuged. Subsequently, samples were incubated at RT for an additional 5 min, after which the aqueous phase was transferred to a new tube and put on ice. From here, the Trizol RNA isolation protocol was resumed, from the RNA precipitation step onwards. The presence of *Nanog* pseudogenes asks for rigorous negative controls in RT-PCR experiments [142]. Therefore, RNA was treated with 2 µl DNAse (2,75 Kunitz units/µl; Qiagen, Venlo, The Netherlands) for 20 min at 37°C, after which incubation at 65°C for 10 min inactivated the enzyme. Next, RNA was reverse transcribed to first strand cDNA with Superscript III (Invitrogen) according to the company's instructions. Random primers were used and for each sample an equivalent mixture was prepared, from which Superscript III was omitted, to control for genomic DNA contamination. Reverse transcribed cDNA samples were stored at –20°C before they were used in a polymerase chain reaction. Species-specific primers for *Nanog* were designed with Beacon Designer 4 (PREMIER Biosoft International, Palo Alto, CA, USA; Table 1) Complementary DNA amplification was performed with HotStarTaq (Qiagen) according to the manufacturer's protocol. The reaction mixture contained 2nM MgCl2 and

Table 4: Primers used for RT-PCR and sequence analysis

Gene	Genbank number	Primers	Ta (°C)	Amplicon size
Mouse *Nanog*	NM_028016	F: 5'-AGATGCGGACTGTGTTCTC-3' R: 5'-TGCGTTCACCAGATAGCC-3'	58	281
Canine *NANOG*	XM_543828	F: 5'-CCGTCTCTCCTCTTCCTTC-3' R: 5'-CACTGTTGCTCTCCTTTGG-3'	54,3	348
Porcine *NANOG*	NM_001129971	F: 5'-CTCTCCTCTTCCTTCCTC-3' R: 5'-ATCACACTGTTGCTATTCC-3'	58	345
Human *NANOG*	NM_024865	F1: 5'-CCTCCAGCAGATGCAAGAACTC-3' R1: 5'-GTAAAGGCTGGGGTAGGTAGGTG-3'	58	F1R1: 172
		F2: 5'-TACCTACCCCAGCCTTTACTCTTC-3' R2: 5'-AGGAGAATTTGGCTGGAACTGC-3'		F2R2: 262
eGFP	EU541500	F1: 5'-CTGGTCGAGCTGGACGGCGACG-3' R1: 5'-CACGAACTCCAGCAGGACCATG-3'	59	630

F = forward primer, R = reverse primer. Ta = annealing temperature used in PCR reaction.

0.5 µM of each primer. To 24 µl of mixture, 1 µl of sample was added, after which the PCR was run in a MyCycler (Bio-Rad). Each PCR started with a 15-min dwell at 94ºC, followed by 40 cycles with 3 steps/cycle; 30 sec melting of double strands at 94ºC, 30 sec annealing at the primer specific annealing temperature (see table), and finally 30 sec elongation at 72ºC. For each sample, -RT negative controls were used in all reactions to seclude the possibility of mistaking genomic DNA for transcripts. The amplicons (10 µl) were run on 1% agarose gels and sequence analysis confirmed Nanog transcripts were amplified by the primer pairs in testis cDNA of mouse, dog, pig, and human,.

Sequence analysis

Sequence reactions were performed on 10- to 20-fold dilutions of PCR products with Terminator Ready Reaction mix (Applied Biosystems, Foster City, USA) according to the manufacturer's instructions and with the same primers that were used in the original amplification. Sequence reaction products were then analyzed on an ABI prism 3130*xl* genetic analyzer (Applied Biosystems). Alternatively, PCR products of the appropriate sizes were excised from the gel and purified with a gel purification kit, according to the manufacturer's instructions (Qiagen). Next, purified products were ligated into a pCRII plasmid vector (pCRII; Invitrogen), which was subsequently transformed into competent *E. coli*. Transformants were selected and plasmid DNA was isolated, after which inserts were further amplified by PCR using M13 primers (Table 1). Next, a 10-fold dilution of these products was used in sequence reactions. The sequence reaction mix included Sp6 primers (5'-ATTTAGGTGACACTATAG-3') or T7 primers (5'-GGGATATCACTCAGCATAAT-3').

Immunoblot analysis

Total protein was extracted with lysis buffer containing 25 mM Mes, 150 mM NaCl, 1mM EGTA, protease inhibitors (Roche), and 1% tritonX100. The amount of protein was determined by a DC protein assay (Bio-Rad) and 5-20 µg of total protein, was boiled for 5 min in Laemmli buffer (Bio-Rad) with 0.5 M β-mercaptoethanol and separated by electrophoresis on a 12% Tris–HCl PAGE gel. To determine protein sizes, a benchmark pre-stained protein ladder was run on each gel. After electrophoresis, proteins were transferred to a Trans-Blot nitrocellulose transfer membrane (Bio-Rad). Subsequently, membranes were blocked overnight at 4°C with 5% Blotting Grade Blocker non-fat dry milk (Bio-Rad), in PBST and incubated with 1ug/ml rabbit polyclonal anti-mouse NANOG (Chemicon) in 5% non-fat dry milk for 1 hr at room temperature. Membranes were washed in PBST, and subsequently incubated for 1 hr at RT in a horseradish peroxidase-conjugated goat anti-rabbit IgG (Pierce, Rockford, USA) secondary antibody

Table 5: Antibodies used for immuno applications.

Immunogen	Source	Concentration	Description	Application
AA1-50 mouse NANOG	A300-398A (Bethyl)	10 µg/ml	Rabbit polyclonal	IHC mouse
Full length mouse NANOG fusion protein	AB21603 (Abcam)	1-2 µg/ml	Rabbit polyclonal	IF Dog, human
Synthetic peptide mouse NANOG	AB5731 (Chemicon)	1 µg/ml	Rabbit polyclonal	IB, IF pig
Human NANOG	14-5768 (eBio-science)	1-2 µg/ml	Mouse monoclonal	IF human
GFP (B-2)	SC9996 (Santa Cruz)	1:500	Mouse monoclonal	IHC reporter mouse
Rabbit IgG	31460 (Pierce)	0.16 µg/ml	Goat polyclonal, peroxidase conjugated	IB

AA = Amino Acids, IHC = immunohistochemistry, IF = immunofluorescence, IB = immunoblotting.

solution diluted 1:5000 in 5% non-fat dry milk. Specific binding of the antibodies was visualized using SuperSignal West Dura Extended Duration Substrate (Pierce, Rockford, IL) after which the blots were exposed to film (Kodak). The primary antibody is known to bind non-specifically to a 55 kDa protein and therefore, bands detected at that height were considered non-specific.

Immunohistochemistry, Immunofluorescence, and Confocal Laser Scanning Microscopy

After collection, testes were fixed overnight (o/n) in 4% PFA or Bouins fixative and embedded in paraffin using standard procedures the following day. Sections were cut at 5-7 µm and mounted on superfrost plus slides (Menzel, Braunschweig, Germany), which were dried o/n at 37°C and stored at 4°C until further use. For IHC with the NANOG antibody (Table 2) on mouse sections, endogenous peroxidases were blocked with 1.5% H_2O_2 (Merck) in 40mM Citric Acid and 120 mM Na_2HPO_4 for 15 min at RT. After antigen retrieval with 10mM EDTA buffer (20 min, pH 9), non-specific binding sites were blocked with 1% bovine serum albumin in PBS for 30 min at RT. After blocking, sections were incubated with rabbit anti-nanog (Bethyl, Montgomery, USA) in blocking solution overnight at 4°C. Slides were incubated with a Powervision poly-HRP-anti-rabbit conjugated secondary antibody (ImmunoVision Technologies) for 1 hr at RT. Subsequently, sections were incubated in Fast 3,3'-diaminobenzedine (Sigma-Aldrich) and counterstained with heamatoxylin. Slides were mounted with Pertex (Klinipath, Duiven, The Netherlands).

For immunohistochemistry with the GFP antibody (Table 2), PFA fixed mouse sections were deparaffinized after which endogenous peroxidases were blocked with methanol/ 0.3% H_2O_2. Next, antigen retrieval was performed by boiling the slides for 10 min in EDTA buffer at pH9. Endogenous biotin was blocked by incubation of the sections with avidin and biotine respectively. Subsequently, non-specific binding was blocked with 10% normal goat serum in 0.05% Tween in PBS (PBST) for 30 min at RT after which the blocking solution was replaced by primary antibody solution diluted in 2% normal goat serum (NGS) in PBST (60 min at RT). Sections were then incubated in biotinylated goat anti-mouse IgGs (1:100; Dako, Heverlee, Belgium) in 2% NGS in PBST for 30 min at RT. After 20 min incubation with horseradish peroxidase (HRP)-conjugated streptavidin (DAKO) in 2% NGS in PBST, slides were incubated in AEC solution (Sigma-Aldrich) and counter stained with hemaelin.

For immunofluorescence, slides were deparaffinized in xylol and subjected to antigen retrieval by boiling the slides for 10 min in citrate buffer at pH2 or pH6. For canine testis sections, additional antigen retrieval was performed by putting the slides in methanol for 10 sec. Following antigen retrieval, slides were permeabilized in TBS with 0.05% tween (TBST) and with TritonX100 (0.1%). Permeabilized slides were blocked for 1 hr in TBST with 0,5% BSA (Sigma-Aldrich) followed by o/n incubation with the

primary antibody (Table 2) in blocking solution at 4°C. The following day, slides were incubated in the secondary antibody in blocking solution for 1hr. at 4°C, after which the slides were counterstained with TOPRO-3 (Invitrogen) and mounted in Vectashield. DNA could not be visualized after antigen retrieval at pH2.

For immunofluorescence on sperm cells, semen was fixed in 2% PFA and washed with PBS. Droplets of sperm cell suspension were placed on Poly-L-Lysine coated slides and allowed to dry. From there on, above described staining procedure was continued from the permeabilization step onwards.

Fluorescent images were retrieved at the Center for Cell Imaging at the Faculty of Veterinary Medicine in Utrecht. Fluorescent signals were visualized using a Confocal Laser Scanning Microscope (Bio-Rad) and on an epifluorescence microscope from which pictures were captured with a CCD camera. Within each session, identical settings were used to image NANOG stains and negative controls. For post-capture analysis, only brightness and contrast were used to enhance signals and negative control images were treated in an equal manner.

Chapter VII

Discussion: Major reprogramming events and pluripotency of cells

Major reprogramming events and pluripotency of cells

Early lineage segregation

Mouse pluripotent cell lines can be derived from a few distinct instances of the germline: i.e. the inner cell mass of preimplantation embryos (ES cells), from migrating PGCs (EG cells), and from neonate and adult testis (SSCs and ES-like cells). However, cows and pigs have been resilient to the derivation of pluripotent cell lines. Most attempts in these species have focused on the generation of ES cell lines and the lack of success has been attributed to the differences in embryology between livestock species and the mouse. There are indeed clear morphological differences between these species, but it has been unclear how these contribute to the difference in ES cell derivation or to culture differences necessary for self-renewal. Our knowledge on factors that contribute to lineage segregation and the origin of pluripotent cells in mouse blastocysts has considerably increased over the past few years and OCT4, CDX2, NANOG, and GATA6 have emerged as key players.

As described in chapter 3, careful analysis of the expression of CDX2 and OCT4 in bovine and porcine development demonstrated that these factors are co-expressed in the trophectoderm [37, 38, 115], which suggests that reciprocal inhibition of these two factors does not underlie the first lineage segregation in these two species as it has been suggested for the mouse [17, 20, 21].

Recently, it has been hypothesized that the first lineage segregation of inner cell mass (ICM) and trophectoderm (TE) depends on Ras-mitogen-activated protein kinase (MAPK) signaling [154]. In support of this, ES cells tend to transform to TE cells after constitutive activation of Ras. Furthermore, in ES cells with constitutively activated Ras, expression levels of CDX2 are elevated and expression levels of NANOG are decreased. Remarkably, in this study the previously reported reciprocal inhibition of CDX2 and OCT4 [20] could not be replicated and the authors hypothesize that lineage segregation depends on reciprocal interaction between CDX2 and NANOG instead [154].

In the same study, it is reported that Erk2, a critical downstream intermediate of MAPK signaling, is asymmetrically distributed in 8-cell stage mouse embryos. An apical restriction of Erk2 could promote CDX2 expression and consequently trophectoderm formation in the apically derived daughter cell. In support of this hypothesis, embryos cultured in presence of an inhibitor of the MAP kinase MEK (PD98059) did express decreased levels of CDX2 and were less able to develop to blastocysts when PD98059 was added before the 8-cell stage [154]. However, in contrast, an effect of this inhibitor on mouse blastocyst development was not found in another study [155]. We conducted a pilot study to examine the role for MAPK signaling in *in vitro*-produced bovine embryos, which were cultured in the presence of 25μM PD98059 (dissolved in DMSO) or in DMSO alone (negative control). An effect of the MEK inhibitor PD98059 on blastocyst development was not observed, and blastocyst rates were approximately equal between the control group and the inhibitor group (unpublished results). These data indicate that in bovine development, segregation of ICM and TE does not depend on the MAP kinase MEK.

Another important finding described in chapter 3 is that *NANOG* transcripts and protein

were not detected in expanded *in vitro*- and E5.0 *in vivo*-derived porcine blastocysts, but clear expression of NANOG protein was observed in a few cells of the ICM of bovine blastocysts. Again, this demonstrates variance between mammals in the expression pattern of a transcription factor that is important for pluripotency in murine cells. The group of dr. I. Chambers has demonstrated transgene expression of NANOG, as determined by immunofluorescence, in a cell line that was transfected with porcine NANOG. However, NANOG expression was not detected when that same antibody was used for whole mount immunofluorescence on in vivo-derived early porcine blastocysts (Ian Chambers, personal communication). Elevated expression levels of *NANOG* mRNA can be detected in the epiblast of porcine embryos from E6.5 of development until E10.5 (Leonie du Puy, personal communication). If NANOG protein is also expressed at these later stages of pig development remains to be determined. These findings suggest that temporal expression of *NANOG* is differently regulated in porcine embryos, with the consequence that in this species expression of *NANOG* is no longer correlated with the segregation of primitive endoderm and epiblast.

In mouse blastocysts, the ICM consists of precursors of primitive endoderm and primitive ectoderm that express the transcription factors GATA6 and NANOG respectively. This mosaic expression depends on Grb2-Ras-MAP kinase signaling [30]. Mouse *Grb2*$^{-/-}$ embryos fail to develop primitive endoderm and have a homogenous ICM of which all cells express NANOG but do not express GATA6 [29, 30]. The *Grb2*$^{-/-}$ phenotype is similar to that of mouse embryos lacking *Fgf4* or *FgfR2*, which also fail to develop primitive endoderm [31-33]. Consequently, a model has been proposed in which GRB2 activation through FGF signaling leads to suppression of *Nanog* and activation of *Gata6* [30, 156]. This model has been confirmed by functional studies with chemical inhibitors in mouse ES cells. For example, tyrosine phosphorylation of FGFR2 attenuates FGF signaling, a process that is inhibited by sodium vanadate, a general inhibitor of tyrosine phosphatases [156]. In ES cells treated with sodium vanadate, expression of primitive endoderm markers are increased and expression levels of NANOG are decreased. This effect can be counteracted by treatment with the inhibitor PD98059, which specifically inhibits the MAP kinase MEK [156]. These results suggest that embryos will homogenously express NANOG in the ICM, when cultured in presence of the MEK inhibitor PD98059. To test this hypothesis, we conducted a pilot study in which *in vitro* produced bovine embryos were cultured in the presence of 25µM PD98059 or in DMSO alone. After 7 days of culture, blastocysts were fixed in 4% PFA and subjected to double labeling with whole mount immunofluorescence as described elsewhere [157], with a mouse monoclonal antibody against NANOG (eBioscience) and a rabbit polyclonal against GATA6 (Santa Cruz). Embryos that were cultured in presence of the MEK inhibitor (n = 6) showed a pepper and salt distribution of NANOG and GATA6 expressing cells, similar to embryos in the negative control group (DMSO; n = 6; Fig. 1). However, the number of NANOG positive cells was significantly higher in the embryos cultured in presence of the MEK inhibitor compared to the negative control group (Fig.1). In contrast with these findings, mouse embryos that were cultured in the presence of the MEK inhibitor did not have different numbers of NANOG positive cells compared to control embryos [154]. The findings of this preliminary study suggest that in bovine development, segregation of epiblast and primitive endoderm is influenced by the MAP kinase MEK.

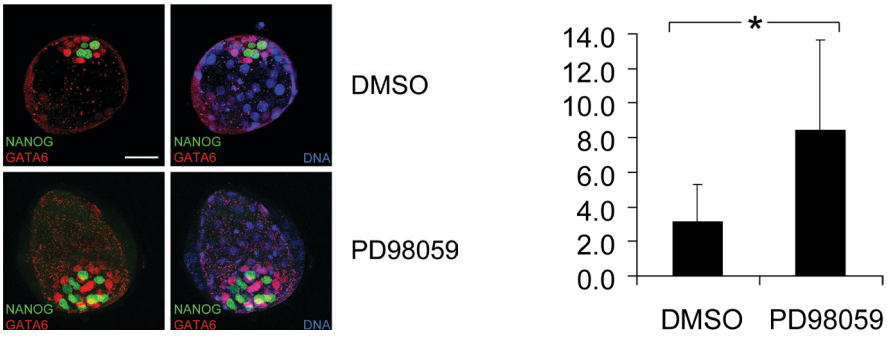

Figure 1: Left: Mottled expression pattern of NANOG and GATA6 in bovine embryos that were cultured in presence of DMSO (negative control; top panels) or in presence of 25µM MEK-inhibitor PD98059, dissolved in DMSO (lower panels). Scale bar = 50 µm; **Right:** Number of NANOG positive cells in bovine embryos that were cultured in presence of DMSO (n = 6; negative control) or in presence of 25µM MEK-inhibitor PD98059 (n = 7; dissolved in DMSO). Asterisk denotes significant difference (2-tailed Student's T-test; $p < 0.05$).

The results described in chapter 3 and in above discussion section clearly demonstrate that parts of the molecular mechanism(s) behind lineage segregation are still obscured. Increasing knowledge on the signaling pathways involved in mouse lineage segregation facilitates the use of functional studies in early development of non-rodent species such as above pilot experiment. These types of studies could provide valuable contributions to the putative establishment of pluripotent ES cell lines from livestock species.

Spermatogonial stem cells and reprogramming

In chapter 4, cell cultures of neonate pig testis are described that express various spermatogonial stem cell markers and somatic cell markers. Furthermore, it is demonstrated that of four commonly used growth factors (LIF, GDNF, EGF, FGF) in mouse SSCs, FGF had the largest influence on the expression of *NANOG*, *GATA4*, and *OCT4* in primary cell cultures derived from porcine neonate testis cells. Presence of FGF negatively influenced *NANOG* expression levels, whereas *GATA4*, and *OCT4*, expression levels were enhanced in cultures with FGF. The findings in this chapter could facilitate the establishment of long-term cultures of porcine male germ cells.

In chapter 5, it is described how TRP53 and PTEN independently suppress *Nanog* in mouse spermatogonial stem cells. Little is known about the mechanism of pluripotency and how developing germ cells are insulated from pluripotency, while maintaining the capacity to contribute to a totipotent zygote. The observations described in chapter 5 give more insight in some of these molecular processes in SSCs. Control of this process would allow induction of pluripotency in SSCs, which could also be applied to future SSC lines from livestock species to obtain an alternative source of pluripotent cells in these species.

The field of stem cell research was revolutionized by the finding that mouse somatic cells can be reprogrammed to a pluripotent state upon retroviral induction of a combination of the factors *c-Myc*, *Klf4*, *Oct4*, and *Sox2* [67]. Shortly thereafter, other studies reported the derivation of induced pluripotent stem (iPS) cells in mouse and human [69, 113, 127]. The generation of patient-specific iPS cell lines should overcome the problem of immune rejection when

these cells are used in cell therapy. Another major advantage of iPS cells is that it circumvents many of the ethical issues that are associated with therapeutic cloning. Since retroviruses are retro-transcribed into the host-genome, questions were raised whether the integration site was important for reprogramming to take place. Furthermore, because of the genomic insertions, the suitability of these cells for cell therapy was questioned. These issues have been addressed by a recent study in which it was demonstrated that pluripotency could be induced without insertional mutagenesis by lentiviral transfection of mouse fibroblasts and mouse liver cells with *c-Myc*, *Klf4*, *Oct4*, and *Sox2* [158].

The approach of iPS cell-research will most certainly be applied to livestock species as yet another source of pluripotent cells. Nevertheless, independent of the source, pluripotency of cells is just one side of the coin in the process of deriving pluripotent cell lines. The other side of the coin is self-renewal; the culture conditions should support proliferation without differentiation. Long-term culture of mouse ES cells depends on the cytokine LIF, that signals through heterodimers of LIFR and GP130. Therefore, it is surprising that embryos that lack LIF, LIFR or GP130, can develop a normal epiblast [159-163]. However, GP130 mutant embryos fail to develop an epiblast if implantation is delayed by diapause; i.e. delayed implantation common to lactating females [164]. It has been hypothesized that LIF signaling suppresses differentiation of epiblast progenitors to epiblast cells, which is consistent with the function of LIF signaling in diapause and mouse ES cells [157].

Human ES cell propagation does not require LIF signaling, but depends on FGF and activin instead [165]. Activin signaling is also essential for self renewal of pluripotent stem cells derived from the epiblast (EpiSCs) of pre-gastrulating mouse embryos [166]. The similarities in requirements, growth characteristics, expression patterns, and developmental potential between EpiSCs and human ES cells have led to the hypothesis that hES cells are akin to late epiblast cells [166]. These observations could implicate that attempts to generate pluripotent cell lines from livestock have a higher chance of success when cells from the pluripotent epiblast are maintained under defined hES cell culture conditions. If pluripotent cells from livestock species will self-renew under these conditions remains to be investigated. A potential strategy could be the generation of induced pluripotent cells that constitutively express the reprogramming factors from doxycycline-inducible transgenes. Removal of doxycycline from the culture medium will result in differentiation of the cells, unless the requirements for self-renewal are fulfilled. With such cells, the effect of culture conditions on self-renewal can be systematically investigated.

Pseudogenes

A remarkable finding of chapter 6 is the expression of *NANOG* pseudogenes in human testes. Retrotransposed genes and more degraded pseudogenes have been considered as fossils of protein encoding genes [167]. Pseudogene sequences that do not code for functional proteins, because of frameshifts or premature stop codons, have been termed junk for the lack of apparent function. This view has changed since the discovery that, in mouse and fruit fly, pseudogene transcripts can regulate transcript levels of closely related protein coding genes through RNA interference [168-172]. Long double stranded RNAs are formed when reversely oriented

transcripts of pseudogenes hybridize to transcripts of the parent genes. These double-stranded RNAs are processed by Dicer, which results in 21-nucleotide siRNAs. Subsequently, the RISC complex and the siRNAs interact to degrade transcripts with complementary sequences such as the parent gene. Alternatively, transcripts of pseudogenes that have a nearby duplication and inversion of the parent gene can fold into a hairpin, which will then enter the RNAi pathway [167].

A large number of retrotransposed copies have been identified of the ES cell-specific genes *Nanog*, *Oct4*, and *Stella* [173]. In the mouse, two retrotransposed genes (*NanogPc* and *NanogPd*) and two more degraded pseudogenes (*NanogPa* and *NanogPb*) have been described for *Nanog*, and in man a total of ten *NANOG* pseudogenes (*NANOGP1-NANOGP10*) and a remnant of an eleventh pseudogene have been described [142, 143]. At the 5' end of *NanogPa*, the 3' half of the region homologous to Nanog exon 4 has inverted and integrated [143]. A blast search of the 3'UTR of mouse *Nanog* demonstrates that this sequence has also inverted and integrated in the pseudogene *NanogPa* sequence. Since *NanogPa* is the evolutionary oldest of mouse *Nanog* pseudogenes [142], the high number of identities with the 3'UTR of its ancestor suggests that selective forces have maintained a large part of the sequence. Human *NANOG* and *NANOGP1* are located on chromosome 12 and have the same orientation [143]. Part of the terminal exon and 3'UTR of NANOGP1 has been duplicated and inserted into the second intron in the reverse orientation [143]. Furthermore, the 3'UTR region of *Homo sapiens NANOG* is 99.07% conserved in *NANOG* pseudogene 8 on chromosome 15, which indicates that this sequence has been subjected to selective pressures. In addition, the reversed orientation of parts of the pseudogenes in mouse and human, suggests that transcripts derived from these pseudogenes can form hairpins, long double-stranded RNAs with transcripts from the actual gene, or long double-stranded RNAs with transcripts from other pseudogenes. Since these products can enter the RNAi pathway, *Nanog* pseudogenes in mouse and human have the potential to regulate expression of the parental *Nanog* gene.

To investigate the expression of pseudogenes in testis further, we performed a single base extension experiment. A single base extension experiment is very similar to a sequencing reaction, but with the difference, that the reaction mixture contains only fluorescently labeled di-deoxynucleotides. As a result, only one base can be added to the primer. Primers were designed that were used to amplify mouse *Nanog* and each *Nanog* pseudogene. Subsequently, a single base extension was performed with four primers that were developed to flank base pairs not conserved between the pseudogenes. The combination of the resulting four bases allowed identification of the origin of the transcripts. In testis cDNA of mouse from the Bl6 strain, *Nanog* transcripts originated from the actual *Nanog* gene and pseudogene-derived transcripts could not be detected. However, in the SV129 background, transcripts originated from *Nanog*, *NanogPa*, and *Nanog Pd* (unpublished results).

Biogenesis of endogenous siRNAs depends on Dicer and a component of the RISC complex called Argonaute2 [168, 169, 171, 172, 174]. A pilot study was conducted to determine if *Nanog* transcript levels are regulated by endogenous siRNAs in mouse testis. Expression levels of Nanog were examined in knockout mouse with Dicer specifically deleted in the germline, kindly provided by Dr Katsuhiko Hayashi [175]. Expression levels of *Nanog* in testis of 2 week-old animals or in FACS sorted Mvh-positive spermatocytes were not different

from control animals that carry an undeleted copy of the transgene. These preliminary findings suggest that *Nanog* transcripts are not degraded by endogenous siRNAs in mouse testis. Nevertheless, the genetic architecture strongly suggests that Nanog-pseudogenes could play a regulative role in the expression of their ancestor. To further examine the function of *Nanog*-pseudogenes, a next step could be the constitutive expression of pseudogenes in mouse ES cells. If pseudogene transcripts can down regulate their parental genes, such an experiment should lead to a decrease in *Nanog* expression levels and consequently differentiation.

The common denominator: pluripotency and epigenetic governance

Cellular phenotypes depend largely on histone modifications and other heritable epigenetic alterations [11, 148]. The cell types from which mouse pluripotent cell lines can be generated are intimately linked with major epigenetic reprogramming events [149, 150]. The cells of the epiblast experience reactivation of the paternal inactive X-chromosome, which is achieved by repression of *Xist* through binding of the pluripotency-associated transcription factors *Nanog*, *Oct4*, and *Sox2* to intron 1 of *Xist* [176, 177]. X-chromosome reactivation is accompanied by a genome-wide increase in trimethylation marks at lysine 27 of histone 3 (H3k27me3) [176, 177]. The resulting epigenetic signature is a prerequisite for successful generation of mouse embryonic stem cells [178].

In mouse PGCs, reprogramming extends from E7.5 to E13.5. PGCs of early embryonic day 7 embryos are at first similar to neighboring somatic cells of the extra-embryonic mesoderm. From E7.5 to E9.5, PGCs experience progressive reprogramming through erasure and acquisition of repressive histone modifications [179]. Epigenetic reprogramming is continued between E10.5 and E13.5, when PGCs colonize the genital ridges, during which the X-chromosome is reactivated [180]. In the same period, differentially methylated regions show rapid genome-wide demethylation [181] and from around E11.5 imprinted genes commence bi-allelic expression [182]. As a consequence of the epigenetic processes, chromatin and expression patterns of reprogrammed PGCs broadly resemble those of ES cells, which is demonstrated by the potential to establish pluripotent cell lines from PGCs and by the renewed expression of pluripotency-associated genes *Nanog*, *Oct4*, and *Sox2* [27, 110, 149, 150, 179, 183].

In the adult mammalian testis, male germ cells undergo major reprogramming in their development towards functional spermatozoa [141]. The fundamental role for various epigenetic modifiers in male germ cells and spermatogenesis has been illustrated by various knockout studies [141, 150, 184]. During the early phases of spermatogenesis, spermatogonia and spermatocytes experience d*e novo* methylation and demethylation of DNA [185]. Interestingly, a genome wide analysis revealed a high correlation of global methylation patterns between promoter regions of sperm cells and ES cells, which suggests that the sperm cells epigenome resembles a pluripotent state [186].

In summary, the cells of the epiblast, developing PGCs, and male germ cells from neonate and adult testis have in common that they experience major reprogramming events. This suggests that these cell types are more liable to acquire pluripotency, because epigenetic gover-

nance is minimal during these reprogramming events. Furthermore, pluripotency associated factors such as NANOG and OCT4 that are involved in reprogramming and pluripotency are expressed in epiblast, developing PGCs, and male germ cells from neonate and adult testis. OCT4 and NANOG are essential for the development of the epiblast and for primordial germ cell survival [13, 26, 28, 187]. The role for these factors at later stages of the germ line remains to be investigated.

Chapter VIII

Summary in Dutch

Summary in Dutch

Hoofdstuk I

Embryonale stam-(ES)cellen van zoogdieren zijn afkomstig van preïmplantatie-embryo's. Ze hebben de eigenschap dat ze langdurig gekweekt kunnen worden zonder verlies van pluripotentie, wat inhoudt dat ze zich nog tot alle celtypen kunnen ontwikkelen. Tot dusverre zijn zulke cellijnen alleen nog maar beschreven bij muizen, mensen en rhesusapen. ES cellen zijn een belangrijk hulpmiddel in de ontwikkelingsbiologie. Zo bieden ES cellen de mogelijkheid om differentiatieprocessen in vitro te onderzoeken en om knock-out en knock-in dieren te maken, waarin respectievelijk een gen onschadelijk is gemaakt of juist toe is gevoegd aan het genoom. Humane ES cellen genieten veel belangstelling vanuit de geneeskunde vanwege de potentiële rol die ze kunnen spelen in de regeneratie van beschadigde weefsels. Het vermogen van ES cellen om beschadigde weefsels te repareren en de daaraan verbonden risico's moeten eerst onderzocht worden in een geschikt modeldier. De muis schiet daarin tekort vanwege de grote verschillen met de mens en voor niet-humane primaten gelden veelal vergelijkbare ethische afwegingen als voor de mens. Het varken is wel een geschikte kandidaat; vanwege de overeenkomsten met de mens in orgaangrootte, de fysiologische levensduur en de fysiologie. Bovendien zijn er minder ethische bezwaren voor het gebruik van het varken als proefdier.

ES cellen van het varken zouden dus een belangrijke rol kunnen hebben bij het ontwikkelen van celtherapieën. Daarnaast kunnen ES cellen van landbouwhuisdieren zoals het varken, maar ook het rund, in theorie gebruikt worden voor het doelmatig genetisch modificeren van deze soorten, bijvoorbeeld om ziekteresistentie te bevorderen. In het verleden hebben diverse groepen geprobeerd om ES cellen te genereren van het varken of het rund, maar tot op heden zijn er voor deze soorten nog geen cellijnen beschreven die langdurig gekweekt kunnen worden zonder verlies van pluripotentie.

Primordiale kiemcellen (geslachtscellen in een ontwikkelend embryo) en spermatogoniale stamcellen zijn ook potentiële bronnen van pluripotente cellen, mits gekweekt onder de juiste omstandigheden. In veel opzichten zijn deze pluripotente cellen vergelijkbaar met ES cellen. Deze alternatieve bronnen van pluripotente cellen zijn weinig onderzocht in andere soorten dan de mens en de muis.

De belangrijkste thema's van dit proefschrift zijn pluripotentie van cellen, moleculaire mechanismen betrokken bij pluripotentie, en overeenkomsten en verschillen tussen soorten in deze mechanismen. Het praktisch werk in dit proefschrift richt zich met name op preïmplantatie-embryo's (hoofdstuk 2 en 3), spermatogoniale stamcellen (hoofdstuk 4 en 5), en de functie van de testis met betrekking tot pluripotentie (hoofdstuk 6).

Hoofdstuk II

Moleculair biologisch onderzoek berust veelal op sequentie informatie en de beschikbaarheid van soortspecifieke antilichamen. Beiden zijn slechts beperkt beschikbaar in het varken en het rund. Met name bij onderzoek aan genen die betrokken zijn bij pluripotentie is dit lastig, omdat de expressie van deze genen zich veelal beperkt tot de vroegembryonale ontwikkeling. De ontwikkeling van de juiste gereedschappen is dan ook een uitdagend aspect bij het onderzoek

naar de factoren die een rol spelen bij pluripotentie van varken en rund.

Een belangrijke techniek bij onderzoek naar genexpressie is de kwantitatieve RT-PCR. Met deze techniek kan bepaald worden wat de mate van expressie van een gen in een weefsel is ten opzichte van een ander weefsel. Daarbij is het belangrijk dat de mate van genactiviteit gecorrigeerd wordt voor eventuele verschillen in uitgangshoeveelheid en behandeling tussen de weefsels. De gangbare methode is door de genexpressie te corrigeren met behulp van de expressie van een interne controle of referentiegen. Expressie van een goed referentiegen reflecteert de totale mate van genactiviteit in een weefsel. Met name tijdens de vroegembryonale ontwikkeling van eicel tot en met blastocyst zijn er grote verschillen in genactiviteit tussen de ontwikkelingsstadia. In eicellen worden grote voorraden maternale RNA moleculen geproduceerd, waarvan een belangrijk gedeelte een rol vervult tijdens de vroege ontwikkeling. In de eerste klievingstadia wordt veel van dit maternale RNA afgebroken terwijl het zygotisch genoom nog amper getranscribeerd wordt en vervolgens neemt de totale hoeveelheid RNA weer sterk toe als het zygotisch genoom geactiveerd wordt. Het is onbekend welke genen gedurende de vroege ontwikkeling van eicel tot blastocyst goed weergeven wat de omvang van het transcriptoom is. Het ontbreken van deze referentiegenen maakt het lastig om de genactiviteit van een gen van interesse tussen verschillende ontwikkelingsstadia te vergelijken, wat vervolgens een studie naar de eventuele rol van deze genen in de ontwikkeling bemoeilijkt.

Het doel van de studie zoals beschreven in hoofdstuk 2 was het identificeren van referentiegenen in het varken die stabiel tot expressie worden gebracht van immature eicel tot blastocyst stadium.

Daartoe werden de expressieniveaus van 7 veelvuldig gebruikte referentiegenen (*B2M*, *BACT*, *GAPDH*, *H2A*, *PGK1*, *S18*, en *UBC*) vergeleken op verschillende stadia van de embryonale ontwikkeling van het varken (Germinal vesicle (GV)-stadium, Metaphase 2 stadium, 2-cellig stadium, 4-cellig stadium, vroege blastocysten, en geëxpandeerde blastocysten). De stabiliteit van de referentiegenen in deze stadia werd onderzocht met behulp van het daartoe ontwikkelde programma geNorm. Na analyse van de transcriptieprofielen bleek dat *GAPDH*, *PGK1*, *S18*, en *UBC* stabiel tot expressie werden gebracht tijdens de vroege ontwikkeling van het varken. Daarentegen was er een sterke regulatie van de transcriptie van *B2M*, *BACT*, en *H2A* tijdens de vroege ontwikkeling. Het wordt aangeraden om in genexpressiestudies van vroege ontwikkelingsstadia van het varken gebruik te maken van de drie referentiegenen *S18*, *UBC*, en *GAPDH* of *PGK1*. Het wordt afgeraden om *B2M*, *BACT*, of *H2A* als referentiegenen te gebruiken in vroege ontwikkelingsstadia van het varken.

Hoofdstuk III

De oorzaak voor het gebrek aan succes in het genereren van ES cellen van varkens en runderen kan gezocht worden in het verschil in embryologische ontwikkeling tussen varkens en runderen enerzijds en muizen en mensen anderzijds. Muizen- en mensen- embryo's implanteren invasief in de baarmoederwand kort na het blastocystenstadium waarna er een zogeheten haemochoriale placenta wordt gevormd. Runder- en varkens- blastocysten vertonen een elongatie van het trofectoderm alvorens non-invasief te implanteren, waarna een epitheliochoriale placenta wordt gevormd.

Deze duidelijke morfologische verschillen verklaren echter nog niet waarom het genereren van ES cellen van embryo's van de ene soort moeilijker is dan dat van de andere soort. Om daar inzicht in te krijgen is het noodzakelijk vergelijkend onderzoek te doen op moleculair biologisch niveau.

Bij muizen zijn al een aantal moleculair biologische factoren bekend die een rol spelen bij de ontwikkeling van peri-implantatie embryo's zoals de twee segregaties die tot de vorming van het trophectoderm (TE), het primitieve endoderm (PE) en het pluripotente primitieve ectoderm leiden. Bij deze segregaties zijn hoofdrollen weggelegd voor de transcriptiefactoren OCT4, CDX2, NANOG en GATA6. Volgens het huidige model worden OCT4 en CDX2 in alle cellen van een morula tot expressie gebracht. Omdat beide factoren elkaar wederzijds onderdrukken zullen sommige cellen dominant OCT4 tot expressie brengen en anderen CDX2. De expressie van CDX2 leidt vervolgens tot de ontwikkeling van cellen met kenmerken van het trophectoderm terwijl de OCT4-positieve cellen de *inner cell mass* (ICM) en vervolgens de epiblast zullen vormen. Volgens het huidige model vindt er na deze eerste segregatie van celtypen een soortgelijk proces plaats tussen de factoren NANOG en GATA6. Wederzijdse onderdrukking zou leiden tot GATA6-dominante cellen die zich ontwikkelen tot PE en NANOG-positieve cellen die zich ontwikkelen tot de pluripotente epiblast. Bij de muis wordt de pluripotente epiblast dus gevormd door achtereenvolgens selectie voor OCT4 positieve cellen en NANOG-positieve cellen.

Omdat bekend is vanuit de literatuur dat runder- en varkens-blastocysten ook OCT4 tot expressie brengen, kan worden verwacht dat de eerste segregatie van celtypen bij deze soorten niet berust op wederzijdse onderdrukking tussen CDX2 en OCT4. De studie in hoofdstuk 3 was erop gericht om meer inzicht te krijgen in hoeverre de andere factoren (CDX2, GATA6 en NANOG) betrokken zijn bij de eerste segregaties tijdens de vroegembryonale ontwikkeling van het varken en het rund. Daartoe werden de expressiepatronen van deze factoren onderzocht met behulp van kwantitatieve PCR in *in vitro*-geproduceerde varkensembryo's en met behulp van immunofluorescentie in *in vitro*-geproduceerde varkens- en runderembryo's en *in vivo*-geproduceerde varkensembryo's.

Varkens- en runderembryo's vertoonden een met de muis vergelijkbaar expressiepatroon van CDX2 en GATA6, wat suggereert dat deze factoren een geconserveerde functie hebben tussen soorten. Het expressiepatroon van NANOG in runderblastocysten was ook vergelijkbaar met dat van de muis. In blastocysten van het varken was NANOG echter niet detecteerbaar. Het is onwaarschijnlijk dat dit een technische oorzaak heeft, want met het gebruikte antilichaam werd wel varkens-NANOG gedetecteerd in gonocyten in de testis van neonate biggen.Verder werd OCT4 niet tot expressie gebracht in het morula stadium van het varken. Op het blastocysten-stadium, werd OCT4 zowel in de ICM als in het trofectoderm tot expressie gebracht.

Op het niveau van belangrijke transcriptiefactoren verschilt de vroege ontwikkeling van het varken met dat van de muis in de expressie van OCT4 en NANOG. Het verschil in expressie van transcriptiefactoren tussen rund en muis beperkte zich tot de al eerder beschreven expressie van OCT4. Hiermee kunnen we concluderen dat de eerste segregatie van ICM en trofectoderm in rund en varken niet zoals bij de muis berust op een wederzijdse inhibitie tussen OCT4 en CDX2, omdat OCT4 samen met CDX2 in het trofectoderm tot expressie wordt

gebracht. Verder geven aan dat de expressiepatronen van GATA6 en NANOG in runderblastocysten dat deze factoren bij het rund een vergelijkbare rol spelen in de ontwikkeling van het PE en het primitief ectoderm als bij de muis. Daarentegen lijkt NANOG niet betrokken te zijn bij de segregatie van PE en het primitief ectoderm bij het varken. Bovengenoemde bevindingen indiceren dat het pluripotente primitieve ectoderm bij het rund en het varken anders tot stand komt dan bij de muis. Dit kan gevolgen hebben voor het genereren en het karakteriseren van pluripotente ES cellen in deze diersoorten.

Hoofdstuk IV

Muizen kunnen relatief eenvoudig gericht genetisch gemodificeerd worden, omdat er voor deze soort cellijnen beschikbaar zijn die deel kunnen nemen aan de kiembaan, zoals embryonale stamcellen en spermatogoniale stamcellen. Varkens vervullen een belangrijke agrarische rol en zijn goed als modeldier voor de mens. Derhalve zou het waardevol zijn indien gerichte mutagenese op het varken toegepast zou kunnen worden op een vergelijkbare manier als bij de muis. Cellijnen die deel kunnen nemen aan de kiembaan zijn echter nog niet beschreven voor het varken. Het onderzoek dat beschreven staat in hoofdstuk 4 richt zich op het isoleren en karakteriseren van testiculaire cellen van het varken met het doel meer inzicht te krijgen welke kweekcondities zelfvernieuwing van spermatogoniale stamcellen van het varken bevorderen. In primaire celkweken van testiculaire cellen van het varken konden gonocyten gedetecteerd worden aan de hand van immunokleuringen voor NANOG en door middel van reactiviteit met DBA lectine. In de primaire celkweek werd een drietal typen kolonies waargenomen, elk met karakteristieke morfologie. Kolonies die morfologisch gelijkenis vertoonden met kolonies van muizen-spermatogoniale stamcellen werden individueel overgezet en verder gekweekt op platen met een coating van laminine. Op deze wijze werden twee cellijnen verkregen die 9 passages gekweekt konden totdat proliferatie stopte. Proliferatie was afhankelijk van de aanwezigheid van de groeifactoren LIF, EGF, GDNF, en FGF. Met behulp van kwantitatieve PCR werd vastgesteld dat beide cellijnen verhoogd *NANOG*, *PLZF*, en *EPCAM*, tot expressie brachten. Expressieniveaus van *GFRα1*, *INTEGRINα6*, en *THY1* waren verlaagd ten opzichte van die in neonate varkenstestis. Met behulp van een factorieel schema werd vervolgens het effect onderzocht van een viertal groeifactoren (LIF, EGF, GDNF, FGF) op de expressie van een marker voor gonocyten (*NANOG*), een pluripotentiemarker (*OCT4*) en een marker voor Sertoli cellen (*GATA4*). FGF had een negatieve invloed op de expressie van *NANOG*, maar een positieve invloed op de expressieniveaus van *OCT4* en *GATA4*. Bij aanwezigheid van EGF werd de positieve invloed van FGF op GATA4 tenietgedaan. Er werden geen effecten waargenomen van LIF of EGF op de expressieniveaus van *NANOG*, *OCT4*, of *GATA4*. Bovenstaande resultaten geven aan dat FGF nadelig kan zijn voor kweek van mannelijke geslachtscellen van het varken.

Hoofdstuk V

Gekweekte spermatogoniale stamcellen kunnen spontaan ES-achtige kolonies vormen waarvan de cellen pluripotent zijn. De tumoronderdrukkers TRP53 en PTEN lijken betrokken te zijn bij het afschermen van spermatogoniale stamcellen van pluripotentie, omdat de stap van unipotente spermatogoniale stamcellen (d.w.z waarvan het ontwikkelingspotentieel beperkt is tot slechts 1 celtype: de spermacel) naar pluripotente ES-achtige cel makkelijker genomen wordt bij afwezigheid van TRP53 of PTEN. Het is onduidelijk hoe TRP53 en PTEN spermatogoniale stamcellen afschermen van pluripotentie. Om meer inzicht te krijgen in dit mechanisme, werd een RNAi experiment uitgevoerd in een spermatogoniale stamcellijn van de muis. Door middel van lipofectamine werden de cellen getransfecteerd met siRNAs gericht tegen het mRNA van *Trp53* of *Pten*, wat in beide gevallen resulteerde in een significante afname van het mRNA van het doelgen. Vervolgens werd het effect van deze afname gemeten op genen die specifiek zijn voor pluripotente cellen (*Nanog*, *Eras*, *c-Myc*, *Klf4*, *Oct4*, en *Sox2*) of voor spermatogoniale stamcellen (*Plzf*) en differentiërende spermatogoniale stamcellen (*Ddx4*). De belangrijkste bevinding van deze studie is dat knockdown van TRP53 en PTEN onafhankelijk van elkaar resulteerde in een toename in expressie van *Nanog*. Het lijkt er dus op dat mannelijke geslachtscellen onder meer afgeschermd worden van pluripotentie door middel van onafhankelijke onderdrukking van *Nanog* door de tumor onderdrukkers TRP53 en PTEN.

Hoofdstuk VI

In de muis beperkt de expressie van de met pluripotentie geassocieerde factor NANOG zich tot cellen van de pluripotente ICM en tot primordiale kiemcellen. Spermatogenese is het complexe proces van differentiatie van mannelijke geslachtscellen en bestaat onder andere uit de meiotische deling en de daaropvolgende differentiatie tot een zeer gespecialiseerde haploïde spermacel die deel uit kan maken van een totipotent embryo met ontwikkelingspotentieel tot alle embryonale en extraembryonale weefsels. Hoewel er een duidelijke link is tussen de functie van de testis en pluripotentie enerzijds en NANOG en pluripotentie anderzijds, is er tot op heden nog geen overtuigende beschrijving van NANOG expressie in de testis. In hoofdstuk 6 wordt een vergelijkende studie naar de expressie van NANOG in testes van verscheidene zoogdieren (muis, hond, varken en mens) beschreven. Expressie van NANOG in testis werd onderzocht met behulp van PCR, immunblot, immunohistochemie, immunofluorescentie en met behulp van een zogeheten NANOG reporter muis, waarvan de expressie van het groen fluorescente eiwit eGFP onder controle staat van de promotor van NANOG. Hoewel NANOG tot op heden geassocieerd werd met ongedifferentieerde stamcellen, werd NANOG gedetecteerd in differentiërende mannelijke geslachtscellen in de testes van muis, hond, varken en mens. Expressie werd waargenomen in spermatocyten in het pachyteen-stadium en in de eerste fase van de spermiogenese. De bevindingen van deze studie suggereren dat er een geconserveerde rol is weggelegd voor NANOG in de meiotische en post-meiotische fase van de spermatogenese.

Hoofdstuk VII

In de muis zijn GATA6 en NANOG betrokken bij de segregatie van epiblast en primitief endoderm. Signalering via Grb2-Ras-MAP leidt tot mozaiek expressie van GATA6 en NANOG in de ICM. NANOG wordt in alle cellen van de ICM tot expressie gebracht in embryo's in afwezigheid van *Grb2*.Dit phenotype lijkt op dat van embryo's zonder *Fgf4* of *Fgfr2*. Tyrosine phosphorylering van FGFR2 vermindert FGF signaaltransductie. Dit kan geremd worden met behulp van sodium vanadaat, een remmer van tyrosine phosphatases. ES cellen die behandeld worden met sodium vanadaat vertonen een verlaging in het expressieniveau van NANOG en een verhoging in de expressieniveaus van genen die karakteristiek zijn voor het primitief endoderm. Dit effect kan tegengewerkt worden door toevoeging van de inhibitor PD98059, waarmee specifiek de activiteit van de MAP-kinase MEK geremd kan worden. Dit geeft aan dat embryo's die gekweekt worden in aanwezigheid van de MEK inhibitor PD98059, homogeen NANOG tot expressie zullen brengen. We hebben dat getoetst door runderembryo's te kweken in aanwezigheid van 25μM PD98059, gevolgd door immunofluorescente labeling van GATA6 en NANOG. In beide groepen werd mozaiek expressie van NANOG en GATA6 waargenomen, maar er waren wel significant meer NANOG positieve cellen in de groep die bij de inhibitor gekweekt werden. Deze resultaten geven aan dat signallering via MEK een rol speelt bij de segregatie van epiblast en primitief endoderm in runderembryo's. Toekomstige vergelijkbare experimenten kunnen een waardevolle bijdrage leveren aan ons inzicht in vroegembryologische processen met betrekking tot de pluripotente celpopulatie, wat vervolgens het genereren van ES cellen kan faciliteren.

Spermatogoniale stamcellen zijn ook een bron van pluripotente cellen. In hoofdstuk 5 wordt onderzocht welke mechanismen ten grondslag liggen aan de conversie van unipotente spermatogoniale stamcel naar pluripotente stamcel. Mogelijkerwijs, kunnen toekomstige spermatogoniale stamcellijnen een bron vormen van pluripotente cellen bij dieren als het varken of het rund.

Een recente revolutionaire ontwikkeling in stamcelonderzoek is de mogelijkheid om gedifferentieerde cellen te herprogrammeren naar een pluripotente cel met behulp van de factoren *c-Myc*, *Klf4*, *Oct4*, *Sox2*. Het induceren van pluripotentie zal ongetwijfeld ook toegepast worden op het varken en het rund. Een belangrijke vraag is of geherprogrammeerde cellen van het rund en het varken ook zichzelf vernieuwen zoals embryonale stamcellen van de muis dat doen. Een mogelijke oplossing voor dit probleem is het gebruik van transgenen waarvan de expressie gereguleerd wordt door doxycycline. Bij afwezigheid van doxycycline zullen de geherprogrammeerde cellen differentieren, tenzij de kweekcondities gunstig zijn voor de zelfvernieuwing van de cellen. Op deze wijze kunnen de kweekcondities onderzocht worden die de zelfvernieuwing van pluripotente cellen bevorderen.

In hoofdstuk zes wordt de opmerkelijke bevinding beschreven dat pseudogenen van *NANOG* in de testis tot expressie worden gebracht. Tot voor kort werden pseudogenen als junk beschouwd, omdat ze door frameshifts en premature stopcodons over het algemeen niet voor functionele eiwitten coderen. Recente bevindingen wijzen echter uit dat transcripten afkomstig van pseudogenen het aantal transcripten van verwante eiwitcoderende genen kan reguleren. Een transcript van de sense-strand van het pseudogen kan bijvoorbeeld hybridiseren met een transcript van de antisense-strand van het eiwitcoderende gen, resulterend in een lang

dubbelstrengs RNA-molecuul, wat vervolgens via RNA interferentie leidt tot degradatie van mRNA moleculen met vergelijkbare sequentie. Omdat we ook expressie van het pseudogen *NanogPa* hebben waargenomen in muizentestis (hoofdstuk 7), vermoeden we een rol voor pseudogenen in de regulatie van het echte gen voor *Nanog* in testes van muis en mens. Voor *Nanog* en andere factoren die geassocieerd worden met pluripotentie (zoals *Oct4*) zijn in muis en mens meerdere pseudogenen beschreven. De bijdrage van pseudogenen aan pluripotentie of differentiatie moet toekomsmstig onderzoek uitwijzen.

Het ontwikkelingspotentieel en het fenotype van een cel, b.v. pluripotent of beperkt tot enkele celtypen, worden voor een groot gedeelte bepaald door epigenetische programma's. Dat zijn niet-genetische programma's die wel erfelijk zijn en van moedercel op dochtercel worden doorgegeven. De cellen van de epiblast, migrerende primordiale kiemcellen en mannelijke geslachtscellen ondervinden aanzienlijke herprogrammering van het epigenoom. We postuleren dat verminderde epigenetische controle tijdens het herprogrammeren ten grondslag ligt aan de mogelijkheid om van deze celtypen pluripotente cellijnen te genereren.

References

References

1. Thomson JA, Itskovitz-Eldor J, Shapiro SS, Waknitz MA, Swiergiel JJ, Marshall VS, Jones JM. Embryonic Stem Cell Lines Derived from Human Blastocysts. Science 1998; 282: 1145-1147.
2. Bronson SK, Smithies O. Altering Mice by Homologous Recombination Using Embryonic Stem Cells. J Biol Chem 1994; 269: 27155-27158.
3. Donovan PJ, Gearhart J. The End of the Beginning for Pluripotent Stem Cells. Nature 2001; 414: 92-97.
4. Murry CE, Keller G. Differentiation of Embryonic Stem Cells to Clinically Relevant Populations: Lessons from Embryonic Development. Cell 2008; 132: 661-680.
5. de Wert G, Mummery C. Human Embryonic Stem Cells: Research, Ethics and Policy. Hum Reprod 2003; 18: 672-682.
6. Yang X, Smith SL, Tian XC, Lewin HA, Renard JP, Wakayama T. Nuclear Reprogramming of Cloned Embryos and Its Implications for Therapeutic Cloning. Nat Genet 2007; 39: 295-302.
7. Brevini TA, Antonini S, Cillo F, Crestan M, Gandolfi F. Porcine Embryonic Stem Cells: Facts, Challenges and Hopes. Theriogenology 2007; 68 Suppl 1: S206-213.
8. Mummery CL. Cardiology: Solace for the Broken-Hearted? Nature 2005; 433: 585-587.
9. Vackova I, Ungrova A, Lopes F. Putative Embryonic Stem Cell Lines from Pig Embryos. J Reprod Dev 2007; 53: 1137-1149.
10. Keefer CL, Pant D, Blomberg L, Talbot NC. Challenges and Prospects for the Establishment of Embryonic Stem Cell Lines of Domesticated Ungulates. Anim Reprod Sci 2007; 98: 147-168.
11. Goldberg AD, Allis CD, Bernstein E. Epigenetics: A Landscape Takes Shape. Cell 2007; 128: 635-638.
12. Palmieri SL, Peter W, Hess H, Scholer HR. Oct-4 Transcription Factor Is Differentially Expressed in the Mouse Embryo During Establishment of the First Two Extraembryonic Cell Lineages Involved in Implantation. Dev Biol 1994; 166: 259-267.
13. Nichols J, Zevnik B, Anastassiadis K, Niwa H, Klewe-Nebenius D, Chambers I, Scholer H, Smith A. Formation of Pluripotent Stem Cells in the Mammalian Embryo Depends on the Pou Transcription Factor Oct4. Cell 1998; 95: 379-391.
14. Niwa H, Miyazaki J, Smith AG. Quantitative Expression of Oct-3/4 Defines Differentiation, Dedifferentiation or Self-Renewal of Es Cells. Nat Genet 2000; 24: 372-376.
15. Beck F, Erler T, Russell A, James R. Expression of Cdx-2 in the Mouse Embryo and Placenta: Possible Role in Patterning of the Extra-Embryonic Membranes. Dev Dyn 1995; 204: 219-227.
16. Chawengsaksophak K, James R, Hammond VE, Kontgen F, Beck F. Homeosis and Intestinal Tumours in Cdx2 Mutant Mice. Nature 1997; 386: 84-87.
17. Strumpf D, Mao CA, Yamanaka Y, Ralston A, Chawengsaksophak K, Beck F, Rossant J. Cdx2 Is Required for Correct Cell Fate Specification and Differentiation

of Trophectoderm in the Mouse Blastocyst. Development 2005; 132: 2093-2102.
18. Rossant J, Chazaud C, Yamanaka Y. Lineage Allocation and Asymmetries in the Early Mouse Embryo. Philos Trans R Soc Lond B Biol Sci 2003; 358: 1341-1348; discussion 1349.
19. Tanaka S, Kunath T, Hadjantonakis AK, Nagy A, Rossant J. Promotion of Trophoblast Stem Cell Proliferation by Fgf4. Science 1998; 282: 2072-2075.
20. Niwa H, Toyooka Y, Shimosato D, Strumpf D, Takahashi K, Yagi R, Rossant J. Interaction between Oct3/4 and Cdx2 Determines Trophectoderm Differentiation. Cell 2005; 123: 917-929.
21. Ralston A, Rossant J. Genetic Regulation of Stem Cell Origins in the Mouse Embryo. Clin Genet 2005; 68: 106-112.
22. Fujikura J, Yamato E, Yonemura S, Hosoda K, Masui S, Nakao K, Miyazaki Ji J, Niwa H. Differentiation of Embryonic Stem Cells Is Induced by Gata Factors. Genes Dev 2002; 16: 784-789.
23. Koutsourakis M, Langeveld A, Patient R, Beddington R, Grosveld F. The Transcription Factor Gata6 Is Essential for Early Extraembryonic Development. Development 1999; 126: 723-732.
24. Kunath T, Arnaud D, Uy GD, Okamoto I, Chureau C, Yamanaka Y, Heard E, Gardner RL, Avner P, Rossant J. Imprinted X-Inactivation in Extra-Embryonic Endoderm Cell Lines from Mouse Blastocysts. Development 2005; 132: 1649-1661.
25. Chambers I, Colby D, Robertson M, Nichols J, Lee S, Tweedie S, Smith A. Functional Expression Cloning of Nanog, a Pluripotency Sustaining Factor in Embryonic Stem Cells. Cell 2003; 113: 643-655.
26. Mitsui K, Tokuzawa Y, Itoh H, Segawa K, Murakami M, Takahashi K, Maruyama M, Maeda M, Yamanaka S. The Homeoprotein Nanog Is Required for Maintenance of Pluripotency in Mouse Epiblast and Es Cells. Cell 2003; 113: 631-642.
27. Yamaguchi S, Kimura H, Tada M, Nakatsuji N, Tada T. Nanog Expression in Mouse Germ Cell Development. Gene Expr Patterns 2005; 5: 639-646.
28. Chambers I, Silva J, Colby D, Nichols J, Nijmeijer B, Robertson M, Vrana J, Jones K, Grotewold L, Smith A. Nanog Safeguards Pluripotency and Mediates Germline Development. Nature 2007; 450: 1230-1234.
29. Cheng AM, Saxton TM, Sakai R, Kulkarni S, Mbamalu G, Vogel W, Tortorice CG, Cardiff RD, Cross JC, Muller WJ, Pawson T. Mammalian Grb2 Regulates Multiple Steps in Embryonic Development and Malignant Transformation. Cell 1998; 95: 793-803.
30. Chazaud C, Yamanaka Y, Pawson T, Rossant J. Early Lineage Segregation between Epiblast and Primitive Endoderm in Mouse Blastocysts through the Grb2-Mapk Pathway. Dev Cell 2006; 10: 615-624.
31. Arman E, Haffner-Krausz R, Chen Y, Heath JK, Lonai P. Targeted Disruption of Fibroblast Growth Factor (Fgf) Receptor 2 Suggests a Role for Fgf Signaling in Pregastrulation Mammalian Development. Proc Natl Acad Sci USA 1998; 95: 5082-5087.
32. Feldman B, Poueymirou W, Papaioannou VE, DeChiara TM, Goldfarb M.

Requirement of Fgf-4 for Postimplantation Mouse Development. Science 1995; 267: 246-249.
33. Wilder PJ, Kelly D, Brigman K, Peterson CL, Nowling T, Gao QS, McComb RD, Capecchi MR, Rizzino A. Inactivation of the Fgf-4 Gene in Embryonic Stem Cells Alters the Growth and/or the Survival of Their Early Differentiated Progeny. Dev Biol 1997; 192: 614-629.
34. Beddington RS, Robertson EJ. An Assessment of the Developmental Potential of Embryonic Stem Cells in the Midgestation Mouse Embryo. Development 1989; 105: 733-737.
35. Behringer RR, Wakamiya M, Tsang TE, Tam PP. A Flattened Mouse Embryo: Leveling the Playing Field. Genesis 2000; 28: 23-30.
36. Enders AC, Carter AM. What Can Comparative Studies of Placental Structure Tell Us?--a Review. Placenta 2004; 25 Suppl A: S3-9.
37. Kirchhof N, Carnwath JW, Lemme E, Anastassiadis K, Scholer H, Niemann H. Expression Pattern of Oct-4 in Preimplantation Embryos of Different Species. Biol Reprod 2000; 63: 1698-1705.
38. van Eijk MJ, van Rooijen MA, Modina S, Scesi L, Folkers G, van Tol HT, Bevers MM, Fisher SR, Lewin HA, Rakacolli D, Galli C, de Vaureix C, Trounson AO, Mummery CL, Gandolfi F. Molecular Cloning, Genetic Mapping, and Developmental Expression of Bovine Pou5f1. Biol Reprod 1999; 60: 1093-1103.
39. Angerer LM, Angerer RC. Animal-Vegetal Axis Patterning Mechanisms in the Early Sea Urchin Embryo. Dev Biol 2000; 218: 1-12.
40. Horstadius S. The Mechanics of Sea Urchin Development, Studied by Operative Methods. In, vol. 14; 1939: 132-179.
41. Venuti JM, Jeffery WR. Cell Lineage and Determination of Cell Fate in Ascidian Embryos. Int J Dev Biol 1989; 33: 197-212.
42. Strome S, Lehmann R. Germ Versus Soma Decisions: Lessons from Flies and Worms. Science 2007; 316: 392-393.
43. St Johnston D, Nusslein-Volhard C. The Origin of Pattern and Polarity in the Drosophila Embryo. Cell 1992; 68: 201-219.
44. Tam PP, Zhou SX. The Allocation of Epiblast Cells to Ectodermal and Germ-Line Lineages Is Influenced by the Position of the Cells in the Gastrulating Mouse Embryo. Dev Biol 1996; 178: 124-132.
45. Lawson KA, Dunn NR, Roelen BA, Zeinstra LM, Davis AM, Wright CV, Korving JP, Hogan BL. Bmp4 Is Required for the Generation of Primordial Germ Cells in the Mouse Embryo. Genes Dev 1999; 13: 424-436.
46. de Sousa Lopes SM, Roelen BA, Monteiro RM, Emmens R, Lin HY, Li E, Lawson KA, Mummery CL. Bmp Signaling Mediated by Alk2 in the Visceral Endoderm Is Necessary for the Generation of Primordial Germ Cells in the Mouse Embryo. Genes Dev 2004; 18: 1838-1849.
47. Ohinata Y, Payer B, O'Carroll D, Ancelin K, Ono Y, Sano M, Barton SC, Obukhanych T, Nussenzweig M, Tarakhovsky A, Saitou M, Surani MA. Blimp1 Is a Critical Determinant of the Germ Cell Lineage in Mice. Nature 2005; 436: 207-213.

48. McLaren A, Lawson KA. How Is the Mouse Germ-Cell Lineage Established? Differentiation 2005; 73: 435-437.
49. Labosky PA, Barlow DP, Hogan BL. Mouse Embryonic Germ (Eg) Cell Lines: Transmission through the Germline and Differences in the Methylation Imprint of Insulin-Like Growth Factor 2 Receptor (Igf2r) Gene Compared with Embryonic Stem (Es) Cell Lines. Development 1994; 120: 3197-3204.
50. Durcova-Hills G, Adams IR, Barton SC, Surani MA, McLaren A. The Role of Exogenous Fibroblast Growth Factor-2 on the Reprogramming of Primordial Germ Cells into Pluripotent Stem Cells. Stem Cells 2006; 24: 1441-1449.
51. Vejlsted M, Offenberg H, Thorup F, Maddox-Hyttel P. Confinement and Clearance of Oct4 in the Porcine Embryo at Stereomicroscopically Defined Stages around Gastrulation. Mol Reprod Dev 2006; 73: 709-718.
52. Takagi Y, Talbot NC, Rexroad CE, Jr., Pursel VG. Identification of Pig Primordial Germ Cells by Immunocytochemistry and Lectin Binding. Mol Reprod Dev 1997; 46: 567-580.
53. Wrobel KH, Suss F. Identification and Temporospatial Distribution of Bovine Primordial Germ Cells Prior to Gonadal Sexual Differentiation. Anat Embryol (Berl) 1998; 197: 451-467.
54. de Rooij DG, Russell LD. All You Wanted to Know About Spermatogonia but Were Afraid to Ask. J Androl 2000; 21: 776-798.
55. Koopman P, Gubbay J, Vivian N, Goodfellow P, Lovell-Badge R. Male Development of Chromosomally Female Mice Transgenic for Sry. Nature 1991; 351: 117-121.
56. Guan K, Nayernia K, Maier LS, Wagner S, Dressel R, Lee JH, Nolte J, Wolf F, Li M, Engel W, Hasenfuss G. Pluripotency of Spermatogonial Stem Cells from Adult Mouse Testis. Nature 2006; 440: 1199-1203.
57. Izadyar F, Pau F, Marh J, Slepko N, Wang T, Gonzalez R, Ramos T, Howerton K, Sayre C, Silva F. Generation of Multipotent Cell Lines from a Distinct Population of Male Germ Line Stem Cells. Reproduction 2008; 135: 771-784.
58. Kanatsu-Shinohara M, Inoue K, Lee J, Yoshimoto M, Ogonuki N, Miki H, Baba S, Kato T, Kazuki Y, Toyokuni S, Toyoshima M, Niwa O, Oshimura M, Heike T, Nakahata T, Ishino F, Ogura A, Shinohara T. Generation of Pluripotent Stem Cells from Neonatal Mouse Testis. Cell 2004; 119: 1001-1012.
59. Kanatsu-Shinohara M, Lee J, Inoue K, Ogonuki N, Miki H, Toyokuni S, Ikawa M, Nakamura T, Ogura A, Shinohara T. Pluripotency of a Single Spermatogonial Stem Cell in Mice. Biol Reprod 2008; 78: 681-687.
60. Seandel M, James D, Shmelkov SV, Falciatori I, Kim J, Chavala S, Scherr DS, Zhang F, Torres R, Gale NW, Yancopoulos GD, Murphy A, Valenzuela DM, Hobbs RM, Pandolfi PP, Rafii S. Generation of Functional Multipotent Adult Stem Cells from Gpr125+ Germline Progenitors. Nature 2007; 449: 346-350.
61. Kanatsu-Shinohara M, Ogonuki N, Inoue K, Miki H, Ogura A, Toyokuni S, Shinohara T. Long-Term Proliferation in Culture and Germline Transmission of Mouse Male Germline Stem Cells. Biol Reprod 2003; 69: 612-616.
62. Chambers I, Smith A. Self-Renewal of Teratocarcinoma and Embryonic Stem Cells.

Oncogene 2004; 23: 7150-7160.
63. Oatley JM, Brinster RL. Regulation of Spermatogonial Stem Cell Self-Renewal in Mammals. Annu Rev Cell Dev Biol 2008.
64. Zamudio NM, Chong S, O'Bryan MK. Epigenetic Regulation in Male Germ Cells. Reproduction 2008; 136: 131-146.
65. Guraya SS. Biology of Spermatogenesis and Spermatozoa in Mammals. Berlin Heidelberg: Springer-Verlag; 1987.
66. Morrisey EE, Tang Z, Sigrist K, Lu MM, Jiang F, Ip HS, Parmacek MS. Gata6 Regulates Hnf4 and Is Required for Differentiation of Visceral Endoderm in the Mouse Embryo. Genes Dev 1998; 12: 3579-3590.
67. Takahashi K, Yamanaka S. Induction of Pluripotent Stem Cells from Mouse Embryonic and Adult Fibroblast Cultures by Defined Factors. Cell 2006; 126: 663-676.
68. Okita K, Ichisaka T, Yamanaka S. Generation of Germline-Competent Induced Pluripotent Stem Cells. Nature 2007; 448: 313-317.
69. Wernig M, Meissner A, Foreman R, Brambrink T, Ku M, Hochedlinger K, Bernstein BE, Jaenisch R. In Vitro Reprogramming of Fibroblasts into a Pluripotent ES-Cell-Like State. Nature 2007; 448: 318-324.
70. Campbell KH, McWhir J, Ritchie WA, Wilmut I. Sheep Cloned by Nuclear Transfer from a Cultured Cell Line. Nature 1996; 380: 64-66.
71. Blomberg LA, Schreier LL, Talbot NC. Expression Analysis of Pluripotency Factors in the Undifferentiated Porcine Inner Cell Mass and Epiblast During in Vitro Culture. Mol Reprod Dev 2007.
72. Van Soom A, Mateusen B, Leroy J, De Kruif A. Assessment of Mammalian Embryo Quality: What Can We Learn from Embryo Morphology? Reprod Biomed Online 2003; 7: 664-670.
73. Kuijk EW, du Puy L, van Tol HT, Haagsman HP, Colenbrander B, Roelen BA. Validation of Reference Genes for Quantitative Rt-PCR Studies in Porcine Oocytes and Preimplantation Embryos. BMC Dev Biol 2007; 7: 58.
74. Okuda A, Fukushima A, Nishimoto M, Orimo A, Yamagishi T, Nabeshima Y, Kuro-o M, Nabeshima Y, Boon K, Keaveney M, Stunnenberg HG, Muramatsu M. Utf1, a Novel Transcriptional Coactivator Expressed in Pluripotent Embryonic Stem Cells and Extra-Embryonic Cells. Embo J 1998; 17: 2019-2032.
75. van den Boom V, Kooistra SM, Boesjes M, Geverts B, Houtsmuller AB, Monzen K, Komuro I, Essers J, Drenth-Diephuis LJ, Eggen BJ. Utf1 Is a Chromatin-Associated Protein Involved in Es Cell Differentiation. J Cell Biol 2007; 178: 913-924.
76. Brulet P, Babinet C, Kemler R, Jacob F. Monoclonal Antibodies against Trophectoderm-Specific Markers During Mouse Blastocyst Formation. Proc Natl Acad Sci U S A 1980; 77: 4113-4117.
77. Oshima RG, Howe WE, Klier FG, Adamson ED, Shevinsky LH. Intermediate Filament Protein Synthesis in Preimplantation Murine Embryos. Dev Biol 1983; 99: 447-455.
78. Ketola I, Rahman N, Toppari J, Bielinska M, Porter-Tinge SB, Tapanainen JS,

Huhtaniemi IT, Wilson DB, Heikinheimo M. Expression and Regulation of Transcription Factors Gata-4 and Gata-6 in Developing Mouse Testis. Endocrinology 1999; 140: 1470-1480.
79. Evans MJ, Kaufman MH. Establishment in Culture of Pluripotential Cells from Mouse Embryos. Nature 1981; 292: 154-156.
80. O'Brien JK, Dwarte D, Ryan JP, Maxwell WM, Evans G. Developmental Capacity, Energy Metabolism and Ultrastructure of Mature Oocytes from Prepubertal and Adult Sheep. Reprod Fertil Dev 1996; 8: 1029-1037.
81. Marchal R, Feugang JM, Perreau C, Venturi E, Terqui M, Mermillod P. Meiotic and Developmental Competence of Prepubertal and Adult Swine Oocytes. Theriogenology 2001; 56: 17-29.
82. Kumar BM, Jin HF, Kim JG, Ock SA, Hong Y, Balasubramanian S, Choe SY, Rho GJ. Differential Gene Expression Patterns in Porcine Nuclear Transfer Embryos Reconstructed with Fetal Fibroblasts and Mesenchymal Stem Cells. Dev Dyn 2007; 236: 435-446.
83. Gao S, Gasparrini B, McGarry M, Ferrier T, Fletcher J, Harkness L, De Sousa P, Wilmut I. Germinal Vesicle Material Is Essential for Nucleus Remodeling after Nuclear Transfer. Biol Reprod 2002; 67: 928-934.
84. Yuan H, Corbi N, Basilico C, Dailey L. Developmental-Specific Activity of the Fgf-4 Enhancer Requires the Synergistic Action of Sox2 and Oct-3. Genes Dev 1995; 9: 2635-2645.
85. He S, Pant D, Schiffmacher A, Bischoff S, Melican D, Gavin W, Keefer C. Developmental Expression of Pluripotency Determining Factors in Caprine Embryos: Novel Pattern of Nanog Protein Localization in the Nucleolus. Mol Reprod Dev 2006; 73: 1512-1522.
86. Degrelle SA, Campion E, Cabau C, Piumi F, Reinaud P, Richard C, Renard JP, Hue I. Molecular Evidence for a Critical Period in Mural Trophoblast Development in Bovine Blastocysts. Dev Biol 2005; 288: 448-460.
87. Kidson A, Schoevers E, Langendijk P, Verheijden J, Colenbrander B, Bevers M. The Effect of Oviductal Epithelial Cell Co-Culture During in Vitro Maturation on Sow Oocyte Morphology, Fertilization and Embryo Development. Theriogenology 2003; 59: 1889-1903.
88. Petters RM, Reed ML. Addition of Taurine or Hypotaurine to Culture Medium Improves Development of One- and Two-Cell Pig Embryos in Vitro. Theriogenology 1991; 35: 253.
89. Parrish JJ, Susko-Parrish J, Winer MA, First NL. Capacitation of Bovine Sperm by Heparin. Biol Reprod 1988; 38: 1171-1180.
90. Izadyar F, Colenbrander B, Bevers MM. In Vitro Maturation of Bovine Oocytes in the Presence of Growth Hormone Accelerates Nuclear Maturation and Promotes Subsequent Embryonic Development. Mol Reprod Dev 1996; 45: 372-377.
91. Gillio-Meina C, Hui YY, LaVoie HA. Gata-4 and Gata-6 Transcription Factors: Expression, Immunohistochemical Localization, and Possible Function in the Porcine Ovary. Biol Reprod 2003; 68: 412-422.

92. McLaren A. Primordial Germ Cells in the Mouse. Developmental Biology 2003; 262: 1-15.
93. Brinster RL. Germline Stem Cell Transplantation and Transgenesis. Science 2002; 296: 2174-2176.
94. Kubota H, Avarbock MR, Brinster RL. Growth Factors Essential for Self-Renewal and Expansion of Mouse Spermatogonial Stem Cells. Proc Natl Acad Sci U S A 2004; 101: 16489-16494.
95. Kanatsu-Shinohara M, Ikawa M, Takehashi M, Ogonuki N, Miki H, Inoue K, Kazuki Y, Lee J, Toyokuni S, Oshimura M, Ogura A, Shinohara T. Production of Knockout Mice by Random or Targeted Mutagenesis in Spermatogonial Stem Cells. Proc Natl Acad Sci U S A 2006; 103: 8018-8023.
96. Dobrinski I. Germ Cell Transplantation and Testis Tissue Xenografting in Domestic Animals. Anim Reprod Sci 2005; 89: 137-145.
97. Tadokoro Y, Yomogida K, Ohta H, Tohda A, Nishimune Y. Homeostatic Regulation of Germinal Stem Cell Proliferation by the Gdnf/Fsh Pathway. Mech Dev 2002; 113: 29-39.
98. Naughton CK, Jain S, Strickland AM, Gupta A, Milbrandt J. Glial Cell-Line Derived Neurotrophic Factor-Mediated Ret Signaling Regulates Spermatogonial Stem Cell Fate. Biol Reprod 2006; 74: 314-321.
99. Kanatsu-Shinohara M, Miki H, Inoue K, Ogonuki N, Toyokuni S, Ogura A, Shinohara T. Long-Term Culture of Mouse Male Germline Stem Cells under Serum-or Feeder-Free Conditions. Biol Reprod 2005; 72: 985-991.
100. Goel S, Fujihara M, Minami N, Yamada M, Imai H. Expression of Nanog, but Not Pou5f1, Points to the Stem Cell Potential of Primitive Germ Cells in Neonatal Pig Testis. Reproduction 2008; 135: 785-795.
101. Goel S, Sugimoto M, Minami N, Yamada M, Kume S, Imai H. Identification, Isolation, and in Vitro Culture of Porcine Gonocytes. Biol Reprod 2007; 77: 127-137.
102. McCoard SA, Wise TH, Fahrenkrug SC, Ford JJ. Temporal and Spatial Localization Patterns of Gata4 During Porcine Gonadogenesis. Biol Reprod 2001; 65: 366-374.
103. Tung PS, Fritz IB. Characterization of Rat Testicular Peritubular Myoid Cells in Culture: Alpha-Smooth Muscle Isoactin Is a Specific Differentiation Marker. Biol Reprod 1990; 42: 351-365.
104. Roberts KP, Banerjee PP, Tindall JW, Zirkin BR. Immortalization and Characterization of a Sertoli Cell Line from the Adult Rat. Biol Reprod 1995; 53: 1446-1453.
105. Costoya JA, Hobbs RM, Barna M, Cattoretti G, Manova K, Sukhwani M, Orwig KE, Wolgemuth DJ, Pandolfi PP. Essential Role of Plzf in Maintenance of Spermatogonial Stem Cells. Nat Genet 2004; 36: 653-659.
106. Anderson R, Schaible K, Heasman J, Wylie C. Expression of the Homophilic Adhesion Molecule, Ep-Cam, in the Mammalian Germ Line. J Reprod Fertil 1999; 116: 379-384.
107. Kubota H, Avarbock MR, Brinster RL. Spermatogonial Stem Cells Share Some, but Not All, Phenotypic and Functional Characteristics with Other Stem Cells. Proc Natl

Acad Sci U S A 2003; 100: 6487-6492.
108. Shinohara T, Avarbock MR, Brinster RL. Beta1- and Alpha6-Integrin Are Surface Markers on Mouse Spermatogonial Stem Cells. Proc Natl Acad Sci U S A 1999; 96: 5504-5509.
109. Fouchecourt S, Godet M, Sabido O, Durand P. Glial Cell-Line-Derived Neurotropic Factor and Its Receptors Are Expressed by Germinal and Somatic Cells of the Rat Testis. J Endocrinol 2006; 190: 59-71.
110. Matsui Y, Zsebo K, Hogan BL. Derivation of Pluripotential Embryonic Stem Cells from Murine Primordial Germ Cells in Culture. Cell 1992; 70: 841-847.
111. Brambrink T, Foreman R, Welstead GG, Lengner CJ, Wernig M, Suh H, Jaenisch R. Sequential Expression of Pluripotency Markers During Direct Reprogramming of Mouse Somatic Cells. Cell Stem Cell 2008; 2: 151-159.
112. Maherali N, Sridharan R, Xie W, Utikal J, Eminli S, Arnold K, Stadtfeld M, Yachechko R, Tchieu J, Jaenisch R, Plath K, Hochedlinger K. Directly Reprogrammed Fibroblasts Show Global Epigenetic Remodeling and Widespread Tissue Contribution. Cell Stem Cell 2007; 1: 55-70.
113. Stadtfeld M, Brennand K, Hochedlinger K. Reprogramming of Pancreatic Beta Cells into Induced Pluripotent Stem Cells. Curr Biol 2008; 18: 890-894.
114. Van Dissel-Emiliani FM, De Boer-Brouwer M, De Rooij DG. Effect of Fibroblast Growth Factor-2 on Sertoli Cells and Gonocytes in Coculture During the Perinatal Period. Endocrinology 1996; 137: 647-654.
115. Kuijk EW, Du Puy L, Van Tol HT, Oei CH, Haagsman HP, Colenbrander B, Roelen BA. Differences in Early Lineage Segregation between Mammals. Dev Dyn 2008; 237: 918-927.
116. Jaillard C, Chatelain PG, Saez JM. In Vitro Regulation of Pig Sertoli Cell Growth and Function: Effects of Fibroblast Growth Factor and Somatomedin-C. Biol Reprod 1987; 37: 665-674.
117. Franca LR, Silva VA, Jr., Chiarini-Garcia H, Garcia SK, Debeljuk L. Cell Proliferation and Hormonal Changes During Postnatal Development of the Testis in the Pig. Biol Reprod 2000; 63: 1629-1636.
118. Aponte P, Soda T, Teerds K, Mizrak S, van de Kant H, Derooij D. Propagation of Bovine Spermatogonial Stem Cells in Vitro. Reproduction 2008.
119. Vandesompele J, De Preter K, Pattyn F, Poppe B, Van Roy N, De Paepe A, Speleman F. Accurate Normalization of Real-Time Quantitative RT-PCR Data by Geometric Averaging of Multiple Internal Control Genes. Genome Biol 2002; 3.
120. Donehower LA, Harvey M, Slagle BL, McArthur MJ, Montgomery CA, Jr., Butel JS, Bradley A. Mice Deficient for P53 Are Developmentally Normal but Susceptible to Spontaneous Tumours. Nature 1992; 356: 215-221.
121. Lam MY, Nadeau JH. Genetic Control of Susceptibility to Spontaneous Testicular Germ Cell Tumors in Mice. Apmis 2003; 111: 184-191.
122. Lin T, Chao C, Saito S, Mazur SJ, Murphy ME, Appella E, Xu Y. P53 Induces Differentiation of Mouse Embryonic Stem Cells by Suppressing Nanog Expression. Nat Cell Biol 2005; 7: 165-171.

123. Kimura T, Tomooka M, Yamano N, Murayama K, Matoba S, Umehara H, Kanai Y, Nakano T. Akt Signaling Promotes Derivation of Embryonic Germ Cells from Primordial Germ Cells. Development 2008; 135: 869-879.
124. Kimura T, Suzuki A, Fujita Y, Yomogida K, Lomeli H, Asada N, Ikeuchi M, Nagy A, Mak TW, Nakano T. Conditional Loss of Pten Leads to Testicular Teratoma and Enhances Embryonic Germ Cell Production. Development 2003; 130: 1691-1700.
125. Moe-Behrens GH, Klinger FG, Eskild W, Grotmol T, Haugen TB, De Felici M. Akt/Pten Signaling Mediates Estrogen-Dependent Proliferation of Primordial Germ Cells in Vitro. Mol Endocrinol 2003; 17: 2630-2638.
126. Takahashi K, Mitsui K, Yamanaka S. Role of Eras in Promoting Tumour-Like Properties in Mouse Embryonic Stem Cells. Nature 2003; 423: 541-545.
127. Yu J, Vodyanik MA, Smuga-Otto K, Antosiewicz-Bourget J, Frane JL, Tian S, Nie J, Jonsdottir GA, Ruotti V, Stewart R, Slukvin, II, Thomson JA. Induced Pluripotent Stem Cell Lines Derived from Human Somatic Cells. Science 2007; 318: 1917-1920.
128. Buaas FW, Kirsh AL, Sharma M, McLean DJ, Morris JL, Griswold MD, de Rooij DG, Braun RE. Plzf Is Required in Adult Male Germ Cells for Stem Cell Self-Renewal. Nat Genet 2004; 36: 647-652.
129. Toyooka Y, Tsunekawa N, Takahashi Y, Matsui Y, Satoh M, Noce T. Expression and Intracellular Localization of Mouse Vasa-Homologue Protein During Germ Cell Development. Mech Dev 2000; 93: 139-149.
130. Fujiwara Y, Komiya T, Kawabata H, Sato M, Fujimoto H, Furusawa M, Noce T. Isolation of a Dead-Family Protein Gene That Encodes a Murine Homolog of Drosophila Vasa and Its Specific Expression in Germ Cell Lineage. Proc Natl Acad Sci U S A 1994; 91: 12258-12262.
131. Resnick JL, Bixler LS, Cheng L, Donovan PJ. Long-Term Proliferation of Mouse Primordial Germ Cells in Culture. Nature 1992; 359: 550-551.
132. Gasteiger E, Gattiker A, Hoogland C, Ivanyi I, Appel RD, Bairoch A. Expasy: The Proteomics Server for in-Depth Protein Knowledge and Analysis. Nucleic Acids Res 2003; 31: 3784-3788.
133. Stambolic V, Suzuki A, de la Pompa JL, Brothers GM, Mirtsos C, Sasaki T, Ruland J, Penninger JM, Siderovski DP, Mak TW. Negative Regulation of Pkb/Akt-Dependent Cell Survival by the Tumor Suppressor Pten. Cell 1998; 95: 29-39.
134. Prives C. Signaling to P53: Breaking the Mdm2-P53 Circuit. Cell 1998; 95: 5-8.
135. Hay B, Jan LY, Jan YN. A Protein Component of Drosophila Polar Granules Is Encoded by Vasa and Has Extensive Sequence Similarity to Atp-Dependent Helicases. Cell 1988; 55: 577-587.
136. Lasko PF, Ashburner M. The Product of the Drosophila Gene Vasa Is Very Similar to Eukaryotic Initiation Factor-4a. Nature 1988; 335: 611-617.
137. Insinga A, Monestiroli S, Ronzoni S, Carbone R, Pearson M, Pruneri G, Viale G, Appella E, Pelicci P, Minucci S. Impairment of P53 Acetylation, Stability and Function by an Oncogenic Transcription Factor. Embo J 2004; 23: 1144-1154.
138. de Jonge HJ, Fehrmann RS, de Bont ES, Hofstra RM, Gerbens F, Kamps WA, de

Vries EG, van der Zee AG, te Meerman GJ, ter Elst A. Evidence Based Selection of Housekeeping Genes. PLoS ONE 2007; 2: e898.
139. Vandesompele J, De Preter K, Pattyn F, Poppe B, Van Roy N, De Paepe A, Speleman F. Accurate Normalization of Real-Time Quantitative RT-PCR Data by Geometric Averaging of Multiple Internal Control Genes. Genome Biol 2002; 3.
140. Silva J, Chambers I, Pollard S, Smith A. Nanog Promotes Transfer of Pluripotency after Cell Fusion. Nature 2006; 441: 997-1001.
141. Zamudio N, Chong S, O'Bryan M. Epigenetic Regulation in Male Germ Cells. Reproduction 2008.
142. Robertson M, Stenhouse F, Colby D, Marland JR, Nichols J, Tweedie S, Chambers I. Nanog Retrotransposed Genes with Functionally Conserved Open Reading Frames. Mamm Genome 2006; 17: 732-743.
143. Booth HA, Holland PW. Eleven Daughters of Nanog. Genomics 2004; 84: 229-238.
144. Russell LDE, R.A.; Sinha Hikim, A. P.; Clegg, E. D. Histological and Histopathological Evaluation of the Testis. Clearwater: Cache River Press, Clearwater, Florida; 1990.
145. Kotaja N, Sassone-Corsi P. The Chromatoid Body: A Germ-Cell-Specific RNA-Processing Centre. Nat Rev Mol Cell Biol 2007; 8: 85-90.
146. Hart AH, Hartley L, Ibrahim M, Robb L. Identification, Cloning and Expression Analysis of the Pluripotency Promoting Nanog Genes in Mouse and Human. Dev Dyn 2004; 230: 187-198.
147. Ezeh UI, Turek PJ, Reijo RA, Clark AT. Human Embryonic Stem Cell Genes Oct4, Nanog, Stellar, and Gdf3 Are Expressed in Both Seminoma and Breast Carcinoma. Cancer 2005; 104: 2255-2265.
148. Roelen BA, de Sousa Lopes SM. Of Stem Cells and Gametes: Similarities and Differences. Curr Med Chem 2008; 15: 1249-1256.
149. Surani MA, Hayashi K, Hajkova P. Genetic and Epigenetic Regulators of Pluripotency. Cell 2007; 128: 747-762.
150. Sasaki H, Matsui Y. Epigenetic Events in Mammalian Germ-Cell Development: Reprogramming and Beyond. Nat Rev Genet 2008; 9: 129-140.
151. Liang J, Wan M, Zhang Y, Gu P, Xin H, Jung SY, Qin J, Wong J, Cooney AJ, Liu D, Songyang Z. Nanog and Oct4 Associate with Unique Transcriptional Repression Complexes in Embryonic Stem Cells. Nat Cell Biol 2008; 10: 731-739.
152. Wang J, Rao S, Chu J, Shen X, Levasseur DN, Theunissen TW, Orkin SH. A Protein Interaction Network for Pluripotency of Embryonic Stem Cells. Nature 2006; 444: 364-368.
153. Fenic I, Hossain HM, Sonnack V, Tchatalbachev S, Thierer F, Trapp J, Failing K, Edler KS, Bergmann M, Jung M, Chakraborty T, Steger K. In Vivo Application of Histone Deacetylase Inhibitor Trichostatin-a Impairs Murine Male Meiosis. J Androl 2008; 29: 172-185.
154. Lu CW, Yabuuchi A, Chen L, Viswanathan S, Kim K, Daley GQ. Ras-Mapk Signaling Promotes Trophectoderm Formation from Embryonic Stem Cells and Mouse Embryos. Nat Genet 2008; 40: 921-926.

155. Paliga AJ, Natale DR, Watson AJ. P38 Mitogen-Activated Protein Kinase (Mapk) First Regulates Filamentous Actin at the 8-16-Cell Stage During Preimplantation Development. Biol Cell 2005; 97: 629-640.
156. Hamazaki T, Kehoe SM, Nakano T, Terada N. The Grb2/Mek Pathway Represses Nanog in Murine Embryonic Stem Cells. Mol Cell Biol 2006; 26: 7539-7549.
157. Ralston A, Rossant J. Cdx2 Acts Downstream of Cell Polarization to Cell-Autonomously Promote Trophectoderm Fate in the Early Mouse Embryo. Dev Biol 2008; 313: 614-629.
158. Stadtfeld M, Nagaya M, Utikal J, Weir G, Hochedlinger K. Induced Pluripotent Stem Cells Generated without Viral Integration. Science 2008.
159. Stewart CL, Kaspar P, Brunet LJ, Bhatt H, Gadi I, Kontgen F, Abbondanzo SJ. Blastocyst Implantation Depends on Maternal Expression of Leukaemia Inhibitory Factor. Nature 1992; 359: 76-79.
160. Li M, Sendtner M, Smith A. Essential Function of Lif Receptor in Motor Neurons. Nature 1995; 378: 724-727.
161. Ware CB, Horowitz MC, Renshaw BR, Hunt JS, Liggitt D, Koblar SA, Gliniak BC, McKenna HJ, Papayannopoulou T, Thoma B, et al. Targeted Disruption of the Low-Affinity Leukemia Inhibitory Factor Receptor Gene Causes Placental, Skeletal, Neural and Metabolic Defects and Results in Perinatal Death. Development 1995; 121: 1283-1299.
162. Nakashima K, Wiese S, Yanagisawa M, Arakawa H, Kimura N, Hisatsune T, Yoshida K, Kishimoto T, Sendtner M, Taga T. Developmental Requirement of Gp130 Signaling in Neuronal Survival and Astrocyte Differentiation. J Neurosci 1999; 19: 5429-5434.
163. Yoshida K, Taga T, Saito M, Suematsu S, Kumanogoh A, Tanaka T, Fujiwara H, Hirata M, Yamagami T, Nakahata T, Hirabayashi T, Yoneda Y, Tanaka K, Wang WZ, Mori C, Shiota K, Yoshida N, Kishimoto T. Targeted Disruption of Gp130, a Common Signal Transducer for the Interleukin 6 Family of Cytokines, Leads to Myocardial and Hematological Disorders. Proc Natl Acad Sci U S A 1996; 93: 407-411.
164. Nichols J, Chambers I, Taga T, Smith A. Physiological Rationale for Responsiveness of Mouse Embryonic Stem Cells to Gp130 Cytokines. Development 2001; 128: 2333-2339.
165. Vallier L, Alexander M, Pedersen RA. Activin/Nodal and Fgf Pathways Cooperate to Maintain Pluripotency of Human Embryonic Stem Cells. J Cell Sci 2005; 118: 4495-4509.
166. Brons IG, Smithers LE, Trotter MW, Rugg-Gunn P, Sun B, Chuva de Sousa Lopes SM, Howlett SK, Clarkson A, Ahrlund-Richter L, Pedersen RA, Vallier L. Derivation of Pluripotent Epiblast Stem Cells from Mammalian Embryos. Nature 2007; 448: 191-195.
167. Sasidharan R, Gerstein M. Genomics: Protein Fossils Live on as RNA. Nature 2008; 453: 729-731.
168. Watanabe T, Totoki Y, Toyoda A, Kaneda M, Kuramochi-Miyagawa S, Obata Y,

Chiba H, Kohara Y, Kono T, Nakano T, Surani MA, Sakaki Y, Sasaki H. Endogenous siRNAs from Naturally Formed dsRNAs Regulate Transcripts in Mouse Oocytes. Nature 2008; 453: 539-543.
169. Kawamura Y, Saito K, Kin T, Ono Y, Asai K, Sunohara T, Okada TN, Siomi MC, Siomi H. Drosophila Endogenous Small RNAs Bind to Argonaute 2 in Somatic Cells. Nature 2008; 453: 793-797.
170. Ghildiyal M, Seitz H, Horwich MD, Li C, Du T, Lee S, Xu J, Kittler EL, Zapp ML, Weng Z, Zamore PD. Endogenous siRNAs Derived from Transposons and mRNAs in Drosophila Somatic Cells. Science 2008; 320: 1077-1081.
171. Czech B, Malone CD, Zhou R, Stark A, Schlingeheyde C, Dus M, Perrimon N, Kellis M, Wohlschlegel JA, Sachidanandam R, Hannon GJ, Brennecke J. An Endogenous Small Interfering RNA Pathway in Drosophila. Nature 2008; 453: 798-802.
172. Tam OH, Aravin AA, Stein P, Girard A, Murchison EP, Cheloufi S, Hodges E, Anger M, Sachidanandam R, Schultz RM, Hannon GJ. Pseudogene-Derived Small Interfering RNAs Regulate Gene Expression in Mouse Oocytes. Nature 2008; 453: 534-538.
173. Pain D, Chirn GW, Strassel C, Kemp DM. Multiple Retropseudogenes from Pluripotent Cell-Specific Gene Expression Indicates a Potential Signature for Novel Gene Identification. J Biol Chem 2005; 280: 6265-6268.
174. Okamura K, Chung WJ, Ruby JG, Guo H, Bartel DP, Lai EC. The Drosophila Hairpin RNA Pathway Generates Endogenous Short Interfering RNAs. Nature 2008; 453: 803-806.
175. Hayashi K, Chuva de Sousa Lopes SM, Kaneda M, Tang F, Hajkova P, Lao K, O'Carroll D, Das PP, Tarakhovsky A, Miska EA, Surani MA. MicroRNA Biogenesis Is Required for Mouse Primordial Germ Cell Development and Spermatogenesis. PLoS ONE 2008; 3: e1738.
176. Mak W, Nesterova TB, de Napoles M, Appanah R, Yamanaka S, Otte AP, Brockdorff N. Reactivation of the Paternal X Chromosome in Early Mouse Embryos. Science 2004; 303: 666-669.
177. Okamoto I, Otte AP, Allis CD, Reinberg D, Heard E. Epigenetic Dynamics of Imprinted X Inactivation During Early Mouse Development. Science 2004; 303: 644-649.
178. O'Carroll D, Erhardt S, Pagani M, Barton SC, Surani MA, Jenuwein T. The Polycomb-Group Gene Ezh2 Is Required for Early Mouse Development. Mol Cell Biol 2001; 21: 4330-4336.
179. Seki Y, Hayashi K, Itoh K, Mizugaki M, Saitou M, Matsui Y. Extensive and Orderly Reprogramming of Genome-Wide Chromatin Modifications Associated with Specification and Early Development of Germ Cells in Mice. Dev Biol 2005; 278: 440-458.
180. Tam PP, Zhou SX, Tan SS. X-Chromosome Activity of the Mouse Primordial Germ Cells Revealed by the Expression of an X-Linked Lacz Transgene. Development 1994; 120: 2925-2932.
181. Hajkova P, Erhardt S, Lane N, Haaf T, El-Maarri O, Reik W, Walter J, Surani MA.

Epigenetic Reprogramming in Mouse Primordial Germ Cells. Mech Dev 2002; 117: 15-23.
182. Szabo PE, Hubner K, Scholer H, Mann JR. Allele-Specific Expression of Imprinted Genes in Mouse Migratory Primordial Germ Cells. Mech Dev 2002; 115: 157-160.
183. Western P, Maldonado-Saldivia J, van den Bergen J, Hajkova P, Saitou M, Barton S, Surani MA. Analysis of Esg1 Expression in Pluripotent Cells and the Germline Reveals Similarities with Oct4 and Sox2 and Differences between Human Pluripotent Cell Lines. Stem Cells 2005; 23: 1436-1442.
184. La Salle S, Oakes CC, Neaga OR, Bourc'his D, Bestor TH, Trasler JM. Loss of Spermatogonia and Wide-Spread DNA Methylation Defects in Newborn Male Mice Deficient in Dnmt3l. BMC Dev Biol 2007; 7: 104.
185. Oakes CC, La Salle S, Smiraglia DJ, Robaire B, Trasler JM. Developmental Acquisition of Genome-Wide DNA Methylation Occurs Prior to Meiosis in Male Germ Cells. Dev Biol 2007; 307: 368-379.
186. Farthing CR, Ficz G, Ng RK, Chan CF, Andrews S, Dean W, Hemberger M, Reik W. Global Mapping of DNA Methylation in Mouse Promoters Reveals Epigenetic Reprogramming of Pluripotency Genes. PLoS Genet 2008; 4: e1000116.
187. Kehler J, Tolkunova E, Koschorz B, Pesce M, Gentile L, Boiani M, Lomeli H, Nagy A, McLaughlin KJ, Scholer HR, Tomilin A. Oct4 Is Required for Primordial Germ Cell Survival. EMBO Rep 2004; 5: 1078-1083.

Acknowledgements

Acknowledgements

Tijdens mijn promotieonderzoek heb ik veel geleerd en met bijzonder veel plezier in of rond het lab gewerkt. Daaraan hebben de volgende mensen in woord en daad bijgedragen die ik bij deze graag wil bedanken:

Bernard Roelen voor je nimmer aflatende optimisme en het vertrouwen dat je in mij en dit project hebt gesteld. Ik heb buitengewoon veel van je geleerd en ik heb met enorm veel plezier met je samengewerkt. Je bent een uitzonderlijk goed begeleider en je steekt veel tijd en energie in je AIO's, zelfs als ze gratis zijn. Ik had me geen betere begeleider kunnen wensen en ik zal met veel plezier terugdenken aan de tijd dat ik op je lab heb mogen werken.

Mijn promotoren: Ben Colenbrander voor je wijze lessen die zelden rechtstreeks geuit werden maar juist veelal tussen de regels door hoorbaar waren. Ik denk met plezier terug aan de conversaties die we samen gehad hebben; Henk Haagsman voor je bijdrage tijdens de maandagochtendbesprekingen; Jan Rothuizen voor je belangstelling voor mijn vorderingen.

Mijn kamergenoten: mijn zeer fijne collega Eric Schoevers voor je hulp met de IVF en de embryokweek, maar ook voor de muzikale opluistering (Musicology); Patricia da Silva, I enjoyed the period we shared our office and I am happy to say that the plants I inherited from you after your thesis defense have survived until now, although they have grown accustomed to somewhat harsher conditions since then; en verder Hilde Aardema, Sridevi, Gustaaf en Annemarie.

De andere (oud-)collega's van Landbouwhuisdieren: Leni van Tol voor jouw hulp op vele fronten en de goede gesprekken op het lab ('we dwalen af') ; Christine Oei voor alle restembryo's van de runderkweek en voor het behandelen van mijn spoedbestellingen als Leni met vakantie was; Elly Zeinstra voor het bij nood altijd weer vinden van een toepasselijk protocol of instrument; Arend Rijneveld en zeer gewaardeerd oud-collega Peter Ursem voor het prettige gezelschap en de hulp bij de opslag van cellen; Omran Algriany, hasan sadiq, thank you for your kindness and your help with the QPCR; Frans van Kooij, Jamal en Nordin: shukran jazilan voor jullie hulp bij het halen van het slachthuismateriaal; efcharisto poly Fros Tonidis-Gkektsis voor je ondersteuning bij het secretariaat; en verder Regiane Rodrigues dos Santos, Edita Sostaric, Min, Karianne Peterson, Ineke Daemen en Mabel Beitsma.

Lotgenoten (succes allemaal met de laatste loodjes): Jurriaan Hölzenspies voor de goede gesprekken en de zinvolle uitwisseling van protocollen, ideeën en muziek, ik heb veel van je geleerd; Leonie du Puy voor je interesse en hulp bij diverse experimenten; Karlijn Wilschut voor je hulp met enkele immuno-gebaseerde experimenten; Jason Tsai for your help with western blotting (enjoy your family life!); khorb koon Chatchote Thitaram for your friendliness; Jeffrey de Gier voor de plezierige samenwerking; Arjan Boerke voor de goede gesprekken voor, tijdens en na het blotten.

De collega's bij Gezelschapsdieren: Louis Penning voor je hulpvaardigheid bij diverse experimenten; Bart Spee voor de goede discussies en de hulp bij het opzetten van de QPCR; Nagesha Rao, thanks for buying that sofa of mine through marktplaats; Bas Brink-

hof voor je inzet voor het RNAi experiment; Frank Riemers voor de diverse keren dat je me uit de brand hebt geholpen; Peter Leeghwater voor je goede tips op het gebied van genanalyse; en verder Frank van Steenbeek, Baukje Schotanus, Brigitte Arends, Hedwig Kruitwagen, Elpetra Timmermans-Sprang, Monique van Wolferen, Adri Slob, Jeannette Wolfswinkel en Manon Vos-Loohuis.

Anko de Graaff en Richard Wubbolts van het Centrum voor Cellulaire Beeldvorming voor jullie assistentie bij de confocale microscopie en voor de lading datadiscs.

De mensen van het Hubrecht lab: Christine Mummery voor het vertrouwen dat je aan me hebt gegeven door me op je lab te laten werken; Robert Passier voor het leren van technieken die ik gedurende mijn promotieonderzoek herhaaldelijk heb gebruikt; obrigado Susana Chuva de Sousa Lopes voor je hulp bij diverse experimenten, wie weet kunnen we in de toekomst nog samenwerken; Dorine Ward-van Oostwaard, Stieneke van den Brink en Marga van Rooijen voor de technieken die ik van jullie geleerd heb en de hulpvaardigheid tijdens, maar ook na mijn verblijf op het Hubrecht lab.

De collega's bij Biochemie / Celbiologie: Federica van Dissel-Emiliani voor je hulpvaardigheid bij het isoleren, kweken en karakteriseren van gonocyten van het varken; Mieke de Boer, voor de hulp bij het maken van coupes; Bart Gadella voor je interesse in mijn voortgang en je hulp bij de verlenging van mijn aanstelling; Toine ten Broeke voor het geven van diverse antilichamen; en verder Willem Stoorvogel, Carla Zijlstra en Esther van 't Veld.

De collega's bij paard: Damien Paris, I enjoyed your company very much, keep up the good work; en verder Tom Stout, Karin Hendriks en Björn Rambags.

Ingrid Vos voor het surplus muizenmateriaal; Ian Chambers, Ans van Pelt, Dick de Rooij, Ian Brewis en Peter de Boer for the good discussions and the fruitful collaborations.

De studenten die bij me stage hebben gelopen: Tessel Rigter en Alain van Mil, bedankt voor jullie inzet.

Familie en vrienden: in het bijzonder mijn ouders voor alle steun die ik door de jaren heen heb gekregen, ongeacht de keuzes die ik maakte; en verder: Marjolein, Ruul, Marten, Hielkje, Cor, Maria, Susanne, Arjan, Marieke, Lennart, Janneke, Joep, Huub, Anneke, Elizabeth, Monique, Ernst, Jostijn, Donatien, Marietje, Jet, Veronique, Wilco v. D., Martine, Willem, Livio en Kate; allemaal bedankt voor de interesse die julle getoond hebben in de voortgang van dit project en/of de afleiding waar jullie in die tijd voor gezorgd hebben.

Erno en Wilco, het is een grote eer voor mij dat jullie mijn paranimfen willen zijn.

De meeste dank gaat uit naar Karin voor de steun tijdens het tot stand komen van dit proefschrift.

Curriculum Vitae

Curriculum Vitae

Ewart Kuijk werd 12 januari 1975 geboren te Eindhoven. In 1994 behaalde hij zijn VWO-diploma aan het Hertog-Jan College te Valkenswaard. Hij studeerde Biologie aan de Universiteit Utrecht en specialiseerde zich in evolutiebiologie en ethologie. Tijdens zijn specialisatie voerde hij twee onderzoeksstages uit: eerst onderzocht hij sociaal gedrag van hommels aan de afdeling Sociale Oecologie van de Universiteit Utrecht; vervolgens onderzocht hij de kosten van reproductie bij Koolmezen aan het Centrum voor Terrestrische Oecologie van het Nederlands Instituut voor Oecologisch Onderzoek te Heteren. Na het afronden van zijn studie, heeft Ewart voor de groep van Ronald Plasterk gewerkt aan de afdeling Functional Genomics van het Hubrecht Laboratorium. Vervolgens heeft hij voor de Universiteit van Canterbury gewerkt aan een onderzoek naar het gedrag en de populatiedynamica van Nieuwzeelandse zeeleeuwen. Terug in Nederland werkte hij wederom op het lab van Ronald Plasterk aan een functionele analyse van het genoom van *Caenorhabditis elegans.* In 2004 begon hij aan zijn promotieonderzoek aan de Hoofdafdeling Gezondheidszorg Landbouwhuisdieren van de Faculteit Diergeneeskunde dat resulteerde in dit proefschrift.

Ewart Kuijk was born on January 12th 1975 in Eindhoven, the Netherlands. In 1994, he completed his secondary education at the "Hertog Jan College" in Valkenswaard. Thereafter, he studied Biology at Utrecht University, where he specialized in evolutionary biology and animal behavior. His specialization comprised two research internships: the first was conducted at the Social Ecology department of Utrecht University where he investigated sociality in bumblebees; for his second research internship, he studied the costs of reproduction in Great tits at the Center for Terrestrial Ecology of the Netherlands Institute for Ecology in Heteren. He obtained his biology degree in 2000, after which he worked as a technician for the group of Ronald Plasterk at the Department of Functional Genomics of the Hubrecht Laboratory. In a sabbatical year, he joined the Marine Mammal Research Group from Canterbury University in New Zealand to study population dynamics and behavior of New Zealand fur seals. Subsequently, he returned to the lab of Ronald Plasterk where he participated in a functional genomic analysis of the *Caenorhabditis elegans* genome. In 2004 he started his PhD project at the Department of Farm Animal Health of the Faculty of Veterinary Medicine, which resulted in the present thesis.

Publications:

Zijlstra C, Kidson A, Schoevers EJ, Daemen AJ, Tharasanit T, Kuijk EW, Hazeleger W, Ducro-Steverink DW, Colenbrander B, Roelen BA. 2008. Blastocyst morphology, actin cytoskeleton quality and chromosome content are correlated with embryo quality in the pig. *Theriogenology*.

Kuijk EW, Du Puy L, Van Tol HT, Oei CH, Haagsman HP, Colenbrander B, Roelen BA. 2008. Differences in early lineage segregation between mammals. *Dev Dyn* **237**:918-927.

Kuijk EW, du Puy L, van Tol HT, Haagsman HP, Colenbrander B, Roelen BA. 2007. Validation of reference genes for quantitative RT-PCR studies in porcine oocytes and preimplantation embryos. *BMC Dev Biol* **7**:58.

Passier R, Oostwaard DW, Snapper J, Kloots J, Hassink RJ, Kuijk E, Roelen B, de la Riviere AB, Mummery C. 2005. Increased cardiomyocyte differentiation from human embryonic stem cells in serum-free cultures. *Stem Cells* **23**:772-780.

Simmer F, Moorman C, van der Linden AM, Kuijk E, van den Berghe PV, Kamath RS, Fraser AG, Ahringer J, Plasterk RH. 2003. Genome-wide RNAi of C. elegans using the hypersensitive rrf-3 strain reveals novel gene functions. *PLoS Biol* **1**:E12.